CLINICAL PHARMACOLOGY OF MILTEFOSINE

Application of modeling and simulation to advance treatment of leishmaniasis

Semra Palić

Clinical pharmacology of miltefosine

Application of modeling and simulation to advance treatment of leishmaniasis

Semra Palić

Clinical pharmacology of miltefosine

Application of modeling and simulation to advance treatment of leishmaniasis

Klinische farmacologie van miltefosine
Toepassing van modellering en simulatie ter bevordering van de behandeling van
leishmaniasis
(met een samenvatting in het Nederlands)

Proefschrift

ter verkrijging van de graad van doctor aan de Universiteit Utrecht
op gezag van derector magnificus, prof.dr. H.R.B.M. Kummeling,
ingevolge het besluit van het college voor promoties
in het openbaar te verdedigen op

vrijdag 10 september 2021 des middags te 4.15 uur

door

Semra Palić

geboren op 3 maart 1994
te Žepa, Bosnië en Herzegovina

Promotor:
 Prof. dr. J.H. Beijnen

Copromotor:
 Dr. T.P.C. Dorlo

Mojoj majci

Preface

Leishmaniasis is a neglected tropical infectious disease caused by the protozoan parasite *Leishmania*, transmitted by sand flies. Affecting the poorest of the poor in low- and middle-income countries, leishmaniasis remains one of the major public health concerns. There are over 20 different *Leishmania* parasite species, and over 90 types of sandflies which carry and transmit *Leishmania* (1). Heterogeneity in parasite species leads to different clinical manifestation of the disease, with cutaneous leishmaniasis (CL) as the most prevalent form of disease. It was estimated in 2018 that up to 1 million new CL cases occur worldwide, with 95% of those occurring in South America, the Middle East and Central Asia. CL is presented by cutaneous ulcers, as the parasite remains localized in the skin. Depending on the parasite subspecies, CL can be self-healing (2). However, more severe CL inevitably leads to disfigurement of the affected skin areas, leaving permanent and stigmatizing scars. Additionally, the most severe and devastating form of leishmaniasis is visceral leishmaniasis (VL). It is characterized by enlargement and swelling of the internal organs affected by parasite, such as spleen and liver. Without adequate treatment, VL is lethal within months. Absence of treatment options accessible by patients in need, ensued VL as the second largest parasitic killer in the world, following malaria (3). An estimated 50 – 90 thousand new cases occur annually, mainly in the countries of East Africa and Southeast Asia (2). Furthermore, in some patients who are treated for VL, a dermatological condition called post kala-azar dermal leishmaniasis (PKDL) develops months or years after treatment completion. PKDL is mainly characterized by papular, nodular or macular skin lesions.

Miltefosine is an alkylphosphocholine agent that demonstrated a broad spectrum of antiparasitic properties, and emerged as the first oral drug against leishmaniasis. Before miltefosine, only highly toxic drugs with invasive routes of administration, such as antimonials, were used in the treatment of leishmaniasis. Miltefosine can be administered orally and as such it represented an enormous step forward in the antileishmanial therapeutic arsenal, especially in the management of VL. Understanding of miltefosine pharmacokinetics (PK) and pharmacodynamics (PD) was limited before the drug was approved in the treatment of VL in 2002 (4). Over the past two decades, various clinical and pharmacokinetic studies documented high variability in PK as well as differences in treatment efficacy among different patient populations, e.g. children versus adults, Eastern African versus Indian patients, etc. (5, 6). In this thesis we present the most recent findings about miltefosine clinical

pharmacology. The PK and PD data from clinical studies were analyzed by advanced pharmacometric methods, to provide a better understanding of miltefosine PK and PD in the treatment of leishmaniasis.

Chapter I provides a comprehensive review on the most recent developments in clinical pharmacology of miltefosine in treatment of CL, VL and PKDL, and evaluates the current dosing regimens with miltefosine. **Chapter II** elaborates on non-linear PK of miltefosine in the treatment of pediatric VL in Eastern African patients. We performed a model-based analysis of pediatric data from two different dosing regimens of miltefosine: a conventional or linear mg/kg dosing regimen and an allometric weight-based dosing regimen, where we quantified and explained the observed non-linearities. This chapter further provides first population PK results of miltefosine following an allometric dosing regimen in the treatment of PKDL. In addition, **chapter III** explores clinical PD of immune responses following treatment with miltefosine. Here we characterize the PK-PD relationship between miltefosine exposure and neopterin dynamics and discuss its association with the clinical outcome. This chapter also includes a systematic review of immunomodulatory effects of miltefosine. Furthermore, **chapter IV** focuses on PK and PD of miltefosine in the skin during the treatment of the dermal infection PKDL. In this chapter we present first evidence of miltefosine exposure in skin tissue from PKDL patients which can be regarded as a proxy of target-site exposure at the site of infection. Moreover, in this chapter we evaluated miltefosine PK following an allometric weight-based dosing regimen of 12 weeks, and related it to skin healing dynamics in pediatric and adolescent PKDL patients. At last, **chapter V** presents conclusions of this thesis, and summarizes authors' views on future perspectives with regard to miltefosine treatment in leishmaniasis.

References

1. Alvar J, Vélez ID, Bern C, Herrero M, Desjeux P, Cano J, Jannin J, de Boer M. 2012. Leishmaniasis worldwide and global estimates of its incidence. PLoS One.

2. WHO. Leishmaniasis.

3. Saporito L, Giammanco GM, De Grazia S, Colomba C. 2013. Visceral leishmaniasis: Host-parasite interactions and clinical presentation in the immunocompetent and in the immunocompromised host. Int J Infect Dis 17:e572–e576.

4. Dorlo TPC, Balasegaram M, Beijnen JH, de Vries PJ. 2012. Miltefosine: a review of its pharmacology and therapeutic efficacy in the treatment of leishmaniasis. J Antimicrob Chemother 67:2576–2597.

5. Dorlo TPC, Kip AE, Younis BM, Ellis SJ, Alves F, Beijnen JH, Njenga S, Kirigi G, Hailu A, Olobo J, Musa AM, Balasegaram M, Wasunna M, Karlsson MO, Khalil EAG. 2017. Visceral leishmaniasis relapse hazard is linked to reduced miltefosine exposure in patients from Eastern Africa: a population pharmacokinetic/pharmacodynamic study. J Antimicrob Chemother 72:3131–3140.

6. Palić S, Kip AE, Beijnen JH, Mbui J, Musa A, Solomos A, Wasunna M, Olobo J, Alves F, Dorlo TPC. 2020. Characterizing the non-linear pharmacokinetics of miltefosine in paediatric visceral leishmaniasis patients from Eastern Africa. J Antimicrob Chemother.

7. Mbui J, Olobo J, Omollo R, Solomos A, Kip AE, Kirigi G, Sagaki P, Kimutai R, Were L, Omollo T, Egondi TW, Wasunna M, Alvar J, Dorlo TPC, Alves F. 2018. Pharmacokinetics, safety and efficacy of an allometric miltefosine regimen for the treatment of visceral leishmaniasis in Eastern African children: an open-label, phase-II clinical trial. Clin Infect Dis.

Contents

Introduction

Chapter 1

An update on the clinical pharmacology of miltefosine in the treatment of leishmaniasis

Semra Palić[1], Jos H. Beijnen[1], Thomas P. C. Dorlo[1]

1. Department of Pharmacy & Pharmacology, The Netherlands Cancer Institute
    - Antoni van Leeuwenhoek Hospital, Amsterdam, The Netherlands

Chapter 1.1

Abstract

Miltefosine is an alkylphosphocholine agent with a broad spectrum of antiparasitic properties. For over two decades now, miltefosine remains the first and only oral drug licensed and used in treatment of the neglected tropical disease leishmaniasis. An extensive review on the pharmacology of miltefosine was last published in 2012, while additional data on the clinical pharmacokinetics (PK) and pharmacodynamics (PD) of miltefosine became available in the past decade, along with ongoing and future studies in this area. Miltefosine PK are characterized by slow absorption and elimination resulting in accumulation of drug in plasma until the end of treatment. Several recent studies established exposure-response relationships for various treatment regimens of miltefosine in the treatment of visceral and cutaneous leishmaniasis, leading to the identification of PK parameters predictive of clinical relapse and outcome. This review provides an update on the most recent developments in the area of clinical pharmacology of miltefosine, including a discussion of the current dosing regimens.

1. Introduction

Miltefosine is an alkylphosphocholine agent which demonstrated a broad spectrum of antiparasitic properties, and emerged as the first oral drug in the therapeutic arsenal for leishmaniasis (1). Leishmaniasis is a spectrum of clinical diseases caused by the protozoan *Leishmania* parasite which are transmitted by sand flies. Affecting mainly the poorest of the poor in low- and middle-income countries, leishmaniasis remains a major public health concern (2). The most severe form of leishmaniasis is visceral leishmaniasis (VL) where internal organs such as spleen, liver and bone marrow are affected, leading to fatality if left untreated. Severity of VL and absence of adequate treatment options accessible by those in need, ensued VL as the second largest parasitic killer in the world, following malaria (3, 4). In addition, the most prevalent clinical presentation of leishmaniasis which mainly affects the skin, is known as cutaneous leishmaniasis (CL). CL is presented by cutaneous ulcers as the parasite remains localized in the skin. Depending on the parasite subspecies, CL can be self-healing after a period of time, while more severe CL inevitably leads to disfigurement of the affected skin areas as a result of stigmatizing scars (5, 6). Moreover, another form of leishmaniasis of the skin is post-kala-azar dermal leishmaniasis (PKDL), which develops as a complication following treatment for VL, where *Leishmania* parasites evade into the skin after VL treatment. PKDL is mainly characterized by papular, nodular or macular skin lesions (7–9).

Today, miltefosine remains a major therapeutic advance against leishmaniasis, especially against VL (10). Since 2010, this drug has been included in the World Health Organization (WHO) List of Essential Medicines and is up to date the only oral drug effective in the treatment of leishmaniasis (WHO. *https://www.who.int/*). Various comprehensive reviews on the clinical development of miltefosine have been published in the past, such as our previous review on the pharmacology of miltefosine from 2012 (12–15). More recently new clinical pharmacokinetic and pharmacodynamic data have become available aiding the further optimization of miltefosine regimens in leishmaniasis. Therefore, the present article provides an updated review, primarily focusing on clinical pharmacokinetic and pharmacodynamic studies of miltefosine in the treatment of leishmaniasis published after 2012.

1.1 Physiochemical properties, metabolism and mechanism of action

Miltefosine (hexadecyl 2-(trimethylazaniumyl)ethyl phosphate), is marketed as Impavido, an oral capsule formulation (2, 16). In pharmacological terms, miltefosine is an antiprozoal agent, while by its chemical structure it is an alkylphosphocholine analog consisting of a phosphorylcholine ester of a long-chain alcohol (17). Miltefosine is a structural analog of lecithin and is structurally related to platelet aggregation factor. The chemical formula for miltefosine is $C_{21}H_{46}NO_4P$ and has a molar mass of 407.576 g·mol^{-1}. The molecular structure for miltefosine is provided in *figure 1*.
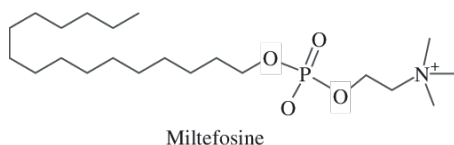
Miltefosine

Figure 1: chemical structure of miltefosine

Miltefosine has a high plasma protein binding, ranging from 96% to 98%, to both serum albumin and low-density lipoprotein (18). It is metabolized by phospholipase D and C, breaking down into choline and choline-containing metabolites, which are further reused in the biosynthesis of long-chain fatty acids and cell membranes (19, 20). Furthermore, miltefosine has a high affinity for lipid rafts, and is incorporated in the membrane lipid bilayer by interacting with membrane sterols, cholesterol and/or egosterol (21, 22). Its direct mechanism of action has been associated with disturbing the membrane metabolism and composition of the *Leishmania* parasite and induction of apoptosis-like cell death. Furthermore, besides direct parasite killing, a summary of preclinical and clinical studies have documented additional mechanisms of action for miltefosine in terms of immunomodulation (15, 23). These studies documented miltefosine targeting the T-helper cell type 1 (Th-1) signaling, mediating a cascade of pro-inflammatory cytokines required for clearance of the *Leishmania* parasite. By increasing concentrations of pro-inflammatory Th-1 cytokines such

as interferon gamma, and interleukin 12, miltefosine is also able to induce a shift of the macrophage phenotype, which is essential for the clearance of intracellular pathogens (23).

2. Dosing of miltefosine in the treatment of leishmaniasis

Several reviews have previously summarized efficacy and tolerance of miltefosine-based treatment regimens (15, 24, 25), thus inhere we summarized the current dosing recommendations for miltefosine for the various clinical presentations of leishmaniasis.

2.1 Visceral leishmaniasis

In treatment of VL, miltefosine demonstrated high efficacy rates in adult patients treated with the conventional linear body weight-based dosing regimen of 2.5 mg/kg/day for 28 days in both Eastern Africa and Southeast Asia, resulting in a final cure rate of 86% and 97% at 6 months follow-up for Eastern African and Indian patients respectively (26, 27). Unfortunately, this dosing regimen appeared less effective in children, with particularly substantially lower cure rates in Nepal and Eastern Africa (59% at 6 months follow-up), as well as approximately 30% lower systemic exposure (28, 29). In response to this, an optimal allometric weight-based dosing regimen was designed following model-based clinical trial simulations (30) and investigated in children, where a relatively higher mg/kg daily dose (up to 3.9 mg/kg) was administered to patients with lower body weights for a duration of 28 days, aimed at providing similar exposure as observed in adults receiving 2.5 mg/kg/day (27). Moreover, lower variability in drug exposure was observed following the allometric dose, which resulted in 90% cure rate at 6 month follow-up (31, 32). Given these results, allometric weight-based dosing of miltefosine is further recommended in pediatric patients for the treatment of pediatric VL.

2.2 Cutaneous and mucocutaneous leishmaniasis

Current dosing recommendations according to the label for miltefosine in the treatment of CL caused by *L. major, L. braziliensis, L. guyanensis, L. infantum and L. panamensis* indicate 50 mg twice daily dosing for patients between 30 and 44 kg, and for patients ≥ 45 kg, a flat dose of 50 mg three times daily in a duration of 28 days (5, 33–35). In addition, miltefosine allometric weight-based dosing regimen has been further recommended in the treatment of pediatric CL in Colombia due to *L. panamensis* (36). Limited evidence exists for miltefosine to

treat CL due to *L. mexicana* and *L. tropica.* For Old World mucocutaneous leishmaniasis (MCL) the same dosing regimen is recommended, while for New World MCL 150 mg daily for 28 days has been recommended (37).

2.3 Post-kala-azar dermal leishmaniasis

At present, there are no standard dosing recommendations for miltefosine in the treatment of PKDL, although 12-week regimens have been suggested and used in South Asia (38). However, there are several trials currently ongoing in Sudan, Bangladesh and India, investigating efficacy of allometric weight-based dosing regimens in treatment of PKDL in various combinations and durations (39–41).

3. Clinical pharmacokinetics

3.1 Bioanalytical assays

Concentrations of miltefosine can be quantified in blood plasma using liquid chromatography coupled to tandem mass spectrometry (LC-MS/MS). A previously validated method for miltefosine had a lower limit of quantification of 4 ng/mL in plasma, which is sensitive enough to measure miltefosine up to 5 months post-treatment (42). Additionally, a method has been developed to quantify miltefosine in peripheral blood mononuclear cells (PBMC) by LC-MS/MS. This assay serves as target site assay to indicate intracellular accumulation of miltefosine (43). Furthermore, assays to measure miltefosine concentration in whole blood were developed using dried blood spot (DBS) on filter paper, and using a novel volumetric absorptive microsampling (VAMS) device (44, 45). Both DBS and VAMS are field-adapted sampling opportunities for clinical PK studies in rural and remote areas. Samples obtained through these methods are stable for months on temperatures up to 37°C, and therefore do not require freezing on site. Ongoing efforts include development of bioanalytical assays to quantify miltefosine in skin tissue, which is of critical importance towards understanding disposition of miltefosine in the skin following systemic administration in the treatment of CL and PKDL (46).

3.2 Clinical Pharmacokinetics

Several studies with a focus on miltefosine plasma PK following both linear weight-based and allometric weight-based dosing regimens have been performed over the past few years, in various patient populations including both adult and pediatric patients, in VL and CL. This further allowed estimation of PK parameters and their between-subject variability from the clinical PK data by employing the methods of population pharmacokinetic modeling. A summary of the reported PK parameter estimates obtained from population PK analyses performed since 2012 is provided in *table 1*.

Absorption of miltefosine is slow and the rate of absorption has been estimated ranging between 1.6 to 9.6 day^{-1} (32). Recent evidence documented an approximately 70% decrease in miltefosine bioavailability in the first treatment week in Eastern African patients suffering from VL, presumably due to malnourishment or disease-associated malabsorption (32, 47). Furthermore, in Eastern African pediatric patients, following the allometric weight-based dosing regimen, miltefosine bioavailability appeared to stagnate at the end of the treatment potentially due to saturation of absorption related to the cumulative dose (32). Initial elimination half-life has been estimated between 4 and 7 days, with a terminal half-life of 31 days (32, 47). In addition, given the long half-life with a twice or thrice daily dose administered, miltefosine concentrations keep accumulating during treatment. Commonly, most patients reach steady-state plasma concentrations roughly after 5 half-lives of treatment, which would be around the fourth week of treatment or later. Moreover, miltefosine was found to accumulate within PBMCs, resulting in nearly twice higher concentrations compared to plasma, indicating a high target-site exposure for miltefosine as the main site of action is intracellularly in infected macrophages (43). Additionally, plasma C_{max} was reported in the range from 17.2 to 42.4 μg/mL in adult patients following the linear weight-based dosing regimen, while 14.4–37.7 μg/mL was reported for pediatric patients following the allometric weight-based dosing regimen (31, 48). Volume of distribution appears rather constant, as estimated in various PK studies (30, 32, 47). In respect to metabolism and excretion, miltefosine is nearly fully eliminated by the enzymes noted above, with little excretion unchanged. Clearance of miltefosine is slow, and estimated at approximately 4 L/day for a typical individual of 70 kg (30).

For a total treatment duration of 28 days, as is conventional for the treatment of both VL and CL, total exposure to miltefosine during the treatment period as represented by the area under the plasma concentration-time curve (AUC) from days 0 to 28 (AUC_{d0-28}) was calculated in adult VL patients in Eastern Africa who were treated with a linear 2.5 mg/kg/day weight-based dosing regimen (conventional dose), which was on average 29% higher than in pediatric VL patients treated with a similar mg/kg dosage (497 versus 352 µg·day/mL, respectively). Moreover, overall exposure was more variable in pediatric patients treated with a similar mg/kg dose (47). The allometric dosing regimen in pediatric Eastern African VL patients resulted in nearly twice higher treatment exposure in the first treatment week, and 16.4% higher AUC_{d0-28} in comparison to the linear 2.5 mg/kg/day regimen (31, 32). In addition, in CL patients from Colombia, markedly higher exposures were observed using a similar linear 2.5 mg/kg/day dosing regimen for 28 days, with mean AUC_{d0-28} values of 789 µg·day/mL for adults (59% higher than previously observed in adult VL patients in Eastern Africa) and 545 µg·day/mL for pediatrics (55% higher than in pediatric VL patients in Eastern Africa) (49). Moreover, also in Indian adult VL patients treated with 2.5 mg/kg/day for 28 days a much higher median AUC_{d0-28} of 645 µg·day/mL (30% higher than in adults VL patients in Eastern Africa) has been found (30). These high differences in exposure between clinical leishmaniasis phenotypes and geographical regions might be related to the previously described non-linearities in the bioavailability of miltefosine in Eastern African patients, which are highly likely to be population specific.

Table 1: Overview of population pharmacokinetic models since 2012 describing miltefosine pharmacokinetics in the treatment of visceral (VL) and cutaneous leishmaniasis (CL).

Study	Clinical presentation	Number of patients (pediatric patients)	Median bodyweight (range) in kg	Dose and treatment duration	Structural model	Absorption rate estimate (day[-1])	Clearance from the central compartment (estimate (l/day))	Volumes of distribution estimate (l)
Dorlo et al.(30)	CL and VL	82 (39)	15 (9 – 23) 35.5 (16 – 58) 85 (70 – 113)	2.5 mg/kg/day for 28 days	two-compartment	9.6	3.99[A]	V_d/F 40.1[A] and V_p/F 1.75
Kip et al.(49)	CL	51 (29)	71.1 (50.4–102)	1.8-2.5 mg/kg/day for 28 days.	three-compartment	9.6 fixed	4.6[A]	V_c/F 28.5[A] and V_p/F 2.85, V_{p2}/F 1.85
Palić et al.(32)	VL	51 (51)	24 (16–34)	linear dose 2.38(1.25–333) mg/kg/day or allometric dose 3.2 (2.7–3.9) mg/kg/day for 28 days	two-compartment	1.61	2.44[B]	V_d/F 22.9[B] and V_p/F 2.27
Dorlo et al. (29)	VL	81 (20)	40 (8–56)	1.5–2.5 mg/kg, for 28 days	two-compartment	NA	3.69[A]	V_c/F 38.5[A] and V_p/F 1.69
Dorlo et al.(47)	VL	48 (19)	33.5 (16–65)	2.59 (2.02–3.33) mg/kg/day for 28 days	two-compartment	1.49	4.29[A]	V_c/F 51.7[A] and V_p/F 2.25

[A] Normalized to a standardized fat-free mass of 53 kg

[B] Normalized to a standardized fat-free mass of 18

4. Clinical pharmacodynamics

Miltefosine exposure has been related to the clinical outcome in VL, by means of logistic regression using a binary outcome variable (cure vs treatment failure/relapse) and a time-to-event approach using the time to clinical disease relapse as outcome variable within a 6- or 12-months follow-up period (47). For CL a relationship was established between miltefosine exposure and binary treatment outcome, where cure was defined as complete reepithelization of lesions at 6-months follow-up (49).

Based on these PK-PD analyses, several PK targets have been proposed for CL and VL, associated with a favorable PD response. Specifically, a PK target for CL was proposed at $AUC_{d0-28} > 535\,\mu g \cdot day/mL$ corresponding to > 95% probability of cure (49). Next, in VL, the time that the plasma concentration was above the in vitro susceptibility EC_{90} ($t > EC_{90}$, for Eastern Africa) or above $10 \times EC_{50}$ (for Nepal) was related to the probability of cure and relapse hazard. First, in a Nepalese VL patient cohort, $t > 10 \times EC_{50}$ was determined as a predictor for treatment outcome within 12 months follow-up, using a $10 \times EC_{50}$ equivalent to 17.9 µg/mL (29, 50). There the mean $t > 10 \times EC_{50}$ was 30.2 days, which was associated with a relapse rate of 19.5%. Second, in Eastern African VL patients, $t > EC_{90}$ using a region-specific EC_{90} value equivalent to 10.6 µg/mL was associated with relapse hazard using a time-to-event model. A PKPD target was suggested based on this analysis with a $t > EC_{90}$ 29.5 days, with only 1/9 relapses having a $t > EC_{90}$ higher than this value for miltefosine monotherapy (47). There was a substantial difference in $t > EC_{90}$ following a linear dosing regimen between adult and pediatric VL patients, with a median 27.8 (range 4.3 − 43.8) versus 22 (range 11 − 34) days, respectively. While with the allometric dose regimen the overall $t > EC_{90}$ was slightly higher in pediatric VL patients compared to the linear dose regimen with a median 24.5 (range 17.46 − 33.3) days, time to reach this target was on median reduced by 17.4 % after the allometric dose in comparison with the linear dose regimen (32). Given that the clinical efficacy of the allometric dosing regimen was much improved and considered adequate in pediatric VL patients, it might be considered that this time to reach the target might also be of importance for the efficacy of miltefosine.

In addition, several biomarkers have been proposed for evaluation of treatment outcome with regard to miltefosine (51). Parasite clearance in the blood during the first week of treatment of miltefosine monotherapy was first reported to be delayed when compared to other treatments, likely due to slow accumulation of miltefosine in plasma in the first week of

treatment (27). Given the long follow-up times required to establish clinical cure, there is a strong interest to identify early markers of cure, and parasite load measured in blood by real-time quantitative PCR (qPCR) became an attractive marker to monitor treatment response. A recent study used pooled data from several clinical trials measuring blood parasite load to investigate the potential of this marker as a predictor of clinical relapse. Data from three VL clinical trials in Eastern Africa were included, where two trials investigated miltefosine monotherapy, and one trial investigated miltefosine in combination with liposomal amphotericin B (AmBisome), while other treatment regimens were fexinidazole monotherapy and sodium stibogluconate (SSG) in combination with AmBisome. Here it was shown that having an absolute parasite load > 20 parasites/mL in blood on day 56 was a sensitive and specific predictor of relapse after treatment of VL (52).

Furthermore, as the parasite replicates in active VL, more macrophages become attracted and activated and levels of inflammation increase (22). Therefore, it has been hypothesized that markers of macrophage activation could be used in monitoring and predicting the treatment response. In particular, IFN-γ further leads to the macrophage stimulated production of a peritidine called neopterin, which is found to be highly elevated in active VL infection (53, 54). In VL patients from Eastern Africa treated with miltefosine and AmBisome, neopterin was evaluated, suggesting that the neopterin concentration ratio day 60/day 28 was a sensitive and specific predictor of clinical outcome within 6 months follow-up, with a sensitivity of 93% to predict relapse (55). The effect of miltefosine concentrations on *Leishmania*-driven neopterin production was modelled subsequently using a direct effect population PK-PD model. Model-based simulations showed that the predicted day 40/day 28 neopterin concentration ratio potentially had a high sensitivity for identification of relapsing patients, which could be used to identify patients requiring more frequent clinical follow-up (submitted work). Nonetheless, specificity of neopterin-derived parameters at various time points for miltefosine was relatively low, limiting its use as a final test of cure. Therefore, at the moment, both neopterin and the blood parasite load are attractive and promising tools for evaluating miltefosine PD. However, in order to use these markers in clinical trial settings or individual patient management, additional studies and optimization is required.

At last, in respect to toxicity, the primary site for miltefosine related adverse events (AE) is the gastrointestinal (GI) system. Most patients experience at least one of the GI AEs, including nausea, vomiting, diarrhea, and/or loss of appetite (27, 56, 57). Most leishmaniasis patients

experience GI-related AEs in the first treatment weeks. However, as the systemic exposure is highest at the end of treatment, GI-related AEs are probably caused by a direct effect of the absolute amount of miltefosine administered with each dose on the lining of the GI. For this reason, it has been reported that administering a lower dose of miltefosine twice or thrice daily instead of one daily dose decreases GI-related adverse effects and intake of (fatty) food together with the dose might be considered, although it is unclear which effect this has on miltefosine's bioavailability (57, 58). Moreover, miltefosine is found to cause embriotoxicity, and fetotoxicity, limiting its use in pregnancy, and requiring contraception for two to five months after miltefosine treatment, depending on the duration of treatment (59, 60).

5. Combination therapies with miltefosine

Various combination therapies with miltefosine have been initiated in the treatment of VL, with goals to increase treatment efficacy, decrease probability of eliciting drug resistance in parasites, reduce treatment and hospitalization costs and duration. Investigated drugs in combination with miltefosine mainly include AmBisome and paromomycin. From 2008 to 2012, a phase III combination therapy trial was conducted in India, investigating AmBisome single dose of 7.5 mg/kg in combination with 14 days of miltefosine at a dosage of 2.5 mg/kg/day (61). Additionally, there are several ongoing trials investigating combination therapies including miltefosine (62). Specifically in 2017 a large-scale phase III trial was reported on short course combination therapies including miltefosine and paromomycin for treatment of VL in Bangladesh, including regimens of 5 mg/kg single dose of AmBisome together with 7 days of miltefosine (2.5 mg/kg/day) and 10 days of paromomycin (15 mg/kg/day) together with miltefosine (2.5 mg/kg/day) (63). PK of miltefosine in combination with AmBisome were previously described, while the combination treatment appears well tolerated, without drug-drug interactions reported to increase frequency of AEs (27). Other paromomycin-miltefosine combination regimens are currently being investigated in Eastern African VL patients, including a 14 day regimen of paromomycin plus allometrically dosed miltefosine (64). Next, with respect to treatment of CL, a combination of miltefosine, with antimonials and thermotherapy are being evaluated in a phase II trial to assess the safety and efficacy of these combination therapies. Preliminary results in American patients elucidated that a combination of thermotherapy with a shorter course of oral miltefosine is more effective than thermotherapy alone (65).

Furthermore, combination therapies for patients with human immunodeficiency virus (HIV) and VL co-infection have been particularly needed. VL is challenging to treat in immunocompromised patients, since a sterilizing cure is considered impossible and additionally drug-drug interactions might complicate therapeutic management. In Eastern African VL-HIV patients, treatment with miltefosine 50 mg twice daily for 28 days in combination with AmBisome was evaluated against a background of various antiretroviral drugs, including nevirapine and efavirenz. Median day 28 miltefosine concentrations were observed significantly higher for patients treated with nevirapine (25,100 ng/mL) in comparison to those treated with efavirenz (18,000 ng/mL), possibly related to protein binding competition. More importantly, overall miltefosine exposure was considerably lower in HIV-coinfected patients compared to VL patients in Eastern Africa not coinfected with HIV. These results warrant further optimization of the miltefosine dose regimen in order to achieve a favorable exposure in VL-HIV coinfected patients (manuscript accepted for publication doi:10.1093/jac/dkab013).

6. Concluding remarks and future perspectives

The development of miltefosine took an unplanned turn from being an experimental anticancer drug to emerging as the first oral drug available for the treatment of leishmaniasis. Here we summarize recent clinical PK and PD studies following either conventional or allometric dosing regimens in both CL and VL in Eastern African, South Asian and South American patients, including adult and pediatric patients. Taken together, it is evident from these studies that miltefosine PK is variable among patients, especially among VL patients in the Eastern Africa, requiring dose adjustments from conventional dosing to allometric dosing in children and adolescents.

Moreover, in the past decade, several PK targets were proposed, for both CL and VL, which were derived from characterizations of PK-PD relationships with clinical outcome and biomarkers. Drug exposure was associated with both treatment outcome for CL and VL, and relapse hazard for VL. Evaluation of PD markers such as blood parasite load and neopterin provided further insight in treatment responses which allowed for a more accurate identification of patients at risk of relapse. Future studies are necessary to further optimize and validate these potential biomarkers of treatment response, ultimately to allow early

selection of drug regimens in development, as well as tailor individual treatment management.

In summary, although treatment of leishmaniasis was highly improved by optimizing miltefosine treatment in various clinical phenotypes and patient populations, a search for more rational treatments continues. Due to the slow accumulation of miltefosine, a substantial period of time is needed to achieve desirable exposure, as discussed in this review. The target $t > EC_{90}$ of 29 days for miltefosine monotherapy to achieve treatment success in VL is rather long and to ensure patient adherence, directly observed therapy is required which in clinical practice is difficult in remote areas. Further optimization of miltefosine should be directed at combination regimens with other antileishmanial drugs to shorten the treatment course, particularly in both VL and PKDL. Currently there are ongoing clinical trials for treatment of PKDL in Sudan, India and Bangladesh, testing different treatment combinations with miltefosine, AmBisome and paromomycin. Ideally, future miltefosine-based combination treatments for VL will include one of the orally available new chemical entities that are currently in early clinical development, to result in an all oral short treatment which could be administered on an out-patient basis (66).

References

1.   Widmer F, Wright LC, Obando D, Handke R, Ganendren R, Ellis DH, Sorrell TC. 2006. Hexadecylphosphocholine (miltefosine) has broad-spectrum fungicidal activity and is efficacious in a mouse model of cryptococcosis. Antimicrob Agents Chemother 50:414–421.

2.   Alves F, Gillon J-Y, Arana B, Dorlo TPC. 2017. Chapter 3. From Bench to Bedside: Development and Optimization of Clinical Therapies for Visceral Leishmaniasis, p. 37–54. *In* Drug Discovery for Leishmaniasis.

3.   Murray HW, Berman JD, Davies CR, Saravia NG. 2005. Advances in leishmaniasis. Lancet 366:1561–1577.

4.   Bern Crayn. Visceral leishmaniasis: Clinical manifestations and diagnosis - UpToDate.

5.   Eissa MM, Amer EI, Mossallam SF, Gomaa MM, Baddour NM. 2012. Miltefosine for Old World cutaneous leishmaniasis: An experimental study on Leishmania major infected mice. Alexandria J Med 48:261–271.

6.   Ameen M. 2007. Cutaneous leishmaniasis: Therapeutic strategies and future directions. Expert Opin Pharmacother 8:2689–2699.

7.   Zijlstra EE. 2016. The immunology of post-kala-azar dermal leishmaniasis (PKDL). Parasit Vectors 9:464.

8.   Islam S, Kenah E, Bhuiyan MAA, Rahman KM, Goodhew B, Ghalib CM, Zahid MM, Ozaki M, Rahman MW, Haque R, Luby SP, Maguire JH, Martin D, Bern C. 2013. Clinical and immunological aspects of post-kala-azar dermal leishmaniasis in Bangladesh. Am J Trop Med Hyg 89:345–353.

9.   Zijlstra EE, Musa AM, Khalil EA, el-Hassan IM, el-Hassan AM. 2003. Post-kala-azar dermal leishmaniasis. Lancet Infect Dis2003/02/01. 3:87–98.

10.   Sindermann H, Engel J. 2006. Development of miltefosine as an oral treatment for leishmaniasis. Trans R Soc Trop Med Hyg 100 Suppl:S17-20.

11.   WHO Model Lists of Essential Medicines.

12.   Sindermann H, Engel J. 2006. Development of miltefosine as an oral treatment for leishmaniasis. Trans R Soc Trop Med Hyg 100.

13.   Soto J, Soto P. 2006. Miltefosine: Oral treatment of leishmaniasis. Expert Rev Anti Infect Ther 4:177–185.

14.   Croft SL, Engel J. 2006. Miltefosine – discovery of the antileishmanial activity of phospholipid derivatives. Trans R Soc Trop Med Hyg 100:S4–S8.

15.   Dorlo TPC, Balasegaram M, Beijnen JH, de Vries PJ. 2012. Miltefosine: a review of its pharmacology and therapeutic efficacy in the treatment of leishmaniasis. J Antimicrob Chemother 67:2576–2597.

16.   Monge-Maillo B, Norman FF, Cruz I, Alvar J, López-Vélez R. 2014. Visceral Leishmaniasis and HIV Coinfection in the Mediterranean Region. PLoS Negl Trop Dis 8.

17.   Croft SL, Seifert K, Duchêne M. 2003. Antiprotozoal activities of phospholipid analogues. Mol Biochem Parasitol. Mol Biochem Parasitol.

18.   Ménez C, Buyse M, Dugave C, Farinotti R, Barratt G. 2007. Intestinal Absorption of Miltefosine: Contribution of Passive Paracellular Transport. Pharm Res 24:546–554.

19.   Kötting J, Marschner NW, Neumüller W, Unger C, Eibl H. 1992. Hexadecylphosphocholine and octadecyl-methyl-glycero-3-phosphocholine: a comparison of hemolytic activity, serum binding and tissue distribution. Prog Exp tumor Res Fortschritte der Exp Tumorforschung Progrès la Rech expérimentale des tumeurs 34:131–142.

20.   Ménez C, Buyse M, Farinotti R, Barratt G. 2007. Inward Translocation of the Phospholipid Analogue Miltefosine across Caco-2 Cell Membranes Exhibits Characteristics of a Carrier-mediated Process. Lipids 42:229–240.

21.   Baumer W, Wlaz P, Jennings G, Rundfeldt C. 2010. The putative lipid raft modulator miltefosine displays immunomodulatory action in T-cell dependent dermal inflammation models. Eur J Pharmacol 2009/11/18. 628:226–232.

22.   Mukherjee AK, Gupta G, Adhikari A, Majumder S, Kar Mahapatra S, Bhattacharyya Majumdar S, Majumdar S. 2012. Miltefosine triggers a strong proinflammatory cytokine response during visceral leishmaniasis: role of TLR4 and TLR9. Int Immunopharmacol 2012/03/01. 12:565–572.

23.   Palić S, Bhairosing P, Beijnen JH, Dorlo TPC. 2019. Systematic Review of Host-Mediated Activity of Miltefosine in Leishmaniasis through Immunomodulation. Antimicrob Agents Chemother 63.

24.   Ware JM, O'Connell EM, Brown T, Wetzler L, Talaat KR, Nutman TB, Nash TE. 2020. Efficacy and Tolerability of Miltefosine in the Treatment of Cutaneous Leishmaniasis. Clin Infect Dis https://doi.org/10.1093/cid/ciaa1238.

25.   Sundar S, Singh A, Chakravarty J, Rai M. 2015. Efficacy and safety of miltefosine in treatment of post-kala-azar dermal leishmaniasis. Sci World J 2015.

26.   Sundar S, Jha TK, Thakur CP, Engel J, Sindermann H, Fischer C, Junge K, Bryceson A,

Berman J. 2002. Oral Miltefosine for Indian Visceral Leishmaniasis. N Engl J Med 347:1739–1746.

27.   Wasunna M, Njenga S, Balasegaram M, Alexander N, Omollo R, Edwards T, Dorlo TPC, Musa B, Ali MHS, Elamin MY, Kirigi G, Juma R, Kip AE, Schoone GJ, Hailu A, Olobo J, Ellis S, Kimutai R, Wells S, Khalil EAG, Strub Wourgaft N, Alves F, Musa A. 2016. Efficacy and Safety of AmBisome in Combination with Sodium Stibogluconate or Miltefosine and Miltefosine Monotherapy for African Visceral Leishmaniasis: Phase II Randomized Trial. PLoS Negl Trop Dis https://doi.org/10.1371/journal.pntd.0004880.

28.   Rijal S, Ostyn B, Uranw S, Rai K, Bhattarai NR, Dorlo TPC, Beijnen JH, Vanaerschot M, Decuypere S, Dhakal SS, Das ML, Karki P, Singh R, Boelaert M, Dujardin J-C. 2013. Increasing Failure of Miltefosine in the Treatment of Kala-azar in Nepal and the Potential Role of Parasite Drug Resistance, Reinfection, or Noncompliance. Clin Infect Dis 56:1530–1538.

29.   Dorlo TPC, Rijal S, Ostyn B, de Vries PJ, Singh R, Bhattarai N, Uranw S, Dujardin J-C, Boelaert M, Beijnen JH, Huitema ADR. 2014. Failure of Miltefosine in Visceral Leishmaniasis Is Associated With Low Drug Exposure. J Infect Dis 210:146–153.

30.   Dorlo TPC, Huitema ADR, Beijnen JH, de Vries PJ. 2012. Optimal dosing of miltefosine in children and adults with visceral leishmaniasis. Antimicrob Agents Chemother 56:3864–72.

31.   Mbui J, Olobo J, Omollo R, Solomos A, Kip AE, Kirigi G, Sagaki P, Kimutai R, Were L, Omollo T, Egondi TW, Wasunna M, Alvar J, Dorlo TPC, Alves F. 2018. Pharmacokinetics, safety and efficacy of an allometric miltefosine regimen for the treatment of visceral leishmaniasis in Eastern African children: an open-label, phase-II clinical trial. Clin Infect Dis.

32.   Palić S, Kip AE, Beijnen JH, Mbui J, Musa A, Solomos A, Wasunna M, Olobo J, Alves F, Dorlo TPC. 2020. Characterizing the non-linear pharmacokinetics of miltefosine in paediatric visceral leishmaniasis patients from Eastern Africa. J Antimicrob Chemother https://doi.org/10.1093/jac/dkaa314.

33.   Eiras DP, Kirkman LA, Murray HW. 2015. Cutaneous Leishmaniasis: Current Treatment Practices in the USA for Returning Travelers. Curr Treat options Infect Dis 7:52–62.

34.   FDA. Impavido (miltefosine) Capsule, 50 mg.

35.   Ware JM, O'Connell EM, Brown T, Wetzler L, Talaat KR, Nutman TB, Nash TE. 2020. Efficacy and Tolerability of Miltefosine in the Treatment of Cutaneous Leishmaniasis. Clin Infect Dis https://doi.org/10.1093/cid/ciaa1238.

36.   Del Mar Castro M, Gomez MA, Kip AE, Cossio A, Ortiz E, Navas A, Dorlo TPC, Saravia

NG. 2017. Pharmacokinetics of miltefosine in children and adults with Cutaneous leishmaniasis. Antimicrob Agents Chemother 61.

37.   Blum J, Buffet P, Visser L, Harms G, Bailey MS, Caumes E, Clerinx J, van Thiel PPAM, Morizot G, Hatz C, Dorlo TPC, Lockwood DNJ. LeishMan recommendations for treatment of cutaneous and mucosal leishmaniasis in travelers, 2014. J Travel Med 21:116–29.

38.   Pijpers J, Den Boer ML, Essink DR, Ritmeijer K. 2019. The safety and efficacy of miltefosine in the long-term treatment of post-kala-azar dermal leishmaniasis in South Asia – a review and meta-analysis. PLoS Negl Trop Dis 13.

39.   Trial Public: New treatment regimens for treatment of Post Kala Azar Dermal Leishmaniasis patients in India and Bangladesh region Scientific Title of Study An Open label, Randomized, Clinical Trial of Two Regimens to Assess the Safety and Efficacy for Tre.

40.   Mondal D, Hasnain MG, Hossain MS, Ghosh D, Ghosh P, Hossain H, Baker J, Nath R, Haque R, Matlashewski G, Hamano S. 2016. Study on the safety and efficacy of miltefosine for the treatment of children and adolescents with post-kala-azar dermal leishmaniasis in Bangladesh, and an association of serum vitamin E and exposure to arsenic with post-kala-azar dermal leishmaniasis: A. BMJ Open 6.

41.   New treatments for PKDL | DNDi.

42.   Dorlo TPC, Hillebrand MJX, Rosing H, Eggelte TA, de Vries PJ, Beijnen JH. 2008. Development and validation of a quantitative assay for the measurement of miltefosine in human plasma by liquid chromatography–tandem mass spectrometry. J Chromatogr B 865:55–62.

43.   Kip AE, Rosing H, Hillebrand MJX, Castro MM, Gomez MA, Schellens JHM, Beijnen JH, Dorlo TPC. 2015. Quantification of miltefosine in peripheral blood mononuclear cells by high-performance liquid chromatography-tandem mass spectrometry. J Chromatogr B Anal Technol Biomed Life Sci 998–999:57–62.

44.   Kip AE, Kiers KC, Rosing H, Schellens JHM, Beijnen JH, Dorlo TPC. 2017. Volumetric absorptive microsampling (VAMS) as an alternative to conventional dried blood spots in the quantification of miltefosine in dried blood samples. J Pharm Biomed Anal 135:160–166.

45.   Kip AE, Rosing H, Hillebrand MJX, Blesson S, Mengesha B, Diro E, Hailu A, Schellens JHM, Beijnen JH, Dorlo TPC. 2016. Validation and clinical evaluation of a novel method to measure miltefosine in leishmaniasis patients using dried blood spot sample collection. Antimicrob Agents Chemother 60:2081–2089.

46.   Short Course Regimens for Treatment of PKDL (Sudan) - ClinicalTrials.gov.

47.   Dorlo TPC, Kip AE, Younis BM, Ellis SJ, Alves F, Beijnen JH, Njenga S, Kirigi G, Hailu A, Olobo J, Musa AM, Balasegaram M, Wasunna M, Karlsson MO, Khalil EAG. 2017. Visceral leishmaniasis relapse hazard is linked to reduced miltefosine exposure in patients from Eastern Africa: a population pharmacokinetic/pharmacodynamic study. J Antimicrob Chemother 72:3131–3140.

48.   Castro M del M, Gomez MA, Kip AE, Cossio A, Ortiz E, Navas A, Dorlo TPC, Saravia NG. 2017. Pharmacokinetics of Miltefosine in Children and Adults with Cutaneous Leishmaniasis. Antimicrob Agents Chemother 61.

49.   Kip AE, Castro M del M, Gomez MA, Cossio A, Schellens JHM, Beijnen JH, Saravia NG, Dorlo TPC. 2018. Simultaneous population pharmacokinetic modelling of plasma and intracellular PBMC miltefosine concentrations in New World cutaneous leishmaniasis and exploration of exposure–response relationships. J Antimicrob Chemother 73:2104–2111.

50.   Bhandari V, Kulshrestha A, Deep DK, Stark O, Prajapati VK, Ramesh V, Sundar S, Schonian G, Dujardin JC, Salotra P. 2012. Drug susceptibility in Leishmania isolates following Miltefosine treatment in cases of Visceral Leishmaniasis and post Kala-Azar dermal Leishmaniasis. PLoS Negl Trop Dis 6.

51.   Kip AE, Balasegaram M, Beijnen JH, Schellens JHM, De Vries PJ, Dorloa TPC. 2015. Systematic review of biomarkers to monitor therapeutic response in leishmaniasis. Antimicrob Agents Chemother. American Society for Microbiology.

52.   Verrest L, Kip AE, Musa A, Schoone GJ, Schallig HDFH, Mbui J, Khalil EAG, Younis BM, Olobo J, Were L, Kimutai R, Monnerat S, Cruz I, Wasunna M, Alves F, Dorlo TPC. 2021. Blood parasite load as an early marker to predict treatment response in visceral leishmaniasis in Eastern Africa. Clin Infect Dis https://doi.org/10.1093/cid/ciab124.

53.   Schriefer A, Barral A, Carvalho EM, Barral-Netto M. 1995. Serum soluble markers in the evaluation of treatment in human visceral leishmaniasis. Clin Exp Immunol 102:535–40.

54.   Manna L, Reale S, Picillo E, Vitale F, Gravino AE. 2008. Interferon-gamma (INF-gamma), IL4 expression levels and Leishmania DNA load as prognostic markers for monitoring response to treatment of leishmaniotic dogs with miltefosine and allopurinol. Cytokine 2008/10/10. 44:288–292.

55.   Kip AE, Wasunna M, Alves F, Schellens JHM, Beijnen JH, Musa AM, Khalil EAG, Dorlo TPC. 2018. Macrophage activation marker neopterin: A candidate biomarker for treatment

response and relapse in visceral leishmaniasis. Front Cell Infect Microbiol 8.

56.   Casado JL, Abad-Fernández M, Moreno S, Pérez-Elías MJ, Moreno A, Bernardino JI, Vallejo A. 2015. Visceral leishmaniasis as an independent cause of high immune activation, T-cell senescence, and lack of immune recovery in virologically suppressed HIV-1-coinfected patients. HIV Med 16:240–248.

57.   Mbui J, Olobo J, Omollo R, Solomos A, Kip AE, Kirigi G, Sagaki P, Kimutai R, Were L, Omollo T, Egondi TW, Wasunna M, Alvar J, Dorlo TPC, Alves F. 2019. Pharmacokinetics, safety, and efficacy of an allometric miltefosine regimen for the treatment of visceral leishmaniasis in eastern African children: An open-label, phase II clinical trial. Clin Infect Dis 68:1530–1538.

58.   Bhattacharya SK, Sinha PK, Sundar S, Thakur CP, Jha TK, Pandey K, Das VR, Kumar N, Lal C, Verma N, Singh VP, Ranjan A, Verma RB, Anders G, Sindermann H, Ganguly NK. 2007. Phase 4 Trial of Miltefosine for the Treatment of Indian Visceral Leishmaniasis. J Infect Dis 196:591–598.

59.   Ware JM, O'Connell EM, Brown T, Wetzler L, Talaat KR, Nutman TB, Nash TE. 2020. Efficacy and Tolerability of Miltefosine in the Treatment of Cutaneous Leishmaniasis. Clin Infect Dis https://doi.org/10.1093/cid/ciaa1238.

60.   Pagliano P, Ascione T, Di Flumeri G, Boccia G, De Caro F. 2016. Visceral leishmaniasis in immunocompromised: Diagnostic and therapeutic approach and evaluation of the recently released IDSA guidelines. Infez Med 24:265–271.

61.   Goswami RP, Rahman M, Das S, Tripathi SK, Goswami RP. 2020. Combination therapy against Indian visceral leishmaniasis with liposomal amphotericin B (FungisomeTM) and short-course miltefosine in comparison to miltefosine monotherapy. Am J Trop Med Hyg 103:308–314.

62.   van Griensven J, Balasegaram M, Meheus F, Alvar J, Lynen L, Boelaert M. 2010. Combination therapy for visceral leishmaniasis. Lancet Infect Dis. Elsevier.

63.   Rahman R, Goyal V, Haque R, Jamil K, Faiz A, Samad R, Ellis S, Balasegaram M, Boer M den, Rijal S, Strub-Wourgaft N, Alves F, Alvar J, Sharma B. 2017. Safety and efficacy of short course combination regimens with AmBisome, miltefosine and paromomycin for the treatment of visceral leishmaniasis (VL) in Bangladesh. PLoS Negl Trop Dis 11:e0005635.

64.   AfriKADIA Consortium. Available at: https://www.afrikadia.org/.

65.   Drugs for Neglected Diseases initiative. New CL combination therapies. Available at: https://dndi.org/research-development/portfolio/new-cl-combos/

66.   Drugs for Neglected Diseases initiative. 2019 R&D portfolio in review: Leishmaniasis.

Available at: https://dndi.org/news/2020/leishmaniasis-rnd-portfolio-update/

Clinical pharmacokinetics of miltefosine in leishmaniasis

Chapter II

Characterizing the nonlinear pharmacokinetics of miltefosine in paediatric visceral leishmaniasis patients from Eastern Africa

Semra Palić[1], Anke E. Kip[1], Jos H. Beijnen[1], Jane Mbui[2],
Ahmed Musa[3], Alexandra Solomos[4], Monique Wasunna[5],
Joseph Olobo[6], Fabiana Alves[4], Thomas P.C. Dorlo[1]

1. Department of Pharmacy & Pharmacology, The Netherlands Cancer Institute
   - Antoni van Leeuwenhoek Hospital, Amsterdam, The Netherlands
2. Centre for Clinical Research, Kenya Medical Research Institute, Nairobi, Kenya
3. Institute of Endemic Diseases, University of Khartoum, Sudan
4. Drugs for Neglected Diseases initiative, Geneva, Switzerland
5. Drugs for Neglected Diseases initiative, Nairobi, Kenya
6. Department of Immunology and Molecular Biology, College of
   Health Sciences, Makerere University, Kampala, Uganda

Chapter 2.1

Abstract

Background

Conventional miltefosine dosing (2.5 mg/kg/day) for treatment of visceral leishmaniasis (VL) is less effective in children than in adults. A higher allometric dose (median 3.2 mg/kg/day) was, therefore, investigated in paediatric VL patients in Eastern Africa. Results of this trial showed an unforeseen, lower than dose-proportional increase in exposure. Therefore, we performed a pooled model-based analysis of the paediatric data available from both dosing regimens to characterize observed nonlinearities in miltefosine pharmacokinetics (PK).

Methods

Fifty-one children with VL were included in this analysis, treated with either a conventional (n=21) or allometric miltefosine dosing regimen (n=30). PK data were analyzed using nonlinear mixed-effects modelling.

Results

A two-compartment model following first order absorption and linear elimination, with two separate effects on relative oral bioavailability, was found to fit these data best. A 69% lower bioavailability at treatment start was estimated, presumably due to initial malnourishment and malabsorption. Stagnation in miltefosine accumulation in plasma, hampering increased drug exposure, was related to the increase in cumulative dose (mg/kg/day). However, the allometric increased exposure 1.7-fold in the first treatment week, and reduced the time to reach the PK target by 17.4%.

Conclusions

Miltefosine PK in children suffering from VL are characterized by dose-dependent non-linearities that obstruct the initially expected exposure levels. Bioavailability appeared to be affected by the cumulative dose, possibly as a consequence of impaired absorption. Despite this, allometric dosing led to a faster target achievement and increased exposure compared with conventional dosing.

1. Background

Visceral leishmaniasis (VL) or kala-azar is among the most fatal parasitic diseases (1). VL is primarily associated with poverty, and is therefore ranked as one of the most neglected tropical infections (2). Limited treatment options are available for VL, most being hampered by poor or variable efficacy, high toxicity, and parenteral routes of administration (3, 4). Miltefosine is an alkyphosphocholine agent, which was originally assessed for treatment of cutaneous metastases in breast cancer, but has been repurposed for treatment of leishmanial infections (5). Today, miltefosine is the only oral drug available for treatment of VL. Miltefosine pharmacokinetics (PK) is characterized by slow absorption and elimination, leading to long initial (approximately 7 days), as well as terminal (approximately 30 days) half-lives (6, 7). The absorption of miltefosine appears to be concentration dependent with passive paracellular diffusion applicable to the concentration below 20.4 μg/mL. Above this concentration, saturable mechanisms of absorption have been observed in Caco-2 cells (8, 9). The first clinical trials of miltefosine for the treatment of VL were conducted in India, where a 28-day treatment with a linear dose of 2.5 mg/kg/day in both children (age 2-11) and adults (older than 15 years of age) resulted in a cure rate of 90% for children and of 97% for adults (10, 11). In a phase II trial in Sudan and Kenya, a conventional 28-day treatment with miltefosine alone resulted in an overall cure rate of 72% at 6 months follow up (12). Results from this trial indicated decreased efficacy in patients younger than 12 years (59%) in comparison to patients $\geq$ 12 years (86%), with discouraging exposure in children who had a body weight lower than 30 kg, which was reported to be 33% lower than in the adult patient cohort (12). Previously, in patients from Nepal, the exposure – effect relationship was determined for the time above 90% effective concentration (EC$_{90}$), indicating that the time miltefosine concentration is below the EC$_{90}$ was related to the probability of treatment failure, due to recrudescence of *Leishmania* parasites (13). The highest probability of treatment success was for 29.5 days > EC$_{90}$ for miltefosine therapy (14).

With the intention of increasing exposure to miltefosine in the paediatric population, model-based simulations were performed, taking into account the difference in fat-free mass (FFM) between children and adults. Predictions derived from these simulations suggested that administering a relatively higher daily mg/kg (allometric) dose of miltefosine to patients with lower FFM would result in children reaching exposure levels equivalent to those of adult patients (15). Consequently, an open label clinical trial was conducted in Kenya and Uganda

with this new allometric dosing regimen (15). The main goal of this trial was to increase exposure to miltefosine in Eastern African children, ultimately improving treatment outcomes. Efficacy in the thirty children with VL (aged 4-12 years) treated with a 28-day allometric miltefosine regimen was indeed increased to 90% at 6 months follow-up (16). However, the results showed an unexpected less than dose-proportional increase in exposure during treatment (AUC from days 0 to 28 (AUC_{d0-28})). In 40% of the observed PK profiles, accumulation of miltefosine in plasma stagnated in the third week of treatment. We have now performed a pooled model-based analysis of the Eastern African paediatric PK data from both the conventional and allometric dose regimens, with the aim of characterizing and elucidating the nonlinearities in miltefosine pharmacokinetics observed in children treated for VL.

2. Methods

2.1 Patient population

Paediatric patients from two clinical trials were included in the current analysis. Both trials were conducted within the context of the Leishmaniasis East Africa Platform (LEAP), and were registered with ClinicalTrials.gov: numbers NCT01067443, for the conventional regimen, and NCT02431143 for the allometric miltefosine dosing regimen (12). The conventional dosing regimen of miltefosine is based on the linear weight-based dosing regimen (in mg/kg of body weight) derived from adult doses of miltefosine. In this trial, a dosage of 2.5 mg/kg of oral miltefosine was administered daily for a duration of 28 days. In contrast, the allometric dosing regimen was based on the previous simulation study, (15) and applied allometric scaling based on the FFM as the descriptor of body size in children, where the lean body weight is closely approximated using body weight, height, and sex, further allowing a higher mg/kg dose for patients with lower body weight (17). In this trial, daily doses between 2.7 and 3.9 mg/kg of oral miltefosine were administered for 28 days.

2.2 Ethics

For the trial with the conventional dosing regimen, ethical approval was granted by the national and local Ethics Committees in Kenya (Kenya Medical Research Institute) and Sudan (Institute of Endemic Diseases) before the trial began. Ethical approval was also granted by the London School of Hygiene and Tropical Medicine (LSHTM) Ethics Committee. For the trial with the allometric dosing regimen, ethical approvals was granted by Kenya Medical Research

Institute, and the Makerere University, Kampala, Uganda. The parents, or legal guardians were informed of the study in their own language and provided written informed consent before trial enrolment was initiated.

2.3 Plasma sample collection and analysis

In both trials, plasma samples were nominally collected on days 0, 7, 14, 28, 56/60, and 210, while in the allometric trial, an additional sample was taken on day 21 after initiation of treatment. The day 0 samples were drawn before the administration of miltefosine, as well as 4 or 8 h post first dose. Blood samples on other days were drawn prior to dose administration. Samples were stored at maximally -20°C in freezers at the clinical sites, during transport to Amsterdam, and at the bio-analytical laboratory of the Netherlands Cancer Institute until they were analysed. When stored accordingly, miltefosine is stable in human plasma for at least 2410 days. A previously validated method of LC-MS/MS was used for drug quantification with a lower limit of quantification of 4 ng/mL (18). Validation of this assay indicated that miltefosine can be accurately quantified in human plasma with intra- and interassay precisions lower than 10.7% and 10.6%, respectively, and accuracies in the range of 95.1 – 109%, for the lowest concentration level (18).

2.4 Population PK analysis and model development

2.4.1 Software

Prior to PK analysis, the patient data were anonymized. Subsequently, data were analyzed using a population approach by non-linear mixed-effects modeling using the first-order conditional estimation method with interaction (FOCE+I) in NONMEM (version 7.3.0, Globomax, USA)(19) using Pirana as interface (version 2.9.6) (20). R studio (version 3.4.3) was used for the generation of the plots used for model evaluation. All computational analyses were carried out on an internal high-performance computing cluster.

2.4.2 Model Building

Model building was carried out in four consecutive steps according to routine procedures: 1) selection of the structural model, 2) selection of the error model, 3) covariate analysis, and 4) model evaluation and validation. For the structural model, we tested both two and three compartment oral PK models assuming linear kinetics for absorption and elimination.

Additionally, we evaluated several alternative models of absorption, such as combined zero- and first-order rates, as well as saturable absorption models. Inclusion of a lag time to all absorption models was also tested. A standard measure of model fit to the data was provided by the objective function value (OFV), expressed as minus twice the log likelihood of the data. Thus, nested hierarchical models were primarily discriminated based on their OFVs and scientific plausibility, where a decrease of 3.84 points in OFV corresponding to a P value <0.05 was considered significant, with 1 degree of freedom following chi-squared distribution. Additional goodness of fit criteria such as diagnostic plots, visual predictive check (VPC), standard errors of parameter estimates, inspection of the correlation matrix, as well as ε- and η-shrinkage were used in assessing the model performance. Between-subject variability (BSV) or ETAs (η, deviation of an individual parameter from the typical population value) were implemented according to equation (1). Residual unexplained variability (RUV) was explored using additive, proportional, and combined error models.

Residual unexplained variability (RUV) was explored using additive, proportional, and combined error models.

Between-subject variability implementation

$$P_i = P_{pop} \cdot e^{\,\eta_{Pi}} \tag{1}$$

where P_i is the individual parameter estimate for an individual i, and P_{pop} is the population parameter estimate, and where η^i is assumed to be distributed N $(0, \omega^2)$.

2.4.3 Covariate analysis

Covariate modeling was performed to identify covariates that could explain BSV, where covariates were tested univariately based on scientific plausibility. For the covariate model, various factors were considered, such as age, sex, FFM (17), albumin levels, baseline parasite load in blood, individual z-scores for BMI for age, height, weight, concomitant infections, co-medication, as well as dose-derived covariates. Covariates were tested on all PK parameters according to equations 2 and 3. Exploration of potential covariate relationships was conducted by separately visualizing estimated BSV values against covariates. Calculated FFM as a descriptor of body size was included as covariate on clearance (CL/F) and volume of distribution in the central compartment (Vc/F) (21, 22). Furthermore, age, sex, concomitant

infections, comedication, total cumulative dose administered in mg/day (TD), and cumulative daily dose in mg/kg/day (CD) were explored as covariates on CL, volumes of distribution of central and peripheral compartments, absorption rate constant k_a, and relative oral bioavailability (F). In addition, we assessed the effects of child growth and malnutrition on F by evaluating z-scores for body mass index (BMI) for age, weight for age, and height for age in relationship with decreased F in the first treatment week. AnthroPlus software developed by World Health Organization was used to calculate z-scores (23, 24). Continuous covariates were explored by various parametrizations, including both full and piece-wise covariate implementation due to observed time-associated changes in parameters as shown in the equations below. An example equation (2) is shown for the linear model in full covariate implementation, while other functional forms such as exponential and power models were also tested. Moreover, equation (3) is a power model for piece-wise covariate implementation, and in a similar fashion we also tested the piece-wise linear and exponential models.

Full covariate implementation

$$P_{cov} = P_{pop} \cdot (1 + \Theta \cdot (COV - COV_{median}) \cdot e^{\eta Pi})$$ (2)

Piece-wise covariate implementation

$$P_{cov} \begin{cases} P_{pop} \cdot [(COV/COV_{threshold}) \wedge \Theta \cdot e^{\eta Pi}] \text{ when} \geq \text{ threshold} \\ P_{pop} \text{ when } COV < _{threshold} \end{cases}$$ (3)

where P_{cov} is the estimated individual parameter value for subjects who share a common covariate pattern, P_{pop} the estimated population parameter value, and η_{Pi} is the individual subject deviation from the population value for parameter P and individual i, assuming normal distribution around zero for the parameter variance in the population. COV is the tested covariate, while Θ represents the estimated effect of that covariate on P_{pop}. The threshold is any value between the minimum and maximum values of the respected covariate. The piece-wise functions above assume linear relationships between the parameter and covariate until a threshold point is reached, after which a different linear relationship is applied. The final value of the threshold was chosen based on a sensitivity analysis.

2.4.4 Model evaluation

Parameter precision estimates were obtained through a bootstrap analysis with replacement using Perl-speaks-NONMEM (PsN, version 4.7) (25) where 1000 datasets were resampled from the original dataset to refit the model. In addition, VPCs of 1000 simulations using the final population model parameters were evaluated and stratified for each clinical trial.

2.4.5 Assessment of achieved exposure levels

The model developed was used to calculate individual patient estimates of secondary pharmacokinetic parameters, based on the predictions of their individual PK profiles. Various parameters for exposure were compared, as represented by the AUC from day 0 till the end of the first treatment week (day 7; AUC_{d0-7}), as well as until the end of the treatment (day 28; AUC_{d0-28}), and the last day of the follow-period (day 210; AUC_{d0-210}). In addition, the time above the target, and the time to reach the target were calculated, where the target was defined as the EC_{90} equivalent to 10.6 µg/mL. This value was established by *in vitro* experiments investigating intracellular susceptibility of *Leishmania donovani* amastigotes from Eastern Africa to miltefosine (14).

Table 1: Patient demographics and dosing of miltefosine

	Conventional dosing regimen	Allometric dosing regimen
Miltefosine dose (mg/kg/day), median (range)	2.38 (1.25–3.33)	3.2 (2.7–3.9)
Total number of patients	21	30
Kenya	7	21
Sudan	14	—
Uganda	—	9
Sex: female (%)	24%	27%
Age (years), median (range)[a]	10 (7–12)	7 (4–12)
Body weight (kg), median (range)	24 (16–34)	21.8 (13.0–29.50)
Height (m), median (range)	1.35 (1.07–1.53)	1.25 (0.99–1.45)
FFM (kg), median (range)	20.75 (12.84–28.54)	18.16 (10.75–24.25)
BMI (kg/m^2), median (range)	13.77 (12.07–17.04)	13.66 (12.36–15.71)
z-score for BMI for age[b]	−1.87 (−3.76 to 1.01)	−1.64 (−2.93 to 2.58)
z-score for weight for height[b]	−0.95 (−3.08 to −0.36)	−1.00 (−2.23 to 0.76)
z-score for height for age[b]	−0.08 (−2.83 to 1.46)	0.08 (−1.99 to 3.07)

[a] Inclusion criteria for the minimal age differed between the trials: with the conventional dose, the youngest treated child was 7 years, and 4 years with the allometric dose.

[b] z-score for BMI for age was evaluated in children aged between 5 and 12 years. For children younger than 5 years, z-score for weight for height was used. Children younger than 5 years were considered underweight when their z-score was <−2 and overweight when their z-score was >2. Children aged between 5 and 12 years were considered underweight when their z-score was <−2 and overweight when their z-score was >1.
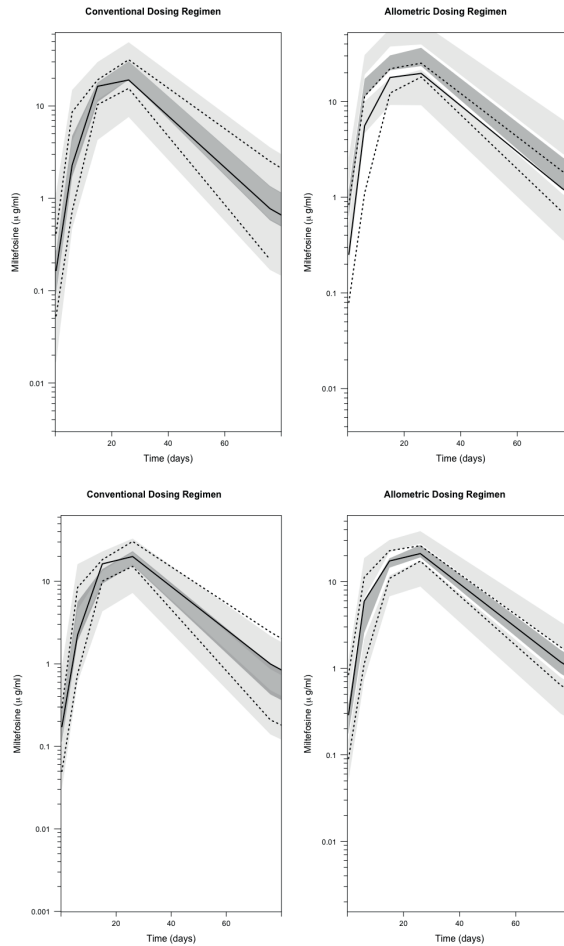
Figure 1: Prediction corrected VPCs based on 1000 simulations for the previously published PK model (14) (upper plots) as well as the newly developed model (lower plots) for the miltefosine PK in the paediatric VL patients from East Africa. The solid lines represent the median concentrations observed in each of the trials, and dark grey shading shows the simulated values. The dotted lines are representative of the 5th and 95th percentiles of the observed data, while light grey shaded areas represent the 95% CI for the simulated data.

3. Results

3.1 Patients

Details of the patient demographics and dosing schedules are given in *Table 1*. Fifty-one patients were included in this population PK analysis, of which 30 were treated with oral miltefosine based on the allometric dosing regimen, and 21 based on the conventional dosing regimen. In total, 343 miltefosine plasma concentrations during and after the treatment period were available and used for building the model. Only two measurements were below the limit of quantification, and were excluded from this analysis.

3.2 Structural PK model

Post-hoc individual predictions for the PK data of patients receiving the allometric regimen, based on the PK model previously developed from the conventional dosing regimen trial data,(14) showed overprediction of miltefosine accumulation in the last week of treatment as illustrated by the upper VPC plots (Figure 1). Therefore, an adjusted PK model was estimated to adequately fit the observed PK profiles of both dosing regimens (Figure 2). A two-compartment model assuming first-order absorption and linear elimination, with two separate non-linearities influencing F (Figure 3), was found to describe these data best. Parameter estimates and respective bootstrap values are given in Table 2. Similar to previous results,(13) a 69% (95% CI 61%–77%) lower F was estimated in the first treatment week (ΔOFV -19.4), presumably due to initial malnourishment and malabsorption. This decrease in F appeared highly variable between patients, and inclusion of BSV in this parameter improved the fit substantially (BSV 86.4%, 95%CI 21%–101%, ΔOFV −223.9). Model-based simulations as indicated in VPC plots (Figure 1, lower plots) showed a satisfactory median prediction, while the variability at the end of the treatment period was slightly overpredicted for the allometric regimen in comparison with the conventional regimen.
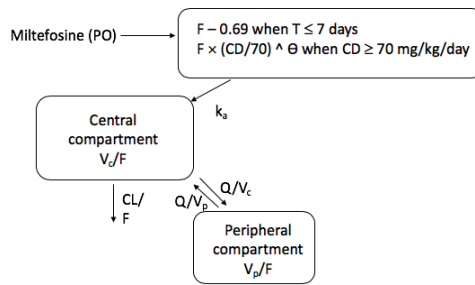
Figure 2: Schematic representation of the developed model for miltefosine PK. Vp, volume of distribution in the peripheral compartment; Q, intercompartmental clearance; T, time, h, estimated effect of CD on F.
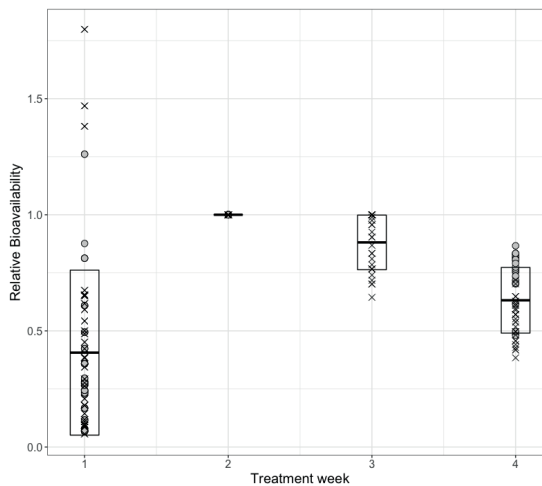

Figure 3: Miltefosine relative oral bioavailability during the course of treatment: two non-linearities described (i) a variable decrease in bioavailability during the first week of treatment (ΔOFV −223.9), most probably due to patient initial malnourishment and malabsorption, and (ii) an effect of the cumulative dose on bioavailability in the later phase of treatment (ΔOFV −22). Circles represent the estimates for individual patients treated with the conventional miltefosine regimen, while the crosses represent the same for patients treated with the allometric regimen. Error bars show the standard error of the mean.

3.3 Covariate assessment

Evaluation of z-scores for BMI, height, weight, concomitant infections, parasite load at baseline, or medication could not explain the variability in miltefosine PK. In addition, a retrospective evaluation of albumin plasma levels in children treated with the allometric dosing regimen indicated that only one patient had increased albumin levels between days 14 and 21 suggesting no possible explanation for the stagnation during this time period in miltefosine accumulation in plasma. Furthermore, TD and CD were examined with respect to exposure differences observed among the two dose regimens. CD implemented as a piece-wise power function (Equation 3) on F was associated with the largest ΔOFV (-11.8), compared with CL (ΔOFV – 4.5), V_c (ΔOFV -3.78) or k_a (ΔOFV -3.24). A threshold value was chosen based on a sensitivity analysis (values ranging from 10 to 110 mg/kg/day, i.e. minimum to maximum CD values throughout the treatment), which indicated that a threshold of 70 mg/kg/day was the most appropriate. Plots of the goodness of fit of the final model are shown in Figure 4. Precision of parameter estimates is given in Table 2.
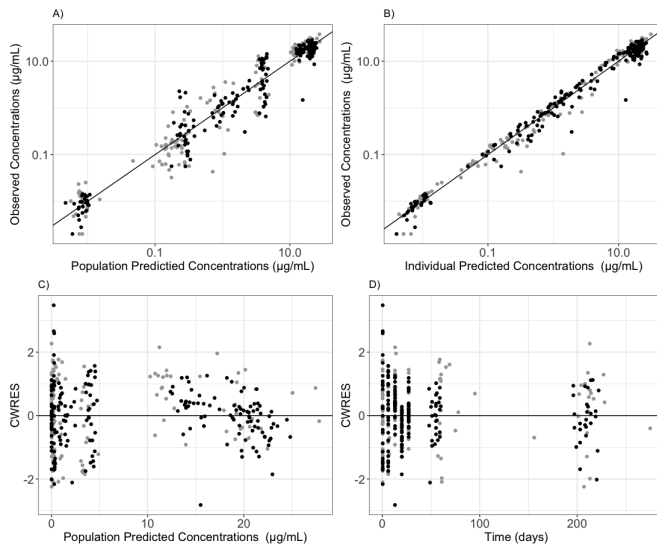

Figure 4: Goodness-of-fit plots for the final PK model depicting both data from the allometric (grey) and conventional dosing (black) regimens. (a) Observed versus population predicted miltefosine concentrations, (b) observed versus individually predicted miltefosine

concentrations, (c) conditional weighted residuals (CWRES) versus population predicted concentrations and (d) CWRES versus time after start of treatment.

Table 2: Parameter estimates and precisions of the final PK model

Parameter (unit)	Estimate [shrinkage %]	Bootstrap estimates [a] median (5%–95% CI)[b]
Fixed effects		
CL/F (L/day)	2.44	2.42 (2.25–2.61)
V_c/F (L)	22.9	22.8 (21.4–24.39)
k_a (day^{-1})	1.61	1.63 (1.07–2.15)
Q/F (L/day)	0.0233	0.023 (0.019–0.027)
V_p/F (L)	2.27	2.26 (2.04–2.49)
F	1 fixed	1 fixed
relative decrease F first week	−0.69	−0.69 (−0.77 to −0.61)
exponent of power relationship between CD and F[c]	−1.72	−1.69 (−2.34 to −1.11)
Between-subject variability		
CL/F (%)	19.5 [28%]	19.3 (11.4–25.1)
decreased F at treatment start (%)	86.4 [2%]	85.3 (21.7–101)
Residual unexplained variability		
proportional error (%)	37 [9%]	36.5 (10.3–40.1)

V_p, volume of distribution in the peripheral compartment; Q, intercompartmental clearance.

[a] Obtained from 665 bootstrap samples.

[b] Non-parametric CI.

[c] Applies after a CD of 70 mg/kg/day is reached, see equation (3).

3.4 PK target attainment

PK parameters reflecting achieved exposure levels at various timepoints during and after treatment were calculated for all patients using the final PK model, and are provided in *Table 3*. The allometric dosing regimen resulted in a 1.7-fold higher exposure in the first treatment week compared with conventional therapy, with a median AUC_{d0-7} of 22 µg*day/mL versus 13 µg*day/mL for patients receiving the allometric and conventional dosing regimens, respectively. The median exposure during the treatment period (AUC_{d0-28}) was 16.4% higher for the allometric dose than for the conventional dosing regimen. The time above EC_{90} ($T > EC_{90}$) was quite similar for both dosing regimens, while the time to reach EC_{90} was 17.4% shorter for the allometric dosing regimen, where some patients had already reached the target on day 3 of treatment, while for the conventional dosing regimen no patient reached the target until day 7 *(Table 3)*. Target achievement within the first treatment days is especially clinically meaningful given that the parasite load is highest in this period of the treatment. Nonetheless, by the end of the third treatment week, with the allometric dosing regimen 99% of the patients reached the target exposure, while 38% of the patients remained below the target with the conventional dosing regimen in the same treatment period.

Table 3: Individual model-based estimates of the miltefosine exposure and target attainment

Exposure parameter (unit)	Conventional dosing regimen		Allometric dosing regimen	
	median	range	median	range
AUC_{d0-7} (µg·day/mL)	13.00	3.07–42.87	22.85	4.14–96.02
AUC_{d0-28} (µg·day/mL)	321.9	261.2–478.0	385.5	271.0–651.7
AUC_{d0-210} (µg·day/mL)	550.5	404.1–891.6	588.6	396.0–875.7
$T > EC_{90}$ (days)	23.4	17–32.3	24.5	17.46–33.3
Time to reach EC_{90} (days)	12.21	6.44–14.15	10.26	2.51–13.41

4. Discussion

This is the first study to compare the conventional and allometric dosing regimen of miltefosine in children suffering from VL, as well as to characterize the observed non-linearities in miltefosine PK following these dosing regimens. The newly developed population PK model for miltefosine was adequate for assessing miltefosine exposure in both the conventional and allometric dosing regimens, and accounts for dose-related effects on the apparent F, previously not observed in the conventional dosing regimen. A faster achievement of the target exposure is clinically important leading to a fewer underexposed individuals, who might be more at risk for eventual treatment failure.

In addition, our model includes two separate non-linearities, accounting for both the effects of malnourishment and increased dose on miltefosine PK. Initial malabsorption by the patients at the start of treatment resulted in a 69.3% decrease in F. Food was added during miltefosine administration in both trials as much as feasible to avoid gastrointestinal side effects, which might have resulted in improved drug absorption. Furthermore, arrest of miltefosine accumulation in the third week of treatment was observed in 40% of the children treated with the allometric dose. Considering the 28% median increase in the dose in the allometric trial, exposure was lower than initially anticipated according to dose proportionality. The median plasma concentration at the end of treatment was 20.9 µg/mL compared with the earlier model-predicted concentration of 29.7 µg/mL. As a result, children who received the allometric dose still had lower exposure compared with that observed in adults after conventional dosing (16). Patient populations in both trials share demographic characteristics and there were no observed differences between sex, or age. Other factors potentially influencing the credibility of the observed miltefosine concentrations could be excluded, since sampling and transport procedures were the same in the two separate trials, as well as procedures regarding sample preparation and quantification of the analyte in the laboratory. Therefore, we evaluated whether z-scores for BMI, height, weight, albumin levels, concomitant infections, or medication during the treatment with miltefosine could have potentially led to the observed halt in miltefosine accumulation in the last weeks of treatment, but no differences were found in the dynamics of these factors between patients receiving either dosing regimen.

Next, we evaluated dosing-related covariates TD and CD on all PK parameters of interest, using various parametrizations. We established that a reduction of miltefosine F is with an

increasing CD above 70 mg/kg/day best explained the arrest in miltefosine accumulation in the third week of treatment in the allometric dosing regimen. A possible explanation for this phenomenon could be the slow and saturable transcellular transport of miltefosine over the gastrointestinal membrane (9). *In vitro* studies have previously suggested the involvement of saturable processes of absorption for miltefosine and the incorporation of miltefosine in the cellular membrane lipid bilayer (8, 9, 26, 27). This is corroborated by the slow oral absorption rates for miltefosine that have been estimated in various population PK studies, including this one (7, 13, 22). Data sparseness in the absorption phase prevented more mechanistic parametrizations of potential distinction between absorption by passive diffusion at low concentrations, and saturable processes after higher concentrations accumulated in plasma, although some attempts were made (see Methods). Nevertheless, the estimated k_a in this study indicated very slow absorption kinetics, which is line with previous studies (7, 14). Extrapolations using this model outside of the observed dosing range should be done with great caution, given the non-mechanistic nature of the relationship between CD and miltefosine bioavailability.

In addition, with the increase in dose in the allometric regimen, safety profiles observed were comparable to those with the conventional regimen. With the allometric regimen, 43% of patients experienced treatment-emerging adverse effects, such as gastrointestinal disorders, commonly related to treatment with miltefosine, also in adults, but none of the patients discontinued treatment due to an adverse effect, (16) which is comparable to the conventional regimen (12).

In conclusion, this study characterized the dose-related non-linearities in miltefosine PK. Adequate early exposure to miltefosine is of critical importance for treatment response, due to the highest parasite load in this period. Regardless of the unforeseen lack of dose proportionality for miltefosine exposure during treatment with the allometric dosing regimen, the nearly doubled miltefosine exposure in the first week which led to fewer underexposed individuals and earlier and higher PK target attainment, potentially resulted in the observed improved treatment efficacy, which increased from 59% for the conventional miltefosine regimen to 90% for the allometric regimen (95% CI: 73–98%). This study, therefore, highlights the importance of adopting an allometric weight-based dosing schedule for miltefosine treatment of VL in peediatric patients.

References

1. Alvar J, Vélez ID, Bern C, Herrero M, Desjeux P, Cano J, Jannin J, de Boer M. 2012. Leishmaniasis worldwide and global estimates of its incidence. PLoS One.

2. Boelaert M, Meheus F, Sanchez A, Singh SP, Vanlerberghe V, Picado A, Meessen B, Sundar S. 2009. The poorest of the poor: a poverty appraisal of households affected by visceral leishmaniasis in Bihar, India. Trop Med Int Heal 14:639–644.

3. Kedzierski L, Sakthianandeswaren A, Curtis JM, Andrews PC, Junk PC, Kedzierska K. 2009. Leishmaniasis: Current treatment and prospects for new drugs and vaccines. Curr Med Chem 16:599–614.

4. Chappuis F, Sundar S, Hailu A, Ghalib H, Rijal S, Peeling RW, Alvar J, Boelaert M. 2007. Visceral leishmaniasis: what are the needs for diagnosis, treatment and control? Nat Rev Microbiol 5:S7–S16.

5. Dorlo TPC, Balasegaram M, Beijnen JH, de Vries PJ. 2012. Miltefosine: a review of its pharmacology and therapeutic efficacy in the treatment of leishmaniasis. J Antimicrob Chemother 67:2576–2597.

6. Bianciardi P, Brovida C, Valente M, Aresu L, Cavicchioli L, Vischer C, Giroud L, Castagnaro M. 2009. Administration of Miltefosine and Meglumine Antimoniate in Healthy Dogs: Clinicopathological Evaluation of the Impact on the Kidneys. Toxicol Pathol 37:770–775.

7. Dorlo TPC, van Thiel PPAM, Huitema ADR, Keizer RJ, de Vries HJC, Beijnen JH, de Vries PJ. 2008. Pharmacokinetics of Miltefosine in Old World Cutaneous Leishmaniasis Patients. Antimicrob Agents Chemother 52:2855–2860.

8. Ménez C, Buyse M, Dugave C, Farinotti R, Barratt G. 2007. Intestinal Absorption of Miltefosine: Contribution of Passive Paracellular Transport. Pharm Res 24:546–554.

9. Ménez C, Buyse M, Farinotti R, Barratt G. 2007. Inward Translocation of the Phospholipid Analogue Miltefosine across Caco-2 Cell Membranes Exhibits Characteristics of a Carrier-mediated Process. Lipids 42:229–240.

10. Sundar S, Jha T, Sindermann H et al. 2003. Oral miltefosine treatment in children with mild to moderate Indian visceral leishmaniasis. Pediatr Infect Dis J 22:434–438.

11. Sundar S, Jha TK, Thakur CP, Engel J, Sindermann H, Fischer C, Junge K, Bryceson A, Berman J. 2002. Oral Miltefosine for Indian Visceral Leishmaniasis. N Engl J Med 347:1739–1746.

12. Wasunna M, Njenga S, Balasegaram M, Alexander N, Omollo R, Edwards T, Dorlo TPC,

Musa B, Ali MHS, Elamin MY, Kirigi G, Juma R, Kip AE, Schoone GJ, Hailu A, Olobo J, Ellis S, Kimutai R, Wells S, Khalil EAG, Strub Wourgaft N, Alves F, Musa A. 2016. Efficacy and Safety of AmBisome in Combination with Sodium Stibogluconate or Miltefosine and Miltefosine Monotherapy for African Visceral Leishmaniasis: Phase II Randomized Trial. PLoS Negl Trop Dis.

13. Dorlo TPC, Rijal S, Ostyn B, de Vries PJ, Singh R, Bhattarai N, Uranw S, Dujardin J-C, Boelaert M, Beijnen JH, Huitema ADR. 2014. Failure of Miltefosine in Visceral Leishmaniasis Is Associated With Low Drug Exposure. J Infect Dis 210:146–153.

14. Dorlo TPC, Kip AE, Younis BM, Ellis SJ, Alves F, Beijnen JH, Njenga S, Kirigi G, Hailu A, Olobo J, Musa AM, Balasegaram M, Wasunna M, Karlsson MO, Khalil EAG. 2017. Visceral leishmaniasis relapse hazard is linked to reduced miltefosine exposure in patients from Eastern Africa: a population pharmacokinetic/pharmacodynamic study. J Antimicrob Chemother 72:3131–3140.

15. Dorlo TPC, Huitema ADR, Beijnen JH, de Vries PJ. 2012. Optimal dosing of miltefosine in children and adults with visceral leishmaniasis. Antimicrob Agents Chemother 56:3864–72.

16. Mbui J, Olobo J, Omollo R, Solomos A, Kip AE, Kirigi G, Sagaki P, Kimutai R, Were L, Omollo T, Egondi TW, Wasunna M, Alvar J, Dorlo TPC, Alves F. 2018. Pharmacokinetics, safety and efficacy of an allometric miltefosine regimen for the treatment of visceral leishmaniasis in Eastern African children: an open-label, phase-II clinical trial. Clin Infect Dis.

17. Al-Sallami HS, Goulding A, Grant A, Taylor R, Holford N, Duffull SB. 2015. Prediction of Fat-Free Mass in Children. Clin Pharmacokinet 54:1169–1178.

18. Dorlo TPC, Hillebrand MJX, Rosing H, Eggelte TA, de Vries PJ, Beijnen JH. 2008. Development and validation of a quantitative assay for the measurement of miltefosine in human plasma by liquid chromatography–tandem mass spectrometry. J Chromatogr B 865:55–62.

19. Keizer RJ, Karlsson MO, Hooker A. 2013. Modeling and Simulation Workbench for NONMEM: Tutorial on Pirana, PsN, and Xpose. CPT Pharmacometrics Syst Pharmacol 2:e50.

20. Keizer RJ, van Benten M, Beijnen JH, Schellens JHM, Huitema ADR. 2011. Piraña and PCluster: A modeling environment and cluster infrastructure for NONMEM. Comput

Methods Programs Biomed 101:72–79.

21. Janmahasatian S, Duffull SB, Ash S, Ward LC, Byrne NM, Green B. 2005. Quantification of Lean Bodyweight. Clin Pharmacokinet 44:1051–1065.

22. Kip AE, Castro M del M, Gomez MA, Cossio A, Schellens JHM, Beijnen JH, Saravia NG, Dorlo TPC. 2018. Simultaneous population pharmacokinetic modelling of plasma and intracellular PBMC miltefosine concentrations in New World cutaneous leishmaniasis and exploration of exposure–response relationships. J Antimicrob Chemother 73:2104–2111.

23. WHO. 2018. Application tools: AnthroPlus software. WHO. World Health Organization.

24. WHO. 2018. Global Database on Child Growth and Malnutrition. WHO. World Health Organization.

25. Lindbom L, Ribbing J, Jonsson EN. 2004. Perl-speaks-NONMEM (PsN)—a Perl module for NONMEM related programming. Comput Methods Programs Biomed 75:85–94.

26. Malta de Sá M, Sresht V, Rangel-Yagui CO, Blankschtein D. 2015. Understanding Miltefosine–Membrane Interactions Using Molecular Dynamics Simulations. Langmuir 31:4503–4512.

27. Barratt G, Saint-Pierre-Chazalet M, Loiseau PM. 2009. Cellular transport and lipid interactions of miltefosine. Curr Drug Metab 10:247–55.

Population pharmacokinetics of a short course allometric miltefosine regimen to treat post kala-azar dermal leishmaniasis in South Asia

Semra Palić[1], Dinesh Mondal[2], Pradeep Das[3], Krishna Pandey[3], Sheeraz Raja[4], Suman Rijal[4], Jos H. Beijnen[1], Shyam Sundar[5], Fabiana Alves[6], Thomas P. C. Dorlo[1]

1. Department of Pharmacy & Pharmacology, The Netherlands Cancer Institute
   - Antoni van Leeuwenhoek Hospital, Amsterdam, The Netherlands
2. International Centre for Diarrhoeal Disease Research, Bangladesh (icddr,b), Dhaka, Bangladesh
3. Rajendra Memorial Research Institute for Medical Sciences, Patna, India
4. Drugs for Neglected Diseases Initiative South Asia, New Delhi, India
5. Department of Medicine, Institute of Medical Sciences, Banaras Hindu University, Varanasi, India
6. Drugs for Neglected Diseases initiative, Geneva, Switzerland

Interim analysis

Abstract

Background

Post-kala-azar dermal leishmaniasis (PKDL) is a dermatological complication of visceral leishmaniasis (VL) treatment, developing months or years after treatment completion. Short courses of miltefosine in combination with other drugs are currently under investigation. This study aims to describe miltefosine pharmacokinetics (PK) following a short course allometric dosing regimen of 3 weeks in PKDL patients.

Methods

Fifteen PKDL patients from Bangladesh and forty-eight from India (age 10 to 59) were treated with oral miltefosine following an allometric weight-based dosing regimen for a duration of 21 days. Plasma samples were collected during the treatment on days 7, 14, 21, 29 and at three months after the treatment end, and were analyzed by liquid chromatography coupled to tandem mass spectrometry. Data were analyzed with a non-linear mixed-effects approach using the first-order conditional estimation method with interaction (FOCE+I) in NONMEM.

Results

In total, 273 miltefosine plasma concentrations were available for model building. A two-compartment model following first-order absorption and elimination fitted the data best. A 32% decrease in apparent oral bioavailability was estimated (95% CI 5-55%; between-subject variability 18%,) in the second and third treatment week to account for stagnating plasma accumulation of the drug, which appeared not directly related to observed gastrointestinal adverse events. The developed model was used to calculate the area under the concentration-time curve until day 21 AUC_{d0-21}) which was on median 525 (range 100 − 713) µg·day/mL.

Conclusion

This study characterized PK following a short course allometric miltefosine regimen in the treatment of PKDL in India and Bangladesh, indicating a decreased bioavailability in the last 2 weeks of treatment.

1. Introduction

Post-kala-azar dermal leishmaniasis (PKDL) is a dermatological complication of kala-azar or visceral leishmaniasis (VL) treatment, that develops months or years after treatment end. While VL is a disease affecting the internal organs, PKDL is manifested by macular, maculopapular or nodular lesions on the skin of patients who otherwise recovered from VL (1, 2). Incidence rates and onset of PKDL appear different among countries baring with this public health problem. For instance, up to 20% of Indian and Bangladeshi patients treated for VL develop PKDL within 1 to 5 years post VL treatment (3, 4). These patients often present chronicity, which may vary over time, but due to contributing to transmission of parasite which causes fatal VL, it has been reported that VL appears to re-occur between 10 and 15 years (5). At the moment, optimal treatment regimens for PKDL are still missing. Previously intravenous amphotericin B (AmBisome) was used in the treatment of PKDL in India but required 60 infusions, and careful clinical and biochemical monitoring which is clinically impractical (6). There is an urgent need for shortened, preferably oral, treatment regimens for PKDL.

Up to now, miltefosine is the only oral drug available for the treatment of leishmaniasis. Various miltefosine regimens have been evaluated for PKDL, resulting in a recommended 12-week monotherapy regimen which is currently part of the guidelines. It has been hypothesized that a shortened regimen of miltefosine plus AmBisome could have sufficient treatment efficacy in PKDL, as well as reduce treatment duration, costs and need for hospitalization. Miltefosine pharmacokinetics (PK) were described in the treatment of VL and cutaneous leishmaniasis (CL), where miltefosine exhibited high efficacy rates (7–10). However, studies on miltefosine PK in the context of PKDL were only recently initiated (11, 12). With respect to PK, it is well known that miltefosine is characterized by a slow absorption and elimination, with a primary half-life reported between 6-7 days. Various population-specific non-linearities in the PK of miltefosine related to its bioavailability have been described (9, 10), which appeared only present in VL patients from Eastern Africa. Little is known about the PK of miltefosine in PKDL patients. In this light, this study aimed to assess miltefosine PK in PKDL patients treated with a shortened allometric weight-based miltefosine dosing regimen of 21 days in combination with AmBisome.

2. Methods

2.1 Clinical trial and patients

A non-comparative, open label, randomized phase II trial was conducted to assess the safety and efficacy of AmBisome and Impavido (miltefosine) in PKDL treatment in patients from Bangladesh region (study site of the International Centre for Diarrhoeal Disease Research) and India (study sites of Rajendra Memorial Research Institute of Medical Sciences (ICMR Institute) at Patna, Bihar and Kala Azar Medical Research Centre, Muzzafarpur). This study is registered with the clinical trial registry in India under the reference "CTRI/2017/04/008421". Oral miltefosine (Impavido, Paladin Labs, Montréal, Canada) was administered twice daily following a previously suggested allometric weight-based dosing regimen (9, 13), for a duration of 21 days. Eligible patients had to have confirmed PKDL by clinical presentation and demonstration of parasites following either methods of microscopy or qPCR on skin smear/skin slit. Patients with stable or progressive disease lasting longer than 4 months were also included. Inclusion criteria allowed patients' between 6 to 60 years of age, while written informed consent from patients, or patient's parent or guardian for children younger than 18 years were required before the treatment initiation. In addition, patients with a previous PKDL treatment in the last two years were excluded from the study. Additionally, the study excluded pregnant and lactating women, patients with contaminant infection such as tuberculosis or HIV, and severe underlying disease such as cardiac, renal or hepatic diseases. At last, severely malnourished patients were also excluded, where malnourishment was assessed by the body mass index (BMI) for age according to the World Health Organization (WHO) reference curves for sex, Z score < -3 for subjects 6 - 19 years; BMI < 16 for subjects > 19-years old.

2.2. Pharmacokinetic sample collection and bioanalysis

Miltefosine plasma samples were collected on day 7, day 14, day 21, and day 29 after treatment onset correspondent to scheduled study visits on days 8, 15, 22, 30, as well as at three months after the treatment start. Miltefosine was quantified in plasma by liquid chromatography coupled to tandem mass spectrometry (LC-MS/MS) with a limit of detection of 2.0 ng/mL. Samples were stored and transported frozen at minimally -20 ˚C and eventually measured at the bioanalytical laboratory of Lambda Therapeutic Research, in Ahmedabad, India.

2.3 Population PK model development

2.3.1 Software

Data were analyzed following a population pharmacokinetic approach using nonlinear mixed-effects modeling. NONMEM (version 7.4, ICON Development Solutions, USA) was used for nonlinear mixed-effects modelling, using the first-order conditional estimation method with interaction (FOCE+I). Model deployment was automated by Perl-speaks-NONMEM (PsN version 4.7.0), with Pirana (version 2.9.9) used as graphical interface. R and R Studio (versions 3.6.3 and 3.4.3) were employed for data management and visualization. All computational analyses were carried out on a high-performance computing cluster of the NKI-AvL.

2.3.2 Model building

Model building was carried out in four consecutive steps: 1) selection of the structural model; 2) selection of the error model; 3) covariate analysis; and 4) model evaluation and validation. For a structural model one and two-compartment models with first-order absorption and elimination from the central compartment were considered. Between subject variability (BSV) was tested on all PK parameters (equation 1). Furthermore, due to observed variability and time-related differences encountered in the PK profiles, between occasion variability (BOV) was evaluated and characterized for bioavailability (F) (equation 1).

$$P_i = P_{pop} \cdot \exp(\eta_i, BSV + \eta_i, BOV) \qquad\qquad\qquad Eq.(1)$$

Where, P_i is the individual parameter estimate for an individual i, P_{pop} is the typical population parameter estimate. η_i is either BSV or BOV effect for subject individual i where η_i assumes normal distribution following N (0, σ^2). Occasions were defined as each individual treatment week in which plasma samples were obtained.

Next, to describe residual unexplained variability (RUV), a proportional error model and a combination of proportional and additive error models were considered (equation 2).

$$C_{obs,ij} = C_{pred,ij} \cdot (1 + \varepsilon1_{p,ij}) + \varepsilon2_{p,ij} \qquad\qquad\qquad Eq. (2)$$

Where $C_{obs,ij}$ represents the observed concentration for an individual *i* and observation *j*, and respectively $C_{pred,ij}$ represents the individual predicted concentration, while $\varepsilon1_{p,ij}$ represents

the proportional error, and $\varepsilon2_{p,ij}$ the additive error, assuming normal distribution following N $(0, \sigma^2)$.

Additionally, a systematic covariate analysis was performed for the estimated PK parameters. Guided by prior knowledge of fat-free mass (FFM) as a body size descriptor of miltefosine PK in children, calculated FFM was included as covariate on clearance (CL/F) and volume of distribution in the central compartment (V_c/F) (9, 14). Other available covariates including age, sex, and gastrointestinal (GI) adverse events (AE) were tested for statistical significance, where significance of a covariate effect was assessed in comparison of hierarchical models as stated in the following section. Potential covariate relationships were assessed by visualizing empirical Bayes estimates of η values against covariate values. Given the common functional forms of covariate relationships, covariates were tested by linear, power and exponential equations.

2.3.3 Model evaluation

Model evaluation was performed by considering parameter precision, objection function value (OFV), goodness of fit (GOF) plots, prediction corrected visual predictive checks (pcVPC), and inspection of the correlation matrix. A decrease in OFV where a significant improvement was determined by drop of ≥ 6.63 points, corresponding to a $P < 0.01$ (χ^2-distribution with 1 degree of freedom) was used to discriminate hierarchical models. Both GOF and pcVPC were evaluated for their adequacy to fit the observed data. Parameter precision was assessed by standard errors, inspection of the correlation matrix, as well as ε- and η-shrinkage. Lastly, the final parameter precision was obtained using Sampling Importance Resampling (SIR) (15).

3. Results

3.1. Patients

The present study included 15 PKDL patients from Bangladesh and 48 from India, aged between 10 to 59 years. Patient demographics are summarized in table 1. In total 273 miltefosine plasma concentrations were available for the population PK analysis. No measurements were below the limit of quantification.

Table 1: Study population demographics

Parameter	Total	Bangladesh	India
Number of patients (number of females)	63 (34)	15 (10)	48 (24)
Age (years)*	22 (10 – 49)	27 (10 – 49)	21 (10 – 49)
Body weight (kg)*	45 (25 – 75)	44 (33-75)	46 (26 -65)
Height (cm)*	155 (122 – 180)	160 (150 – 180)	153 (122 – 171)

* Values represent median (range)

3.2 Population PK model

A structural two-compartment model with first order absorption and elimination was found to fit the observed data best. Observed data is illustrated in *figure 1.* Estimates of the PK parameters and parameter precisions are provided in *table 2*. Due to lack of data in the absorption phase, the absorption rate constant was fixed to a previous model-based estimate. BSV could only be estimated for CL/F and F in the second and third treatment week. The GOF plots of the two-compartmental model suggested a misspecification due to a stagnation in accumulation of miltefosine in the last two weeks of treatment. BOV was used to evaluate and characterize this observation and indicated a lowered F in week two and three of treatment. Fixing F to 1 in the first week of treatment, resulted in an estimated relative F of 0.68 (95% CI 0.45 – 0.95) in week two and three of treatment that was variable between patients in the second and third treatment week (BSV 18.7%, ΔOFV -11), which explained most of the BOV encountered which was therefore excluded in the final model. Furthermore, BOV on CL/F and V_c/F was tested, and could be estimated, however BOV on F resulted with the best GOF fit. FFM was included *a priori* as covariate on CL/F and V_c/F. Other covariates such as GI AEs did not show an effect on miltefosine PK, as illustrated in *figure 2.* GI AEs are commonly expected for miltefosine in the first treatment week, however frequency of GI AEs documented in this study occurred at random treatment days, from the start till the end. In exception, one patient had severe vomiting which resulted with 30% reduction in total treatment exposure. A proportional error model was found appropriate to quantify RUV.

A further evaluation of the model as indicated by the GOF plots *(figure 3)*, and model-based simulations as by pcVPC *(figure 4)* showed adequate model fit to data. The developed model

was used to calculate treatment exposure until the day 21 as given by area under the plasma concentration over time curve from day 0 to day 21 (AUC_{d0-21}). Resulting AUC_{d0-21} was on median 525 µg·day/mL, and ranged between $100 - 713$ µg·day/mL among patients.

Table 2: Pharmacokinetic parameter estimates and parameter precision

Parameter (unit)	Estimate	95 % CI[B]
Fixed Effects		
Apparent clearance **CL/F** (L/day)[A]	2.1	1.6 - 2.6
Apparent volume of the central compartment **V$_c$/F** (L)[A]	19	$17.4 - 20.6$
Absorption rate constant **k$_a$** (/day)	1.61 fixed [A]	-
Apparent intercompartmental clearance **Q/F** (L/day)[A]	0.039	0.0035 -0.18
Apparent volume of the peripheral compartment **V$_p$/F** (L)[A]	2.33	$0.8 - 3.15$
Apparent Bioavailability **F week 1 of treatment**	1 fixed	-
F week 2 & 3 of treatment	0.68	$0.45 - 0.95$
Between-subject variability (%)		
CL/F	17.1	$7.6 - 36.3$
F	18.7	$4.4 - 46.9$
Residual Unexplained Variability (%)		
Proportional error	27.2	$21.2 - 38$

[A] Estimated for a fat-free mass of 50 kg

[B] Obtained by sampling importance resampling

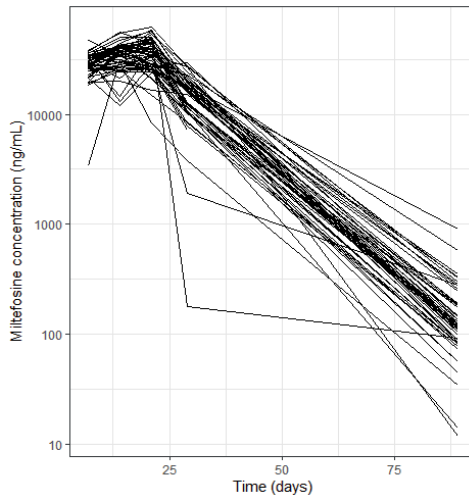[C] Fixed based on the previous estimate following allometric weight-based dosing regimen

Figure 1: Observed pharmacokinetic (PK) profiles of miltefosine following 21-day treatment with the allometric dosing regimen. Each line represents an individual patient PK profile.
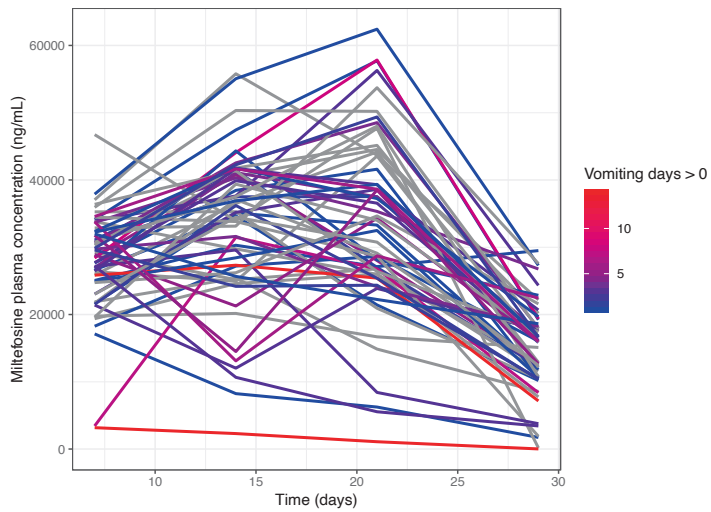

Figure 2: Effect of the gastrointestinal (GI) adverse events (AE) on miltefosine concentration over time profiles stratified for the number of vomiting days.
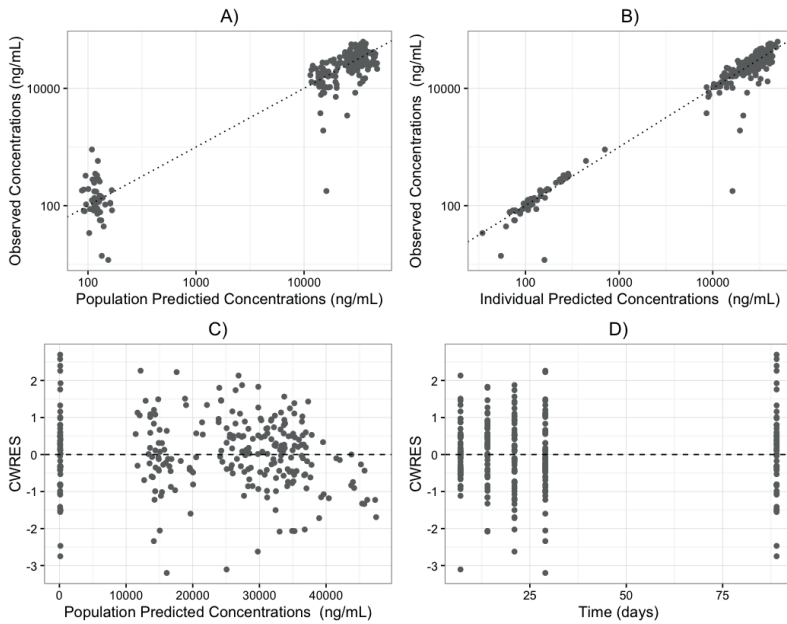
Figure 3: Goodness-of-fit plots for the final PK model. A) Observed versus population predicted miltefosine plasma concentrations, B) observed versus individually predicted miltefosine plasma concentrations, C) conditional weighted residuals (CWRES) versus population predicted concentrations and D) CWRES versus time after start of treatment.
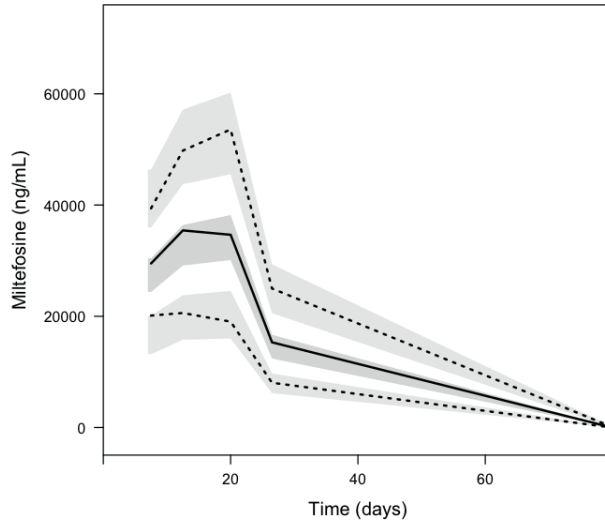
Figure 4: Prediction corrected VPCs based on 1000 simulations for the developed population PK. The solid lines represent the median concentrations observed, and dark grey shading shows the simulated prediction interval. The dotted lines represent the 5th and 95th percentiles of the observed data, while light grey shaded areas represent the 95% prediction interval for the simulated 5th and 95th percentiles.

4. Discussion

This study is the first to characterize PK of miltefosine following a short course (21 days) allometric miltefosine regimen in PKDL patients. The present clinical study is currently still ongoing and evaluates safety and efficacy of AmBisome monotherapy versus a short course regimen of miltefosine in combination with AmBisome in the treatment of PKDL. With respect to miltefosine PK, as per our previous studies, a two-compartment model following first order absorption and elimination was used as a base for the structural model (9, 16). Concentrations of miltefosine in plasma following allometric dosing regimen accumulated faster in these PKDL patients, when compared to VL patients from Eastern Africa treated with a similar allometric dose miltefosine dose regimen for 28 days. Median concentration of miltefosine at day 7 in PKDL patients was 28.9 µg/mL (range 3.4 and 46.7 µg/mL), while day 7 concentration in VL patients treated with the allometric dose were on median 5.9 µg/mL and ranged between 2.5

and 12.4 µg/mL (9). Previously we found a reduction in miltefosine bioavailability in the first treatment week, probably due to patient malnourishment and malabsorption related to this particular Eastern African VL population, while such reduction in bioavailability was not observed in the current PKDL patients, or Indian VL patients (9, 17). In addition, previously we reported arrest in accumulation of miltefosine concentrations in the third or fourth week of treatment in VL patients following this dosing schedule, and related these nonlinearities to saturable absorption of miltefosine. We observed similar nonlinearities in the current patient cohort. Documented patient adherence to medication could not explain these observations, even when accounting for the reported missed doses in the dose input of the model. In this light, we additionally tested the effect of GI-related adverse events such as vomiting, but these could only explain strong deviations in the PK profile for one patient, who had continuous vomiting for the duration of one week. No other physiological explanation could be found for these observations.

A total drug exposure during the 21-day treatment period (AUC_{d1-22}) in this PKDL patient cohort was on median 525 µg·day/mL which is more than dose-proportional to a previously observed 28-day regimen AUC's during treatment (AUC_{d0-28}) in Bangladeshi PKDL children and adolescents treated with an allometric 28-day regimen (AUC_{d0-28} 571 µg·day/mL), but dose-proportional to Indian VL patients treated with a conventional 100 mg/day 28-day regimen (AUC_{d0-28} 654 µg·day/mL) (18). No profound differences in exposure were found between children and adults, nor between the treatment sites. Additional studies are required to establish a relationship between miltefosine plasma PK and target site exposure in the skin, as well as its activity in combination with AmBisome, in order to develop more evidence-based treatment regimens for PKDL.

References

1. Ramesh V, Katara GK, Verma S, Salotra P. 2011. Miltefosine as an effective choice in the treatment of post-kala-azar dermal leishmaniasis. Br J Dermatol 165:411–414.

2. Mondal D, Khan MGM. 2011. Recent advances in post-kala-azar dermal leishmaniasis. Curr Opin Infect Dis 24:418–422.

3. Zijlstra EE, Alves F, Rijal S, Arana B, Alvar J. 2017. Post-kala-azar dermal leishmaniasis in the Indian subcontinent: A threat to the South-East Asia Region Kala-azar Elimination Programme. PLoS Negl Trop Dis. Public Library of Science.

4. Singh RP, Picado A, Alam S, Hasker E, Singh SP, Ostyn B, Chappuis F, Sundar S, Boelaert M. 2012. Post-kala-azar dermal leishmaniasis in visceral leishmaniasis-endemic communities in Bihar, India. Trop Med Int Heal 17:1345–1348.

5. Desjeux P, Ghosh RS, Dhalaria P, Strub-Wourgaft N, Zijlstra EE. 2013. Report of the post Kala-Azar dermal leishmaniasis (PKDL) consortium meeting, New Delhi, India, 27-29 June 2012. Parasites and Vectors 6.

6. Goyal V, Nand V, Das R, Singh SN, Singh RS, Pandey K, Verma N, Hightower A, Rijal S, Das P, Alvar J, Bern C, Alves Id F. 2020. Long-term incidence of relapse and post-kala-azar dermal leishmaniasis after three different visceral leishmaniasis treatment regimens in Bihar, India https://doi.org/10.1371/journal.pntd.0008429.

7. Castro M del M, Gomez MA, Kip AE, Cossio A, Ortiz E, Navas A, Dorlo TPC, Saravia NG. 2017. Pharmacokinetics of Miltefosine in Children and Adults with Cutaneous Leishmaniasis. Antimicrob Agents Chemother 61.

8. Dorlo TPC, van Thiel PPAM, Huitema ADR, Keizer RJ, de Vries HJC, Beijnen JH, de Vries PJ. 2008. Pharmacokinetics of Miltefosine in Old World Cutaneous Leishmaniasis Patients. Antimicrob Agents Chemother 52:2855–2860.

9. Palić S, Kip AE, Beijnen JH, Mbui J, Musa A, Solomos A, Wasunna M, Olobo J, Alves F, Dorlo TPC. 2020. Characterizing the non-linear pharmacokinetics of miltefosine in paediatric visceral leishmaniasis patients from Eastern Africa. J Antimicrob Chemother https://doi.org/10.1093/jac/dkaa314.

10. Dorlo TPC, Kip AE, Younis BM, Ellis SJ, Alves F, Beijnen JH, Njenga S, Kirigi G, Hailu A, Olobo J, Musa AM, Balasegaram M, Wasunna M, Karlsson MO, Khalil EAG. 2017. Visceral leishmaniasis relapse hazard is linked to reduced miltefosine exposure in patients from Eastern Africa: a population pharmacokinetic/pharmacodynamic study. J

Antimicrob Chemother 72:3131–3140.

11. Mondal D, Hasnain MG, Hossain MS, Ghosh D, Ghosh P, Hossain H, Baker J, Nath R, Haque R, Matlashewski G, Hamano S. 2016. Study on the safety and efficacy of miltefosine for the treatment of children and adolescents with post-kala-azar dermal leishmaniasis in Bangladesh, and an association of serum vitamin E and exposure to arsenic with post-kala-azar dermal leishmaniasis: A. BMJ Open 6.

12. Sundar S, Sinha P, Jha TK, Chakravarty J, Rai M, Kumar N, Pandey K, Narain MK, Verma N, Das VNR, Das P, Berman J, Arana B. 2013. Oral miltefosine for Indian post-kala-azar dermal leishmaniasis: a randomised trial. Trop Med Int Heal 18:96–100.

13. Mbui J, Olobo J, Omollo R, Solomos A, Kip AE, Kirigi G, Sagaki P, Kimutai R, Were L, Omollo T, Egondi TW, Wasunna M, Alvar J, Dorlo TPC, Alves F. 2018. Pharmacokinetics, safety and efficacy of an allometric miltefosine regimen for the treatment of visceral leishmaniasis in Eastern African children: an open-label, phase-II clinical trial. Clin Infect Dis.

14. Janmahasatian S, Duffull SB, Ash S, Ward LC, Byrne NM, Green B. 2005. Quantification of Lean Bodyweight. Clin Pharmacokinet 44:1051–1065.

15. Dosne AG, Bergstrand M, Karlsson MO. 2017. An automated sampling importance resampling procedure for estimating parameter uncertainty. J Pharmacokinet Pharmacodyn 44:509–520.

16. Ostyn B, Hasker E, Dorlo TPC, Rijal S, Sundar S, Dujardin J-C, Boelaert M. 2014. Failure of miltefosine treatment for visceral leishmaniasis in children and men in South-East Asia. PLoS One 9:e100220.

17. Dorlo TPC, Rijal S, Ostyn B, de Vries PJ, Singh R, Bhattarai N, Uranw S, Dujardin J-C, Boelaert M, Beijnen JH, Huitema ADR. 2014. Failure of Miltefosine in Visceral Leishmaniasis Is Associated With Low Drug Exposure. J Infect Dis 210:146–153.

18. Dorlo TPC, Huitema ADR, Beijnen JH, de Vries PJ. 2012. Optimal dosing of miltefosine in children and adults with visceral leishmaniasis. Antimicrob Agents Chemother 56:3864–72.

Clinical pharmacodynamics of immune responses following treatment with miltefosine

Systematic Review of Host-Mediated Activity of Miltefosine in Leishmaniasis through Immunomodulation

Semra Palić[1], Patrick Bhairosing[2],
Jos H. Beijnen[1], Thomas P.C. Dorlo[1]

1. Department of Pharmacy & Pharmacology, The Netherlands Cancer Institute
   - Antoni van Leeuwenhoek Hospital, Amsterdam, The Netherlands
2. Scientific Information Service, The Netherlands Cancer Institute, Amsterdam, The Netherlands

Chapter 3.1

Abstract

Host immune responses are pivotal for the successful treatment of the leishmaniases, a spectrum of infections caused by *Leishmania* parasites. Previous studies speculated that augmenting cytokines associated with a type 1 T-helper cell (Th1) response is necessary to combat severe forms of leishmaniasis, and it has been hypothesized that the antileishmanial drug miltefosine is capable of immunomodulation and induction of Th1 cytokines. A better understanding of the immunomodulatory effects of miltefosine is central to provide a rationale regarding synergistic mechanisms of activity to combine miltefosine optimally with other conventional and future antileishmanials that are currently under development. Therefore, a systematic literature search was performed to evaluate to what extent and how miltefosine influences the host Th1 response. Miltefosine's effects observed both in a preclinical and clinical context associated with immunomodulation in the treatment of leishmaniasis are evaluated in this review. A total of 27 studies were included in the analysis. Based on the current evidence, miltefosine is not only capable of inducing direct parasite killing, but also of modulating the host immunity. Our findings suggest that miltefosine-induced activation of Th1 cytokines, particularly represented by increased IFN-γ and IL-12, is essential to prevail over the *Leishmania*-driven Th2 response. Differences in miltefosine-induced host-mediated effects between *in vitro*, *ex vivo,* animal model and human studies are further discussed. All things considered, an effective treatment with miltefosine is acquired by enhanced functional Th1 cytokine responses and may further be enhanced in combination with immunostimulatory agents.

1. Introduction

With an estimated 678,000 cases and about 40,000 fatalities *per annum* worldwide, the neglected tropical disease leishmaniasis is the second largest parasitic killer following malaria (1). Heterogeneity among parasite species results in different clinical manifestations, with visceral leishmaniasis (VL) being the most severe and potentially lethal form of *Leishmania* infection. In VL, parasites replicate within mononuclear phagocytic cells leading to infection of the spleen, liver and bone marrow (2, 3). Other clinical phenotypes include cutaneous (CL), post-kala-azar dermal (PKDL) and mucocutaneous (MCL) leishmaniasis, which are manifested by skin or mucous membrane lesions and/or ulcers (3, 4).

T-helper (Th) cells are the core of adaptive immunity, as their activity underpins almost every adaptive immune response, while impairments to Th cell functioning are found in many autoimmune diseases (5). When activated, naive Th cells divide and commit to a particular effector phenotype including Th type 1 (Th1) or 2 (Th2). Th1 cells secrete cytokines such as interferon (IFN)-α, -β, - γ, interleukin (IL) -1β, -6, -8, -12, -18, -27, intercellular adhesion molecule 1 (ICAM1), and tumor necrosis factor (TNF) α and β. Th1-related cytokines are particularly implicated in clearing intracellular pathogens, such as *Leishmania* parasites, that invade and replicate within reticuloendothelial cells (6, 7). Th2 cells primarily secrete IL-4, -5, -10, and -13: cytokines that activate pathways which are implicated in clearing extracellular pathogens, and the development of allergies. The crucial role of Th1 activation in the treatment of VL has been demonstrated previously by the role of IFN-γ in infection clearance, *e.g.* IFN-γ knockout mice failed to respond to an anti-IL-4 monoclonal antibody treatment, resulting in progressive infection (8). Additionally, in mice with genetically compromised Th1 cytokine production, a dominant Th2 response led to exacerbated VL infection, implying that an active Th1 response is crucial to balance the infection-promoting Th2 response and ultimately control the parasite burden (9).

Although the Th1 versus Th2 dichotomy is typically less clear in human infection, the importance of the Th1/Th2 balance in obtaining control over the *Leishmania* infection has also been observed in clinical studies. Patients suffering from progressive VL showed a consistent lack of Th1 cytokine production (10). Whereas, expression of Th2 markers was detected in PKDL lesional tissues (10, 11). In VL and diffuse CL, an increase in Th2 activity is generally associated with infection progression, and Th1 activity has been associated with infection clearance, and establishing clinical cure (7). IFN-γ has been shown effective as adjunct therapy

in VL and diffuse CL (12–15). However, in the localized CL lesions , the balance between Th1 and Th2 cytokines appears more complex, since even the healing lesions were shown to contain persisting levels of circulating Th2 cytokines (16).

Due to decreasing and disappointing efficacy of various antileishmanial drugs as monotherapy, including miltefosine, implementation of combination therapies is warranted. This is especially needed in East Africa, where antileishmanial drugs systemically show lower efficacy rates (17). To use new and existing therapies in the most optimal synergistic way, more knowledge is required on the direct and indirect mechanisms of action of antileishmanial compounds, *e.g.* through stimulation of the host immune system (18, 19). Miltefosine is an alkylphosphocholine agent, (20) which is currently the only oral drug available on the market for the treatment of leishmaniasis and is widely used both in the treatment of CL and VL (21). Various direct and indirect antileishmanial mechanisms of action have been suggested for miltefosine, including disruption of (membrane) lipid metabolism, apoptosis-like cell death, induction of mitochondrial dysfunction, but also immunomodulatory effects involving Th1 cell response (20). Following the observed effects on Th cells in leishmaniasis, miltefosine has also been investigated in the treatment of other immune-mediated diseases such as cancer, inflammatory bowel disease and atopic dermatitis, showing promising pre-clinical results (22). Given the observed relationship between Th1/Th2 balance and control over the *Leishmania* infection, the potentiation of Th cell activation through the use of immunomodulators in addition to conventional chemotherapy has been hypothesized as a future therapeutic option for leishmaniasis (23, 24). Preclinical studies have *e.g.* suggested that adding Th1-directed immunotherapy to chemotherapy could decrease *Leishmania*-associated suppression of the immune system and result in a more rapid parasite clearance (25–27). There is limited knowledge however about the translational and predictive value of immune effects from *in vitro* and various animal models for humans, which is complicated by intrinsic immunopathological differences between available murine and hamster models (28).

A better understanding of the immunomodulatory effects of miltefosine is central to provide a rationale regarding synergistic mechanisms of activity to combine miltefosine optimally with other conventional and future antileishmanials that are currently under development, and immunotherapeutic interventions. Also, in principle, this may aid understanding of the translational value of the immunomodulatory effects observed in preclinical models for other

antileishmanial drugs. Therefore, our objective was to systematically review how miltefosine affects markers of the host Th1 response associated with its immunomodulatory effect in the treatment of leishmaniasis *in vitro*, in animal models and in human, and to what extent the host-mediated effects in these different models are in congruence.

2. Methods

2.1 Search strategy

A systematic search of the literature was performed in PubMed (MEDLINE), Embase (OVID) and Scopus on September 29th, 2017 and repeated on January 15th, 2018 and November 21st, 2018. Sensitivity of the search was accomplished by including the following terms: "Miltefosine" AND "Leishmaniasis" AND ("Th1-cells" OR "Cytokines" OR "Chemokines" OR "Intercrines" OR "Interleukins"). All terms were searched in MeSH-terms (or equivalent in other databases), title and abstract. The full search strategies are shown in the *supplemental data file I*. Deduplication of the articles was done according to the "Bramer Method" (82).

2.2 Study identification and selection

No limits were used in the search strategy. Inclusion and exclusion of found literature was performed following PRISMA guidelines (*supplemental data file II*) (83). Secondary sources were identified through the referenced literature of the primary identified studies and through additionally querying PubMed using the search term "Miltefosine" AND and ("Immunity" OR "Immunomodulation" OR "Immunomodulatory"). Language restrictions were not applied in the selection of studies. Studies with only titles or abstracts available were not included. Eligible studies had to describe the effects of miltefosine on Th1 activity, demonstrating a change in the levels of any of the following: IFN-α, -β, - γ, IL -1, -6, -8, -12, -18, -27, ICAM1, neopterin, TNF α and β, since these markers have been associated with cellular immunity and subversion of intracellular pathogens. Therefore, studies focusing on other immunological factors such as changes in Th2 cytokines, alterations in toll-like receptor expression were not included. Only original research articles and treatment relevant patient case reports (focused on Th1 response) were included. Therefore, reviews, editorials, commentaries, posters, conference reports, non-immunological case reports *etc.* were excluded. We aimed to evaluate the effects observed both in a preclinical and clinical context; hence we included all *in vitro*, animal and human studies. The literature identified by the

search strategy was screened independently by two authors (SP and TD) for eligibility criteria mentioned above. Disagreements were resolved by discussion between the two authors.

2.3 Data extraction

The following information was retrieved and extracted from each included study: clinical presentation of the leishmaniasis infection (VL, CL, or PKDL), parasite subspecies, number of subjects, population age range, male-to-female ratio, and geographical region, which were applicable only to human studies, and miltefosine dose, route of administration, dosing frequency, treatment duration, sampling schedule, sampling matrix, measured cytokine(s), and direction of observed effects. Where applicable, we also included the dosing schedule of comedication, the presence of comorbid diseases or conditions, the follow-up period, and whether a correlation was observed between the immunological markers of interest and treatment outcomes, such as initial treatment response, relapse, or final cure.

3. Results

A complete search on September 29th, 2017 yielded 56 hits in PubMed (MEDLINE), 94 hits in Embase (OVID), and 132 hits in Scopus. This search was repeated on January 15th, 2018, resulting in 9 new hits, and on November 21st, 2018, 8 more new hits. After removal of the duplicates, 184 unique articles were identified in total.

Our search identified in total 6 *in vitro*, 3 *ex vivo*, 13 in animal and 5 in human studies which investigated Th1 cytokine activity after miltefosine treatment in leishmaniasis *(figure 1)*. In total, 4 *in vitro* studies were available for VL (*L. donovani*) and 1 for CL (*L. braziliensis* and *L. major*), as well as 2 *ex vivo* for VL (*L. donovani*), and 1 for CL (*L. braziliensis)*. In animal studies, 12 identified studies investigated miltefosine effects in VL and 1 in CL, while in human, 3 studies were identified for VL and 2 for PKDL. Finally, a total of 27 studies were included in this systematic review: 23 meeting the inclusion and eligibility criteria from the primary search results, and 4 studies identified through secondary sources. Results from all these studies in the various leishmaniasis disease models are discussed in the following paragraphs.
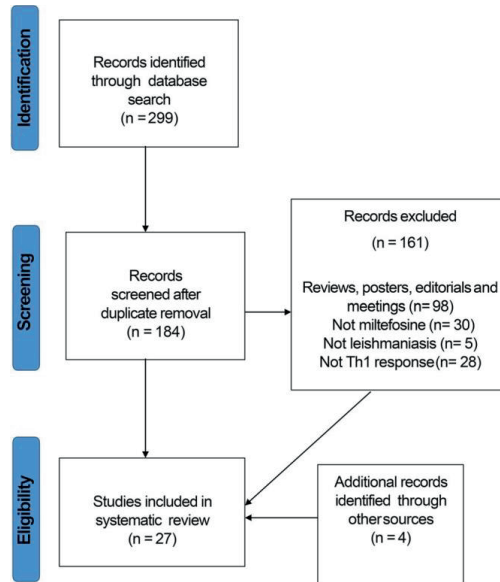
Figure 1: Flowchart of the studies identified, screened and included in this review

3.1 Studies in vitro and ex vivo

In vitro studies *(table 1)* were the first to propose and to demonstrate that miltefosine induces a Th1 response via various immunological pathways. Applying miltefosine to *Leishmania* infected splenocytes resulted in an induction of a Th1 response primarily shown by increased IFN-γ (19, 29–31). IFN-γ enables class switching from immunoglobulin G (IgG) 1 to IgG2. Analysis of IgG isotypes elucidated that IgG1 and IgG3 are significantly higher in patients with active VL, as well as in active lesions in CL, than control reference values in areas of endemicity (32, 33). IgG1 was proposed as a marker of relapse in Indian VL (32). Still, whether certain subclasses of IgG antibodies, such as IgG2 may haprve a protective role in VL and PKDL has not been clearly established. On the other hand, the levels of present antibody subtypes may illustrate the level of activation of cellular Th response (16). For instance, prior vaccination of mouse to increase IgG2 levels was associated with a 5-fold higher IFN-γ level post-treatment (24). Furthermore, IL-12 and IFN-γ were significantly increased in miltefosine treated cells *ex vivo (table 2)*, suggesting miltefosine-driven stimulation of Th1 cytokines (34). One mechanism proposed for the observed miltefosine immunomodulatory effects was inhibition of PI3K-dependent phosphorylation in macrophages and the simultaneous increase in the protein

kinase C dependence, which in turn triggers the production of Th1 cytokines (30, 35). Another proposed mechanism of IFN-γ induction by miltefosine is that miltefosine may increase the expression of IFN-γ receptor, which further promotes signal transducer and activator of transcription 1 (STAT-1) signaling. In VL, STAT-1 phosphorylation is impaired by *Leishmania*-driven sphingosine-1-phosphate (SPH-1) activity. Miltefosine-mediated increases in IFN-γ responsiveness caused a decrease in SPH-1 activation, which in turn also led to an increase in STAT-1 phosphorylation (30).

Table 1: Overview of *in vitro* studies on Th1 cytokine response following miltefosine in treatment of leishmaniasis

Study	Clinical indication	Parasite species	Host cell	Cytokine measured (extracellular)	Direction of effects	Number of subjects (group)	Miltefosine concentration/dose	Number of time points evaluated	Between sampling intervals
Gangalum et al. (29)	VL	*L. donovani*	peritoneal macrophages (mice)	IFN-γ	increase	5 (3)	0.8 µM	1	24 h
Wadhone et al. (30)	VL	*L. donovani*	peritoneal macrophages (mice)	IFN-γ, IL-12	increase	5 (3)	3.2 µM	5	1, 3, 6, 12, and 24 h
Shukla et al.(31)	CL	*L. major*	lymph node mononuclear cells	IFN-γ	increase	8 (8)	n.a.	2	6 h
Ghosh et al. (19)	n.a.	n.a.	peritoneal macrophages (mice)	IFN-γ, TNF-α	increase	5(5)	20 µM	2	24 and 72 h
Shivahare et al. (40)	VL	*L. donovani*	macrophages (J-774A.1 cells) (mice)	IL-12, TNF-α	increase	n.a. (6)	2 and 8 µM	1	48 h
Shivahare et al. (39)	VL	*L. donovani*	macrophages (J-774A.1 cells) (mice)	IL-12, TNF-α	increase	n.a. (5)	2 and 8 µM	1	48 h

CL: cutaneous leishmaniasis, h: hours, IFN: interferon, IL: interleukin, VL: visceral leishmaniasis; n.a.: not availabl

In addition, infections with *L. major* and *L. donovani* are known to suppress the activation of p38 mitogen-activated protein kinases (p38MAPK), which is required for production of pro-inflammatory Th1 cytokines (36). Miltefosine was able to increase the levels of p38MAPK activation in BALB/c-derived peritoneal macrophages, that in turn increased IL-12 levels in a dose-dependent manner within 48 hours post-treatment (19, 29, 30). Moreover, miltefosine treatment of isolated peripheral blood mononuclear cells (PBMCs) derived from monocytes of VL patients resulted in an 8-fold rise in IL-12 levels (37). Also, PBMCs isolated from patients with advanced VL also showed increased Th1 cytokines after *ex vivo* miltefosine treatment, further illustrating miltefosine-driven immunomodulation (38). Additionally, a functional role of miltefosine in the synthesis of TNF-α has been shown *in vitro* (29, 39, 40). BALB/c mouse-derived macrophages with a knock-out platelet aggregation factor (PAF) receptor function displayed a complete lack of response to miltefosine, indicated by diminished miltefosine-induced parasite killing (29). Down-regulation of the PAF receptor was also found to enhance IL-4 production, and suppress IFN-γ levels, resulting in progressive VL infection (29). Miltefosine is a structural analogue of PAF and it was found that miltefosine activation of the PAF receptor led to increased IL-12 and TNF-α, while no effect was observed for PAF receptor-deficient macrophages (29, 41). Similar results were obtained based on CL patient-derived PBMCs (37).

3.2 Studies in animal

Various animal studies *(table 3)* focused on the effects of miltefosine on IFN-γ production in both murine and hamster models of VL (42–49). Following miltefosine administration, all studies reported substantially increased IFN-γ levels in macrophages of *Leishmania* infected animals in contrast to control groups (42–49). Several studies also showed that increases in

Table 2: Overview of *ex vivo* studies on Th1 cytokine response following miltefosine in treatment of leishmaniasis

Study	Clinical indication	Parasite species	Host cell	Cytokine measured	Direction of effects	Number of subjects (group)	Miltefosine concentration/dose	Number of time points evaluated	Between sampling intervals
Joshi et al. (38)	VL	*L. donovani*	lymph node mononuclear cells (hamster), PBMCs (human)	IFN-γ, IL-12	increase	animal 30, human 32 (4)	animal: 40 mg/kg human: n.a.	2	45, 90 days
Mukherjee, A. K. et al.(34)	VL	*L. donovani*	THP1 derived macrophages	IFN-γ, IL-12, TNF-α	increase	10	5 µM	2	24 and 48 h
Gonzalez-Fajardo et al. (37)	CL	*L. braziliensis*	PMBCs (human)**	IFN-γ, TNF-α, and IL-12	increase	22	2, 4, 8, 16, 32 µM	6	6, 12, 24, 48, and 72 h

CL: cutaneous leishmaniasis, h: hours, IFN: interferon, IL: interleukin, PBMC: peripheral blood mononuclear cell, VL: visceral leishmaniasis;

** monocyte-derived macrophages from isolated PBMCs

Table 3: Overview of animal studies on Th1 cytokine response following miltefosine in treatment of leishmaniasis

Study	Clinical indication	Parasite species	Host	Measured cytokine	Matrix	Direction of effects	Number of subjects (treatment groups)	Miltefosine dose	Route of administration	Treatment duration	Number of time points per individual
Shakya et al.(42)	VL	L. donovani	mouse	IFN-γ, IL-12, TNF-α	serum	increase	5-6 (9)	1.25 to 20 mg/kg q.d.	PO	5 days	2
Shakya et al. (43)	VL	L. donovani	mouse	IFN-γ, TNF-α	serum	increase	5-6 (7)	2.5, 5, 20 mg/kg q.d.	PO	7 days	2
Wege et al. (44)	VL	L. donovani	mouse	IFN-γ	spleen	increase	32	2.5 mg/kg q.d.	PO	n.a.	3
Anand et al. (45)	VL	L. donovani	mouse	IFN-γ, IL-12, TNF-α	splenocytes	increase	5 (7)	5, and 25 mg/kg q.d.	IP	5 days	2
Murray et al. (46)	VL	L. donovani	mouse	IFN-γ	pheripheral blood	increase	5 (8)	25 mg/kg q.d.	PO	5 days	3
Schmidt-Ott et al. (47)	CL	L. mexicana	mouse	IFN-γ	lymph nodes	increase	6	1.5 mg q.d.	topical	5 days per week for 5 weeks	2

Reference		Species	Cytokines	Sample	Effect		Dose	Route	Duration	
Shivahare et al. (50)	VL	mouse, hamster	IFN-γ, IL-12, TNF-α	splenocytes	increase	5-6 (9)	5 and 20 mg/kg q.d. (mouse), 5 and 40 mg/kg q.d. (hamster)	PO	5 days	2
Sane et al. (53)	VL	mouse, hamsters	IFN-γ, TNF-α	serum	increase	5 (6)	2.5-40 mg/kg q.d.	PO	5 days	2
Gupta et al. (49)	VL	hamsters	IFN-γ, IL-12, TNF-α	pheripheral blood	increase	8-10 (5)	40 mg/kg q.d.	n.a.	5 days	2
Jaiswal et al. (48)	VL	hamsters	IFN-γ and IL-12	pheripheral blood	increase	30	40 mg/kg q.d.	PO	5 days	3
Tripathi et al. (51)	VL	hamsters	IFN-γ, IL-12	lymphocytes	increase	5-6 (9)	2.5-40 mg/kg q.d.	PO	5 days	2
Manna et al. (55)	VL	dogs	IFN-γ	pheripheral blood	increase	20	2 mg/kg q.d.	PO	30 days	5
Andrade et al. (52)	VL	dogs	IFN-γ	pheripheral blood	increase	14	100, 200 mg/animal q.d.	n.a.	28 or 45 days	3

Species column also lists: *L. donovani*, *L. donovani*, *L. donovani*, *L. donovani*, *L. donovani*, *L. infantum*, *L. chagasi*

b.i.d.: twice daily, CL: cutaneous leishmaniasis, IFN: interferon, IL: interleukin, IP: intraperitoneal, n.a.: not available, PKDL: post-kala-azar dermal leishmaniasis, PO: per os, q.d.: once daily, t.i.d. thrice daily, VL: visceral leishmaniasis

IFN-γ levels were proportional to the dose of miltefosine administered, as well as accompanied by suppression of Th2-associated cytokine levels, together inducing the killing of parasite (43, 45, 50). As indicated by *in vitro* studies, IFN-γ activates macrophages, and miltefosine was shown to enhance the expression of IFN-γ in macrophages of BALB/c mice infected with *L. donovani* (42–44) Moreover, miltefosine was even able to up-regulate IFN-γ levels in T-cell deficient mice (46). In addition, control groups of mice and hamsters which were not treated with miltefosine demonstrated increased or unchanged parasite levels in comparison to those treated with subcurative and curative doses of miltefosine (50). Up to a 9-fold increase in Th1 cytokines was measured in mice splenocytes 4 days post-treatment with miltefosine alone, which was boosted to a 13-fold increase when miltefosine was combined with immunostimulatory compounds such as pyrazolopyridine derivatives (45). These results indicate that the immune response shift towards Th1 is likely due to treatment-induced immunomodulation (51, 52).

Studies in mice have as well documented a dose-proportional increase in IL-12 after standard miltefosine treatment. The host immune system requires IL-12 in order to stimulate the differentiation of Th1 cells, further maintain Th1 responses, and overall stimulate the production of IFN-γ (42, 43). A few studies argued that miltefosine-mediated immunomodulatory effects are more advanced when miltefosine is administered in combination with compounds that stimulate Th1 polarized cytokines (50, 53). As already postulated by *in vitro* studies, an increase in IgG2 antibodies contributed to the development of an effective Th1-mediated immune response (45, 51, 53). Increases in IgG2 expression, as well as consequent suppression of IgG1 dominance were more appropriately illustrated in hamster models, since mice lack the distinct subclasses among IgG antibodies (54). In hamster VL *(L. donovani)* models, upon successful miltefosine treatment, complete cure is reached at day 45, where IFN-γ, IL-12 and TNF-α levels were identified as indicators of treatment outcome (48, 49). Furthermore, two studies evaluated the effects of miltefosine in the treatment of dogs naturally infected with VL *(L. infantum).* A 28 or 45 day treatment with oral miltefosine administered daily (100-200 mg/day) increased IFN-γ in peripheral blood up to two-fold at day 180 post start of treatment (52). Subsequent relapse in these dogs was associated with decreased IFN-γ and reoccurrence of Th2 cytokine production. Relapses were primarily associated with increases in IL-4 and IL-10, which is typically observed at the time of diagnosis (52). Dogs treated with a combination of miltefosine and allopurinol showed a more

prolonged increase of IFN-γ in peripheral blood, with 90% survival at nine months (55). Lastly, a single study investigating the immune effects of miltefosine on CL in BALB/c, CBA/J and C57BL/6 mouse models infected with either *L. major* or *L. mexicana* showed that IFN-γ was elevated in lymph nodes directly during and after five weeks of miltefosine treatment. For *L. major* infection in BALB/c mice, the most significant increase in IFN-γ was 3.1 fold at 3 weeks after the 5-week miltefosine treatment, while the increases in IFN-γ for CBA/J and C57BL/6 mice was 2.8 and 1.9 fold respectively (47). Differences in IFN-γ receptor expression were observed among the various murine species. Miltefosine treatment of *L. mexicana* infection in mice was ineffective and did not result in increased levels of Th1 cytokines, resulting in 9 out of 12 disease relapses (47). However, a relatively low miltefosine dose was administered, thus an optimal exposure might not have been achieved (47). Taken together, preclinical studies show the importance of immune cross-talk in both infection development and clearance. Miltefosine immunomodulation in the animal models appears to be exerted through two major pathways *(figure 2)*: stimulation of Th1 cytokine production that will further drive macrophage activation, as well as activation of the transcription factors within the infected macrophages, which will in addition prime macrophage to increase Th1 cytokine secretion, and eventually counterbalance anti-inflammatory cytokines.

3.3 Studies in human

Although very limited results from studies in human *(table 4)* are available up to date, these appear to be in line with findings from *in vitro* and animal studies. Production of IFN-γ and IL-12 were also found elevated after miltefosine treatment of VL (56). Additionally, in patients with inborn errors in the genes encoding for IL-12, miltefosine was shown ineffective and VL reoccurred multiple times (57). These patients were also more susceptible to other infections such as tuberculosis. This indicates that impaired IFN-γ functioning does not only hamper normal immune function, but also limits miltefosine's action to stimulate macrophage-driven Th1 cytokine production. Importance of restoring the host immunity in VL is particularly demonstrated in immunosuppressed patients, such as those who are co-infected with HIV, where VL is even more challenging to treat, and results in more episodes of relapse and even death (58). Furthermore, neopterin, a Th1 immune marker has been recently evaluated in VL patients after treatment with miltefosine alone or in combination with amphotericin B (59). Neopterin is exclusively produced by macrophages, that are activated by IFN-γ upon

treatment (60, 61). As such, a decline in neopterin levels due to miltefosine treatment may directly reflect a decline in macrophages loaded with parasites.

Additionally, somewhat different immunological responses were observed in PKDL, where both Th1 and Th2 cytokines were found present. Since PKDL patients were already treated for VL, infection is no longer systemic, as the result of treatment-associated increased Th1 cytokine levels. However, Th2 cytokines are still present in the skin, most likely remaining since the primary VL infection (11). One of the case studies identified describes a decrease of IFN-γ in patient's lesional tissue after the treatment with miltefosine (10). Measured CD40 levels were also found enhanced, and probably contributed to evoked Th1 signaling. However, TNF-α levels were found decreased, which may be explained by concomitant treatment of rheumathroid arthritis with immunosuppressant hydroxychloroquine, and previously mistreated leprosy with clofazimine, both known to interact with Th signaling (10). In addition, Mukhopadhyay et al. reported that miltefosine significantly increased secretion of Th1 cytokines and decreased anti-inflammatory Th2 responses in PKDL patients. Similarly to scenarios observed in VL, elevated levels of TNF−α, IL-1β, IL6, and IL-8 in peripheral blood were also accompanied by higher levels of serum nitrate that is known to drive pro-inflammatory monocyte response in PKDL (62). Development of PKDL has been reported after treatment of VL with various antileishmanials including miltefosine, amphotericin B, stibogluconate and paromomycin, but rates of PKDL occurring after any of the treatments has not been studied up to date (63, 64). Understanding immunological responses during VL treatment is therefore of crucial importance for advancing our knowledge about infection reappearance in some patients during asymptomatic intervals.
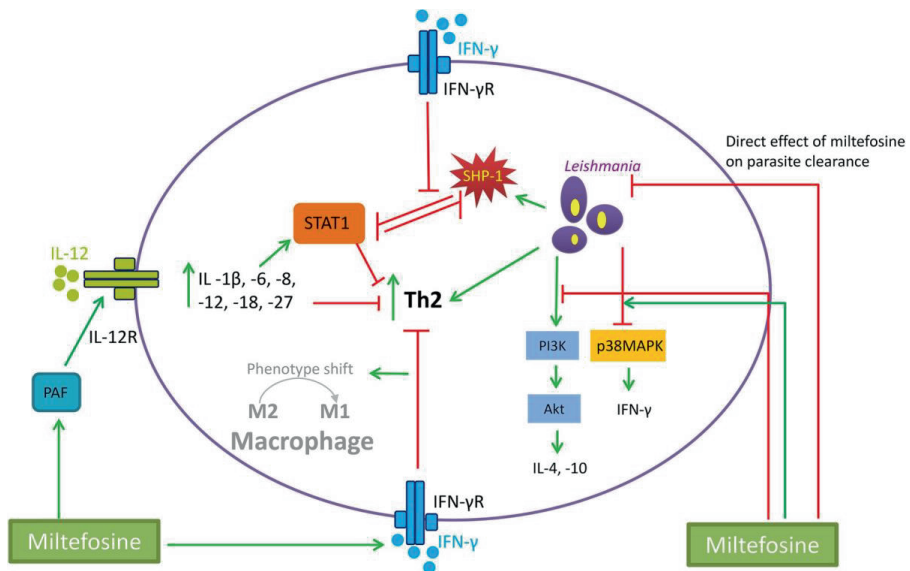
Figure 2: Proposed mechanisms of action for miltefosine

The proposed mechanisms include direct killing of Leishmania parasites and several immunomodulatory effects, which are exerted via (i) platelet aggregation factor (PAF) receptor, increasing production of interleukin (IL)-12, (ii) enhancement of interferon gamma (IFN-) receptor, which in turn lowers the production of T-helper (Th) cell type 2 cytokines (such as IL-4, -5, -10, and -13), (iii) activation of IFN-, reversing sphingosine-1-phosphate (SPH-1) inhibition of signal transducer and activator of transcription 1 (STAT-1), which is translocated to the nucleus and involved in stimulation of the host cellular immunity, (iv) activation of p38 mitogen-activated protein kinase (p38MAPK), which is initially inhibited by Leishmania, and (v) inhibition of PI3 kinase phosphorylation of protein kinase B (Akt), which is initially stimulated by the parasite. Red lines indicate an inhibitory effect, while green arrows indicate a stimulatory effect.

Table 4: Overview of human studies on Th1 cytokine response following miltefosine in treatment of leishmaniasis

Study	Clinical indication	Parasite species	Measured cytokine	Matrix	Direction of effects	Number of subjects (treatment groups)	Miltefosine dose	Route of administration	Treatment duration	Number of time points
Das et al. (56)	VL	L. donovani	IFN-γ, TNF–α	pheripheral blood	increase	23	50 mg b.i.d.	PO	28 days	2
Parvaneh et al. (57)	VL	L. infantum	IFN-γ, IL-12	whole blood	increase	2	n.a.	PO	28 days	n.a.
Kip et al. (59)	VL	L. donovani	neopterin	plasma	decrease	48 (2)	2.5 mg/kg/day	PO	28 days, 10 days	6-7
Ansari et al. (10)	PKDL	L. donovani	IFN-γ, TNF–α	lesional tissue biospy	IFN-γ increase TNF–α decrease	1	50 mg b.i.d./t.i.d.	PO	15 weeks	3
Mukhopadhyay et al. (62)	PKDL	L. donovani	TNF–α, IL-1 β, IL6, IL-8	pheripheral blood	increase	16	100 mg q.d.	PO	16 weeks	2

b.i.d.: twice daily, CL.: cutaneous leishmaniasis, IFN: interferon, IL: interleukin, IP: intraperitoneal, n.a.: not available, PKDL: post-kala-azar dermal leishmaniasis, PO: per os, q.d.: once daily, t.i.d. thrice daily, VL: visceral leishmaniasis

4. Discussion

In the current review, we have systematically evaluated and summarized the proposed immunomodulatory effects in the treatment of various leishmanial infections *in vitro*, *ex vivo*, in animal and in human. To the best of our knowledge, this is the first systematic review of the host-mediated activity of miltefosine through immunomodulation. Several general mechanisms were identified to support miltefosine-mediated immunomodulation. *Leishmania* parasites drive the Th2 response during the course of infections in VL, and miltefosine was found capable of reversing these infection-driven effects, especially demonstrated in VL subjects (49, 65). *Leishmania* reduces the responsiveness of IFN-γ receptors within infected cells, while miltefosine was found to restore the functioning of IFN-γ receptors (66). In having such a direct effect on IFN-γ receptors, miltefosine is able to activate a pro-inflammatory immune response, along parasite killing (67, 68). IFN-γ alone appears insufficient to drive a dominant Th1 response, IL-12 also has an important role in sustaining this Th1 response (51, 69). *In vivo* studies showed that miltefosine induced IL-12 in a dose dependent manner (30). Animal studies further demonstrated that a complete cure at the end of the treatment was associated with a rise in IFN-γ, IL-12 and TNF-α levels, suggesting that these cytokines may indicate initial treatment response (48, 49). Essentially, increased concentrations of pro-inflammatory cytokines will lead the shift in macrophage phenotype from M2, which is dominated by Th2 cytokine expression, to M1 that is driven by Th1 cytokines and ultimately needed to clear the intracellular pathogen. Several studies further reported higher concentrations of Th1 cytokines when miltefosine was combined with compounds known to stimulate the host immunity. It has been long hypothesized that various antileishmanial drugs including miltefosine, amphotericin B, paromomycin and antimonials exert immunomodulatory effects. However, to our knowledge, only a single *in vitro* study made a direct comparison between different antileishmanials and IL-12 levels, where it was reported that miltefosine, amphotericin B, and sodium antimony gluconate treated macrophages produce increased IL-12 levels, but not macrophage treated with paromomycin (19). It remains difficult to evaluate to what extent miltefosine immunomodulatory effects might be different compared to other antileishmanials, or whether observed effects are resulting from decreasing parasite levels or rather direct effects on Th1 cell signaling. However, in contrast to other antileishmanials, only for miltefosine immunomodulatory effects have been reported in immune-mediated disorders such as rheumatoid arthritis,

chronic urticaria, or malignant disease (22). Taken together, these findings illustrate that besides the direct killing of the parasite, miltefosine is also able to affect the host immune system by targeting Th1. These observations indicate not only the mechanisms of miltefosine immunomodulation, but also highlight the importance of Th1 cytokine activation for the clearance of *Leishmania* in VL. Moreover, in spite of the fact that only a few human studies were identified in our review of available literature, the studies that were identified support the role of Th1 cytokine activation by miltefosine in the treatment of VL. This is corroborated by IL-12 deficient VL patients in which miltefosine was non-efficacious. However, a contrasting change in levels of neopterin is observed upon miltefosine treatment in VL patients. While most Th1 cytokines reflect cascades taking place outside, or at the surface of macrophages which are needed for its activation, neopterin reflects an activated macrophage response, whose decline therefore is attributed to a decline in macrophage parasite level.

As mentioned, the immunomodulatory effects of miltefosine have also been demonstrated in the treatment of other immune-mediated disorders such as inflammatory bowel disease (IBD) or chronic urticaria (22). In a mouse model of IBD, miltefosine was shown to block proliferation of Th2 cytokines, subsequently increasing Th1 cytokines, which resulted in decline of inflammation and less severe colitis (70). Moreover, in patients with chronic spontaneous urticaria who do not respond to treatment with antihistamines, miltefosine was able to relieve symptoms such as number of weals and intensity of pruritus (71). Additionally, miltefosine-induced immunomodulation may particularly be important for patients who are co-infected with human immunodeficiency virus (HIV). In this immunocompromised patient population suffering from both HIV and VL, the immune responses are heavily dominated by Th2 cytokine activity, and combined with antiretroviral treatment, miltefosine was proven to have relatively good efficacy (58, 72).

Taken collectively, the identified *in vitro*, *ex vivo*, animal and human studies suggest the therapeutic importance of miltefosine-driven activation of Th1 cytokines in the treatment of VL, diffuse CL and PKDL (30, 45, 73). A direct translation between the various test systems and corresponding therapeutic effects nevertheless may not be easily derived. Underlying reasons are the complex physiological and immunological factors that are known to result in a different pathophysiology and immunopathology between species (74). For example, untreated VL in hamster models results typically in mortality, while in murine models the

parasite is cleared and infected subjects recover even in the absence of treatment (75). Moreover, murine VL models usually reflect acute infections in spleen and liver that may be resolved, and parasite clearance from these organs does not necessarily represent immune sterilization (23). This is contrast to human infection, where the stage of leishmanial infection may not be obvious and patients may suffer from concomitant diseases or infections that may as well compromise the immune system (76). In addition, some immunological aspects observed in human patients could not be accurately reproduced in mice. For example, glucocorticoid-induced tumor necrosis factor receptor family–related protein (GITR) was found increased in VL patients. Pharmacological blockage of its receptor did not induce antiparasitic immunity and even restored IL-10 levels that were initially inhibited by IFN-γ (77, 78). In mice, however, due to contrasting humoral and cellular immune responses, these effects were not observed (75, 77).

Furthermore, differences in activation between Th1 and Th2 cytokines appear more obvious in mice, therefore initial distinction between these cytokines has been derived based on studies in mice. However, studies in human showed that a strict distinction between Th1 and Th2 cytokines is too simplistic, as both the disease and the treatment will drive the balance between these cytokines through inhibitory and positive feedback loops (7, 79). In PKDL specifically, Th17 cytokines such as IL-17 and TNF-α are found upregulated compared to control. Th17 cytokines are known to recruit neutrophils to induce tissue inflammation and link the innate to adaptive responses. Therefore, different leishmanial infections in human appear to drive distinct T cell differentiation, which suggests that immunomodulation between parasite species is also different (78, 79). In essence, *in vitro* studies provide crucial information on how the parasite and separate immune cells respond to the drug. However, these studies may often lack power to illustrate how the complete host immune system may respond to treatment (63). Therefore, in order to translate findings between pre-clinical and clinical studies, we highlight the need of implementing translational pharmacokinetic-pharmacodynamic (PK-PD) modelling. PK-PD modelling and simulation has already been shown superiority over classical extrapolation and translation of preclinical to clinical findings and has demonstrated particularly benefits in the development and evaluation of dosing regimens in special patient populations such as children or pregnant women (80, 81).

According to the identified studies, miltefosine is able to actively influence the host immunity through stimulation of production of Th1 cytokines that participate in *Leishmania* clearance.

In line with this, several preclinical studies also proposed that a combination treatment with immunostimulatory agents may enhance miltefosine's immunomodulation and result in a more favourable treatment outcome, especially in cases where infections are advanced, or where the immune system is further compromised by presence of additional co-infections (39, 42, 50). In conclusion, while targeted immunotherapy in the treatment of VL is still lacking, given its modulatory effects we emphasize the potential of miltefosine in synergy with future anti-leishmanial compounds.

References

1. Alvar J, Vélez ID, Bern C, Herrero M, Desjeux P, Cano J, Jannin J, Boer M den, Team the WLC. 2012. Leishmaniasis Worldwide and Global Estimates of Its Incidence. PLoS One 7:e35671.

2. Murray HW. 2004. Progress in the treatment of a neglected infectious disease: Visceral leishmaniasis. Expert Rev Anti Infect Ther 2:279–292.

3. Murray HW, Berman JD, Davies CR, Saravia NG. 2005. Advances in leishmaniasis. Lancet 366:1561–1577.

4. Von Stebut E. 2007. Cutaneous Leishmania infection: Progress in pathogenesis research and experimental therapy. Exp Dermatol 16:340–346.

5. Murphy K. 2011. Janeway's immunobiology, 8th ed. Garland Science, Oxford, United Kingdom.

6. Kidd P. 2003. Th1/Th2 balance: the hypothesis, its limitations, and implications for health and disease. Altern Med Rev 8:223–46.

7. Ali N, Bhattacharya P. 2013. Translating immune cell cross-talk into a treatment opportunity for visceral leishmaniasis. Immunotherapy2013/10/04. 5:1025–1027.

8. Wang Z-E, Reiner SL, Zheng S, Dalton DK, Locksley RM. 1994. CD4 + Effector Cells Default to the Th2 Pathway in Interferon y-deficient Mice Infected with Leishman/a major. J Exp Med 179.

9. Scott P, Natovitz P, Coffman RL, Pearce E, Sher A. 1988. Immunoregulation of cutaneous leishmaniasis. T cell lines that transfer protective immunity or exacerbation belong to different T helper subsets and respond to distinct parasite antigens. J Exp Med 168:1675–84.

10. Ansari NA, Ramesh V, Salotra P. 2008. Immune response following miltefosine therapy in a patient with post-kala-azar dermal leishmaniasis. Trans R Soc Trop Med Hyg2008/07/22. 102:1160–1162.

11. Zijlstra EE. 2016. The immunology of post-kala-azar dermal leishmaniasis (PKDL). Parasit Vectors 9:464.

12. Sundar S, Murray HW. 1995. Effect of treatment with interferon-gamma alone in visceral leishmaniasis. J Infect Dis 172:1627–9.

13. Badaro R, Johnson WD. 1993. The role of interferon-gamma in the treatment of visceral and diffuse cutaneous leishmaniasis. J Infect Dis 167 Suppl:S13-7.

14. Kima PE, Soong L. 2013. Interferon gamma in leishmaniasis. Front Immunol 4:156.

15. Sundar S, Singh VP, Sharma S, Makharia MK, Murray HW. 1997. Response to interferon-gamma plus pentavalent antimony in Indian visceral leishmaniasis. J Infect Dis 176:1117–9.

16. Castellano LR, Filho DC, Argiro L, Dessein H, Prata A, Dessein A, Rodrigues V. 2009. Th1/Th2 immune responses are associated with active cutaneous leishmaniasis and clinical cure is associated with strong interferon-gamma production. Hum Immunol 70:383–390.

17. Dorlo TPC, Kip AE, Younis BM, Ellis SJ, Alves F, Beijnen JH, Njenga S, Kirigi G, Hailu A, Olobo J, Musa AM, Balasegaram M, Wasunna M, Karlsson MO, Khalil EAG. 2017. Visceral leishmaniasis relapse hazard is linked to reduced miltefosine exposure in patients from Eastern Africa: a population pharmacokinetic/pharmacodynamic study. J Antimicrob Chemother 72:3131–3140.

18. Rijal S, Ostyn B, Uranw S, Rai K, Bhattarai NR, Dorlo TPC, Beijnen JH, Vanaerschot M, Decuypere S, Dhakal SS, Das ML, Karki P, Singh R, Boelaert M, Dujardin J-C. 2013. Increasing Failure of Miltefosine in the Treatment of Kala-azar in Nepal and the Potential Role of Parasite Drug Resistance, Reinfection, or Noncompliance. Clin Infect Dis 56:1530–1538.

19. Ghosh M, Roy K, Roy S. 2013. Immunomodulatory effects of antileishmanial drugs. J Antimicrob Chemother 68:2834–2838.

20. Dorlo TPC, Balasegaram M, Beijnen JH, de Vries PJ. 2012. Miltefosine: a review of its pharmacology and therapeutic efficacy in the treatment of leishmaniasis. J Antimicrob Chemother 67:2576–2597.

21. Sindermann H, Croft SL, Engel KR, Bommer W, Eibl HJ, Unger C, Engel J. 2004. Miltefosine (Impavido): The first oral treatment against leishmaniasis. Med Microbiol Immunol 193:173–180.

22. Verhaar AP, Wildenberg ME, Peppelenbosch MP, Hommes DW, Van Den Brink GR. 2014. Repurposing miltefosine for the treatment of immune-mediated disease? J Pharmacol Exp Ther 350:189–195.

23. Faleiro RJ, Kumar R, Bunn PT, Singh N, Chauhan SB, Sheel M, Amante FH, Montes de Oca M, Edwards CL, Ng SS, Best SE, Haque A, Beattie L, Hafner LM, Sacks D, Nylen S, Sundar S, Engwerda CR. 2016. Combined Immune Therapy for the Treatment of

Visceral Leishmaniasis. PLoS Negl Trop Dis 10:e0004415.

24. Singh OP, Sundar S. 2014. Immunotherapy and targeted therapies in treatment of visceral leishmaniasis: current status and future prospects. Front Immunol 5:296.

25. Shivahare R, Ali W, Singh US, Khattri S, Puri SK, Gupta S. 2016. Evaluation of immunomodulatory activities of lentinan in combination with miltefosine in Balb/c mice against visceral leishmaniasis. Eur J Immunol 46:1090–1091.

26. Charan Raja MR, Velappan AB, Chellappan D, Debnath J, Kar Mahapatra S. 2017. Eugenol derived immunomodulatory molecules against visceral leishmaniasis. Eur J Med Chem 2017/08/22. 139:503–518.

27. Arora S, Tiwari A. 2016. Immune-modulation by a Novel Leishmania antigen facilitates faster clearance of intracellular parasites from infected macrophages and synergizes with anti-leishmanial drugs. Eur J Immunol 46:668.

28. Alves F, Gillon J-Y, Arana B, Dorlo TPC. 2017. From bench to bedside: development and optimization of clinical therapies for visceral leishmaniasis, p 37–54. In Rivas L, Gil C (ed), Drug discovery for leishmaniasis. Royal Society of Chemistry, London, United Kingdom.

29. Gangalum PR, de Castro W, Vieira LQ, Dey R, Rivas L, Singh S, Majumdar S, Saha B. 2015. Platelet-activating factor receptor contributes to antileishmanial function of miltefosine. J Immunol 2015/05/17. 194:5961–5967.

30. Wadhone P, Maiti M, Agarwal R, Kamat V, Martin S, Saha B. 2009. Miltefosine promotes IFN-gamma-dominated anti-leishmanial immune response. J Immunol 2009/05/21. 182:7146–7154.

31. Shukla D, Chandel HS, Srivastava S, Chauhan P, Pandey SP, Patidar A, Banerjee R, Chattopadhyay D, Saha B. 2017. TLR11 or TLR12 silencing reduces Leishmania major infection. Cytokine 2017/10/12.

32. Bhattacharyya T, Ayandeh A, Falconar AK, Sundar S, El-Safi S, Gripenberg MA, Bowes DE, Thunissen C, Singh OP, Kumar R, Ahmed O, Eisa O, Saad A, Silva Pereira S, Boelaert M, Mertens P, Miles MA. 2014. IgG1 as a potential biomarker of post-chemotherapeutic relapse in visceral leishmaniasis, and adaptation to a rapid diagnostic test. PLoS Negl Trop Dis 8:e3273.

33. Buxbaum LU. 2008. A detrimental role for IgG and FcgammaR in Leishmania mexicana infection. Immunol Res 42:197–209.

34. Mukherjee AK, Gupta G, Adhikari A, Majumder S, Kar Mahapatra S, Bhattacharyya Majumdar S, Majumdar S. 2012. Miltefosine triggers a strong proinflammatory cytokine response during visceral leishmaniasis: role of TLR4 and TLR9. Int Immunopharmacol2012/03/01. 12:565–572.

35. Mukhopadhyay D, Saha P, Chatterjee M. 2012. Targets for immunochemotherapy in leishmaniasis. Expert Rev Anti Infect Ther 10:261–264.

36. Bhardwaj S, Srivastava N, Sudan R, Saha B. 2010. Leishmania interferes with host cell signaling to devise a survival strategy. J Biomed Biotechnol 2010:109189.

37. Gonzalez-Fajardo L, Fernández OL, McMahon-Pratt D, Saravia NG. 2015. Ex Vivo Host and Parasite Response to Antileishmanial Drugs and Immunomodulators. PLoS Negl Trop Dis 9.

38. Joshi S, Yadav NK, Rawat K, Tripathi CDP, Jaiswal AK, Khare P, Tandon R, Baharia RK, Das S, Gupta R, Kushawaha PK, Sundar S, Sahasrabuddhe AA, Dube A. 2016. Comparative analysis of cellular immune responses in treated Leishmania patients and hamsters against recombinant Th1 stimulatory proteins of Leishmania donovani. Front Microbiol 7:312.

39. Shivahare R, Ali W, Singh US, Natu SM, Khattri S, Puri SK, Gupta S. 2016. Immunoprotective effect of lentinan in combination with miltefosine on Leishmania-infected J-774A.1 macrophages. Parasite Immunol2016/07/09. 38:618–627.

40. Shivahare R, Ali W, Vishwakarma P, Natu SMM, Puri SK, Gupta S. 2015. Leptin augments protective immune responses in murine macrophages and enhances potential of miltefosine against experimental visceral leishmaniasis. Acta Trop2015/06/30. 150:35–41.

41. Croft SL, Engel J. 2006. Miltefosine – discovery of the antileishmanial activity of phospholipid derivatives. Trans R Soc Trop Med Hyg 100:S4–S8.

42. Shakya N, Sane SA, Haq W, Gupta S. 2012. Augmentation of antileishmanial efficacy of miltefosine in combination with tuftsin against experimental visceral leishmaniasis. Parasitol Res2012/03/07. 111:563–570.

43. Shakya N, Sane SA, Vishwakarma P, Gupta S. 2012. Enhancement in therapeutic efficacy of miltefosine in combination with synthetic bacterial lipopeptide, Pam3Cys against experimental Visceral Leishmaniasis. Exp Parasitol2012/05/26. 131:377–382.

44. Wege AK, Florian C, Ernst W, Zimara N, Schleicher U, Hanses F, Schmid M, Ritter U.

2012. Leishmania major infection in humanized mice induces systemic infection and provokes a nonprotective human immune response. PLoS Negl Trop Dis2012/08/01. 6:e1741.

45. Anand D, Yadav PKP, Patel OP, Parmar N, Maurya RK, Vishwakarma P, Raju KS, Taneja I, Wahajuddin M, Kar S, Yadav PKP. 2017. Antileishmanial Activity of Pyrazolopyridine Derivatives and Their Potential as an Adjunct Therapy with Miltefosine. J Med Chem2017/01/07. 60:1041–1059.

46. Murray HW, Delph-Etienne S. 2000. Visceral leishmanicidal activity of hexadecylphosphocholine (miltefosine) in mice deficient in T cells and activated macrophage microbicidal mechanisms. J Infect Dis2000/02/11. 181:795–799.

47. Schmidt-Ott R, Klenner T, Overath P, Aebischer T. 1999. Topical treatment with hexadecylphosphocholine (Miltex) efficiently reduces parasite burden in experimental cutaneous leishmaniasis. Trans R Soc Trop Med Hyg1999/09/24. 93:85–90.

48. Jaiswal AK, Khare P, Joshi S, Kushawaha PK, Sundar S, Dube A. 2014. Th1 stimulatory proteins of Leishmania donovani: Comparative cellular and protective responses of rTriose phosphate isomerase, rProtein disulfide isomerase and relongation factor-2 in combination with rHSP70 against visceral leishmaniasis. PLoS One 9:1–17.

49. Gupta R, Kushawaha PK, Samant M, Jaiswal AK, Baharia RK, Dube A. 2012. Treatment of Leishmania donovani-infected hamsters with miltefosine: analysis of cytokine mRNA expression by real-time PCR, lymphoproliferation, nitrite production and antibody responses. J Antimicrob Chemother2011/11/29. 67:440–443.

50. Shivahare R, Vishwakarma P, Parmar N, Yadav PK, Haq W, Srivastava M, Gupta S, Kar S. 2014. Combination of liposomal CpG oligodeoxynucleotide 2006 and miltefosine induces strong cell-mediated immunity during experimental visceral leishmaniasis. PLoS One2014/04/16. 9:e94596.

51. Tripathi CD, Kushawaha PK, Sangwan RS, Mandal C, Misra-Bhattacharya S, Dube A. 2017. Withania somnifera chemotype NMITLI 101R significantly increases the efficacy of antileishmanial drugs by generating strong IFN-gamma and IL-12 mediated immune responses in Leishmania donovani infected hamsters. Phytomedicine2017/02/06. 24:87–95.

52. Andrade HM, Toledo VP, Pinheiro MB, Guimaraes TM, Oliveira NC, Castro JA, Silva RN, Amorim AC, Brandao RM, Yoko M, Silva AS, Dumont K, Ribeiro Jr. ML, Bartchewsky W,

Monte SJ, Ribeiro Jr. ML, Bartchewsky W, Monte SJ. 2011. Evaluation of miltefosine for the treatment of dogs naturally infected with L. infantum (=L. chagasi) in Brazil. Vet Parasitol2011/06/07. 181:83–90.

53. Sane SA, Shakya N, Haq W, Gupta S. 2010. CpG oligodeoxynucleotide augments the antileishmanial activity of miltefosine against experimental visceral leishmaniasis. J Antimicrob Chemother2010/05/25. 65:1448–1454.

54. Sharma M, Chauhan K, Shivahare R, Vishwakarma P, Suthar MK, Sharma A, Gupta S, Saxena JK, Lal J, Chandra P, Kumar B, Chauhan PM. 2013. Discovery of a new class of natural product-inspired quinazolinone hybrid as potent antileishmanial agents. J Med Chem2013/04/25. 56:4374–4392.

55. Manna L, Reale S, Picillo E, Vitale F, Gravino AE. 2008. Interferon-gamma (INF-gamma), IL4 expression levels and Leishmania DNA load as prognostic markers for monitoring response to treatment of leishmaniotic dogs with miltefosine and allopurinol. Cytokine2008/10/10. 44:288–292.

56. Das S, Pandey K, Rabidas VN, Mandal A, Das P. 2013. Effectiveness of miltefosine treatment in targeting anti-leishmanial HO-1/Nrf-2-mediated oxidative responses in visceral leishmaniasis patients. J Antimicrob Chemother2013/06/04. 68:2059–2065.

57. Parvaneh N, Barlogis V, Alborzi A, Deswarte C, Boisson-Dupuis S, Migaud M, Farnaria C, Markle J, Parvaneh L, Casanova JL, Bustamante J. 2017. Visceral leishmaniasis in two patients with IL-12p40 and IL-12Rβ1 deficiencies. Pediatr Blood Cancer 64.

58. Adriaensen W, Dorlo TPC, Vanham G, Kestens L, Kaye PM, van Griensven J. 2018. Immunomodulatory Therapy of Visceral Leishmaniasis in Human Immunodeficiency Virus-Coinfected Patients. Front Immunol 8:1943.

59. Kip AE, Wasunna M, Alves F, Schellens JHM, Beijnen JH, Musa AM, Khalil EAG, Dorlo TPC. 2018. Macrophage Activation Marker Neopterin: A Candidate Biomarker for Treatment Response and Relapse in Visceral Leishmaniasis. Front Cell Infect Microbiol 8:181.

60. Mildvan D, Spritzler J, Grossberg SE, Fahey JL, Johnston DM, Schock BR, Kagan J. 2005. Serum Neopterin, an Immune Activation Marker, Independently Predicts Disease Progression in Advanced HIV-1 Infection. Clin Infect Dis 40:853–858.

61. Eisenhut M. 2013. Neopterin in Diagnosis and Monitoring of Infectious Diseases. J biomarkers 2013:196432.

62. Mukhopadhyay D, Das NK, Roy S, Kundu S, Barbhuiya JN, Chatterjee M. 2011. Miltefosine effectively modulates the cytokine milieu in Indian post kala-azar dermal leishmaniasis. J Infect Dis2011/09/22. 204:1427–1436.

63. Pandey K, Das VNR, Singh D, Das S, Lal CS, Verma N, Bimal S, Topno RK, Siddiqui NA, Verma RB, Sinha PK, Das P. 2012. Post-Kala-Azar Dermal Leishmaniasis in a Patient Treated with Injectable Paromomycin for Visceral Leishmaniasis in India. J Clin Microbiol 50:1478–1479.

64. Pandey K, Singh D, Forwood C, Lal C, Das P, Das V. 2013. Development of post-kala-azar dermal leishmaniasis in AmBisome treated visceral leishmaniasis: A possible challenge to elimination program in India. J Postgrad Med 59:226.

65. Baumer W, Wlaz P, Jennings G, Rundfeldt C. 2010. The putative lipid raft modulator miltefosine displays immunomodulatory action in T-cell dependent dermal inflammation models. Eur J Pharmacol2009/11/18. 628:226–232.

66. Dasgupta B, Roychoudhury K, Ganguly S, Kumar Sinha P, Vimal S, Das P, Roy S. 2003. Antileishmanial drugs cause up-regulation of interferon-gamma receptor 1, not only in the monocytes of visceral leishmaniasis cases but also in cultured THP1 cells. Ann Trop Med Parasitol 97:245–257.

67. Murray HW, Montelibano C, Peterson R, Sypek JP. 2000. Interleukin -12 Regulates the Response to Chemotherapy in Experimental Visceral Leishmaniasis. J Infect Dis 182:1497–1502.

68. Das S, Rani M, Rabidas V, Pandey K, Sahoo GC, Das P. 2014. TLR9 and MyD88 are crucial for the maturation and activation of dendritic cells by paromomycin-miltefosine combination therapy in visceral leishmaniasis. Br J Pharmacol2014/03/29. 171:1260–1274.

69. Khademvatan S, Gharavi MJ, Yousefi E, Saki J. 2011. INOS and IFNgamma gene expression in Leishmania major-infected J774 cells treated with miltefosine. Int J Pharmacol 7:843–849.

70. Verhaar AP, Wildenberg ME, te Velde AA, Meijer SL, Vos ACW, Duijvestein M, Peppelenbosch MP, Hommes DW, van den Brink GR. 2013. Miltefosine suppresses inflammation in a mouse model of inflammatory bowel disease. Inflamm Bowel Dis2013/07/03. 19:1974–1982.

71. Magerl M, Rother M, Bieber T, Biedermann T, Brasch J, Dominicus R, Hunzelmann N,

Jakob T, Mahler V, Popp G, Schäkel K, Schlingensiepen R, Schmitt J, Siebenhaar F, Simon JC, Staubach P, Wedi B, Weidner C, Maurer M. 2013. Randomized, double-blind, placebo-controlled study of safety and efficacy of miltefosine in antihistamine-resistant chronic spontaneous urticaria. J Eur Acad Dermatology Venereol 27:e363–e369.

72. Ritmeijer K, Dejenie A, Assefa Y, Hundie TB, Mesure J, Boots G, Den Boer M, Davidson RN. 2006. A Comparison of Miltefosine and Sodium Stibogluconate for Treatment of Visceral Leishmaniasis in an Ethiopian Population with High Prevalence of HIV Infection. Source Clin Infect Dis 43:357–364.

73. Ansari NA, Ramesh V, Salotra P. 2006. Interferon (IFN)–γ, Tumor Necrosis Factor–α, Interleukin -6, and IFN -γ Receptor 1 Are the Major Immunological Determinants Associated with Post–Kala Azar Dermal Leishmaniasis. J Infect Dis 194:958–965.

74. Nylén S, Sacks D. 2007. Interleukin-10 and the pathogenesis of human visceral leishmaniasis. Trends Immunol 28:378–384.

75. Mears ER, Modabber F, Don R, Johnson GE. 2015. A Review: The Current In Vivo Models for the Discovery and Utility of New Anti-leishmanial Drugs Targeting Cutaneous Leishmaniasis. PLoS Negl Trop Dis 9:e0003889.

76. van der Greef J, Adourian A, Muntendam P, McBurney RN. 2006. Lost in translation? Role of metabolomics in solving translational problems in drug discovery and development. Drug Discov Today Technol 3:205–211.

77. Parish CR. 1971. Immune response to chemically modified flagellin. II. Evidence for a fundamental relationship between humoral and cell-mediated immunity. J Exp Med 134:21–47.

78. Katara GK, Ansari NA, Singh A, Ramesh V, Salotra P. 2012. Evidence for involvement of th17 type responses in post kala azar dermal leishmaniasis (pkdl). PLoS Negl Trop Dis 6:e1703.

79. Kaiko GE, Horvat JC, Beagley KW, Hansbro PM. 2008. Immunological decision-making: how does the immune system decide to mount a helper T-cell response? Immunology 123:326–38.

80. De Cock RFW, Piana C, Krekels EHJ, Danhof M, Allegaert K, Knibbe CAJ. 2011. The role of population PK–PD modelling in paediatric clinical research. Eur J Clin Pharmacol 67:5–16.

81.   Agoram BM, Martin SW, Van Der Graaf PH. 2007. The role of mechanism-based pharmacokinetic–pharmacodynamic (PK–PD) modelling in translational research of biologics. Drug Discov Today 12.

82.   Bramer WM, Giustini D, de Jonge GB, Holland L, Bekhuis T. 2016. De-duplication of database search results for systematic reviews in EndNote. J Med Libr Assoc 104:240–3.

83.   Moher D, Liberati A, Tetzlaff J, Altman DG, Group TP. 2009. Preferred Reporting Items for Systematic Reviews and Meta-Analyses: The PRISMA Statement. PLoS Med 6:e1000097.

Pharmacodynamics of the macrophage activation marker neopterin following miltefosine treatment in Eastern African visceral leishmaniasis patients

Semra Palić[1], Jane Mbui[2], Ahmed M. Musa[3], Joseph Olobo[4], Eltahir A.G. Khalil[3], Jos H. Beijnen[1], Fabiana Alves[5], Alwin D.R. Huitema[1,6], Monique Wasunna[7], Thomas P.C. Dorlo[1]

1. Department of Pharmacy & Pharmacology, The Netherlands Cancer Institute - Antoni van Leeuwenhoek Hospital, Amsterdam, The Netherlands
2. Centre for Clinical Research, Kenya Medical Research Institute, Nairobi, Kenya
3. Institute of Endemic Diseases, University of Khartoum, Khartoum, Sudan
5. Drugs for Neglected Diseases initiative, Geneva, Switzerland
4. Department of Immunology and Molecular Biology, College of Health Sciences, Makerere University, Kampala, Uganda
6. Princess Maxima Center for Pediatric Oncology, Utrecht, the Netherlands
7. Drugs for Neglected Diseases initiative, Nairobi, Kenya

Abstract

Introduction

Visceral leishmaniasis (VL) is an infectious disease caused by *Leishmania* parasites, which replicate inside the macrophage, leading to elevated production of neopterin. Recently, it has been proposed that an increase in neopterin levels at 30 days after treatment may identify patients at risk of relapse. The aim of this study was to establish a pharmacokinetic-pharmacodynamic (PK-PD) relationship between miltefosine and neopterin using PK-PD modeling, and investigate model-based neopterin parameters that could be helpful in determining patients at higher risk of relapse, possibly earlier after treatment.

Methods

Non-linear mixed-effects modeling was employed to develop a population PK-PD model of miltefosine effects on neopterin dynamics, including endogenous production of neopterin. Neopterin concentrations were measured by ELISA in 78 Eastern African VL patients (range age 7-41) from two clinical trials. Various model-derived measures were evaluated as identifiers of risk of relapse.

Results

The developed model includes two modes of neopterin production: a healthy endogenous neopterin steady-state production ($N_{endogenous}$) estimated at 16.6 nmol/L (95% CI: 16.5 -16.7), and a VL-induced steady-state concentration ($N_{disease,base}$) estimated at 70 nmol/L, (95% CI: 61 -78). The individual model-based predictions of the neopterin concentration ratio at day 40 to day 28 of 0.8 was found predictive of relapse with 92.86% sensitivity and 56.25% specificity (AUC ROC 68.6%).

Conclusion

In this study we developed a PK-PD model quantifying the relationship of miltefosine PK with neopterin dynamics in the treatment of VL, which was further employed to identify patients at a higher risk of relapse.

1. Background

Visceral leishmaniasis (VL) or kala-azar is the most severe form of the neglected tropical disease leishmaniasis. VL impairs internal organs such as spleen, liver and the bone marrow, and without proper treatment, VL is fatal. Currently, the alkylphosphocholine agent miltefosine is the only oral drug available for treatment of VL. Miltefosine pharmacokinetic (PK) properties are mainly characterized by the long primary and terminal elimination half-lives (approximately 7 and 35 days, respectively) (1, 2). Several mechanisms of actions have been proposed for miltefosine, including direct killing of the *Leishmania* parasite inside of the macrophage where the parasite survives and replicates, as well as immunomodulation of the cytokines involved in clearance of the infection (3–5). Species of *Leishmania* parasites that cause VL are found to interact with the host immune responses, increasing anti-inflammatory cytokine expression, and suppressing the proinflammatory responses. Activation of the cellular immunity is reflected with an increased concentration of interferon gamma (IFN-γ), as one of the major proinflammatory cytokines.(6) IFN-γ further prompts activation of macrophages to simulate the production of neopterin. Therefore measurement of neopterin concentrations has been indicated to reflect the amount of cells from the reticuloendothelial system, including macrophages and monocytes, hence reflecting the level of proinflammatory or T-helper type 1 cell-derived immune activation (3).

Neopterin is a pteridine produced via guanosine triphosphate cyclohydrolase-I from guanosine triphosphate, by activated macrophages, monocytes, dendritic and epithelial cells. Increased circulating neopterin levels are used as a marker of immune activation and macrophage load in various infectious diseases, such as human immunodeficiency virus (HIV), or intracellular bacterial infections such as tuberculosis (7, 8). Endogenous neopterin plasma concentrations in various healthy populations have been reported around between 8 - 13 nmol/L (9). Due to a VL-driven surge in macrophage response and activation, neopterin levels in VL surpass the levels reported for other infectious diseases. In VL, neopterin levels up to 338 nmol/L (13, 14) have been reported, while in pulmonary tuberculosis and HIV serum neopterin levels were up to 37 nmol/L and 50 nmol/L, respectively (10–12).

Till today, there are no early measurable markers used in clinical practice as (surrogate) endpoint to monitor treatment response in clinical trials for VL (15, 16). Currently, final clinical

cure is established at 6 months, while some studies in India have suggested that even longer follow-up periods up to 12 months are required. A major advantage of an early measurable marker is the possibility to identify patients who are at risk of relapse earlier after treatment. Furthermore, the use of markers in clinical trials may allow designing studies with smaller patient cohorts, which is of essential value in trials concerning neglected tropical diseases (17).

A few studies previously proposed that successful antileishmanial treatment significantly lowered neopterin levels, in contrast to relapsed patients (13, 18). This was further evaluated in a study in adult VL patients from Eastern Africa, where an increase from the end of the treatment till day 60 at follow up was suggested as a potentially useful surrogate endpoint in clinical trials, identifying subjects at higher risk of relapse (14). In the present model-based study, we aimed to characterize in detail plasma neopterin dynamics in response to miltefosine exposure in both pediatric and adult VL patients from Eastern Africa. The secondary aim of this study was to identify neopterin parameters which could serve in identifying individuals at risk of relapse earlier in the treatment follow up itinerary than current clinical evaluations.

2. Methods

2.1 Patients and treatment

Data from Eastern African VL patients from two trials investigating miltefosine monotherapy were included in the current analysis. 48 patients (age 7-41) were treated with the conventional miltefosine regimen (median 2.4 mg/kg/day) in Kenya and Sudan (22), while 30 pediatric patients (age 4-12) were treated with the allometric weight-based dosing regimen (median 3.2 mg/kg/day) in Kenya and Uganda (23). Both studies were registered with ClinicalTrials.gov: numbers NCT01067443, for the conventional regimen, and NCT02431143 for the allometric dosing regimen (22). Eligible patients in both trials were primary VL cases and were enrolled in trials upon confirmed parasitological assessment. All patients were HIV-negative and did not present any underlying disease associated with splenomegaly, or concomitant infection such as tuberculosis. In both trials miltefosine was administered once daily during 28 consecutive days. Initial clinical cure was determined at the end of the

treatment at day 28, while the final cure was evaluated at six months after the end of the treatment, defined by the absence of the parasite by microscopy.

2.2 Ethics

Ethical approvals were granted by the national and local Ethics Committees in Kenya (Kenya Medical Research Institute) and Sudan (Institute of Endemic Diseases) for the clinical trial applying the conventional dosing regimen. In addition, an ethical approval was also granted by the London School of Hygiene and Tropical Medicine (LSHTM) Ethics Committee. Furthermore, ethical approvals were granted by Kenya Medical Research Institute, and Makerere University, Kampala, Uganda, for the clinical trial applying the allometric weight-based dosing regimen. Before the initiation of enrollment in both trials, patients were informed of the study in their own language and provided written informed consent. For the pediatric patients, the same was provided to the parents, or legal guardians

2.3 Blood sampling

In both trials, plasma samples were collected for each patient on the first day of treatment, then at day 7, 14, and 28 of treatment, while in the allometric trial an additional sample was taken on day 21 after the treatment initiation. At day 1 samples were drawn prior to the first miltefosine administration, and 4 or 8 hours after the first dose. On other days the blood samples were drawn prior the dose. Additionally, two samples were available at follow-up period: day 56-60 and day 210. Samples were kept at minimally -20°C during storage and transport until they were analyzed.

2.4 Analytical method

Miltefosine concentrations were quantified using a previously validated method of liquid chromatography coupled to tandem mass spectrometry (LC-MS/MS), which has a lower limit of quantification of 4 ng/mL. At the lowest levels, precision of the intra-assay was lower than 10.7%, while the inter-assay was 10.6%, and accuracies in the range of 95.1 − 109% (24). In addition, neopterin concentrations were quantified using commercially available ELISA kits purchased from Demeditec Diagnostics GmbH. For the allometric weight-based regimen trial, each sample was analyzed in duplicates and the average value was subsequently used, while only one measurement per sample was available for the conventional dosing trial. The

calibration curve ranged from 1.4 to 111 nmol/L of neopterin and was fit according manufacturer's instructions using a 4-parameter logistic model using Graphpad Prism 7 (La Jolla, CA, USA). The ^{10}log values of the net luminescence at 595 nm were plotted against the neopterin concentration. The optical density was measured using a 96-well plate reader EL808 (Biotek, Winooski, VT, USA). Calibration curves were not forced through zero, and back-calculated concentrations had to be within 15% of the nominal concentrations for all five calibration standards.

2.5 PK-PD model development

2.5.1 Software

Non-linear mixed effects (NLME) modeling was carried out using NONMEM® version 7.3 (ICON Development Solutions, Ellicott City, MD, USA) and Perl-speaks-NONMEM (PsN, version 4.7.0 using Pirana as interface (version 2.9.7). Data were analysed using the first-order conditional estimation with interaction (FOCE+I) estimation method, while R and R Studio (version 3.6.3 and 3.4.3) were used for graphical evaluation (25).

2.5.2 Structural model

NLME modelling was performed using as a base the structural PK models which were previously developed and validated (2, 19). The structural PK models for both regimens is a two-compartment model following first order absorption and linear elimination, with 69-72% lower bioavailability estimated at the treatment start, presumably due to initial malnourishment and malabsorption. Moreover, the PK model developed based on the allometric dosing regimen further accounts for the effects of increase in cumulative dose (mg/kg/day), reflected in lower miltefosine accumulation in plasma (2). In this regard, previously estimated PK parameters were fixed and subsequently used to link with the PD, with the PK observations kept in the modeling dataset according to the methods of sequential population PK-PD analysis (26). Next, upon graphical inspection of the PD data, various miltefosine concentration – effect relationships were explored to model the neopterin dynamics, including a direct effect, an indirect effect and a turnover model (27, 28). Lastly, a mixture model was assessed, using the $MIXTURE subroutine in NONMEM to differentiate patients who exhibited a neopterin rebound after end of treatment from those who did not (29).

2.5.3 Stochastic model and covariate analysis

BSV within was tested on all PD parameters according to *Eq. 2*:

$$P_i = P \cdot e^{\eta P i} \qquad\qquad Eq.\ 2$$

where P_i is the individual parameter estimate for an individual *i*, and P is the population parameter estimate, and where η_i assumes to distributed N (0, ω^2).

Furthermore, residual unexplained variability (RUV) was explored using additive, proportional, and combined error models, with an example equation for the proportional error model given in *Eq. 3.*

$$Y_{obs,ij} = Y_{pred,ij} \cdot (1 + \varepsilon_{p,ij}) \qquad\qquad Eq.\ 3$$

where $Y_{obs,ij}$ represents the observed concentration for an individual i and observation j, and respectively $Y_{pred,ij}$ represents the individual predicted concentration, while $\varepsilon_{p,ij}$ represents the proportional error assuming N (0, σ^2).

Covariate analysis was conducted to establish whether available covariates could explain the estimated BSV on PD parameters. Covariates were analysed univariately following scientific plausibility and tested statistically (P value <0.05) by using the OFV. Age, sex, and body mass index (BMI), as well as VL relapse were screened as potential covariates.

2.5.4 Model evaluation

Standard measure of model fit to the data was assessed by the OFV which is minus twice the log likelihood of the data. Therefore, nested hierarchical models were discriminated based on their OFVs. A decrease of 3.84 points in OFV corresponding to a P value <0.05 was considered significant (chi-squared distribution with 1-degree freedom). Parameter estimate precisions was obtained by sampling importance resampling (SIR). (30), Moreover, the confidence interval (CI) for the parameter estimates, the correlation matrix and visual improvement of the model fit to data assessed by the standard GOF plots were used for model evaluation.

2.5.5 Evaluation of the model-based predictions of the treatment outcome

The developed PK-PD model was used to estimate the neopterin concentration between end of treatment (day 28) and first follow up point (day 60), with the goal of evaluating whether the patients who are at risk of relapse could already be identified earlier than currently defined in the clinical trials. In this respect, the individual model-derived measures of neopterin dynamics were evaluated as a predictor of relapse using area under the receiver operating characteristics (AUC ROC) curves.

3. Results

3.1 Patients and samples

Neopterin plasma concentrations and miltefosine PK data were available from 78 Eastern African VL patients included in two clinical trials where a 28-day regimen of miltefosine monotherapy was administered *(Table 1)*. In total 478 neopterin plasma concentrations during and after miltefosine treatment were available *(Figure 1)*.

Table 1: Demographics of the patients included in the study

Total number of patients	78
Age (years)	9 (4 – 41) *
Sex (% of females)	37%
Weight (kg)	23 (13 – 65) *
Height (cm)	132 (99 – 185) *
Observed neopterin at the treatment start (nmol/l)	89.76 (15.9 – 338) *
Neopterin at the end of treatment (nmol/l)	27.6 (5.5 – 117.2) *
Miltefosine treatment exposure represented by the AUC (µg · day/mL)	381.5 (223.8 – 769.2) *

* Values represent the median (range), AUC: area under the miltefosine plasma concentration-time curve from day 0 until the end of treatment (day 28)
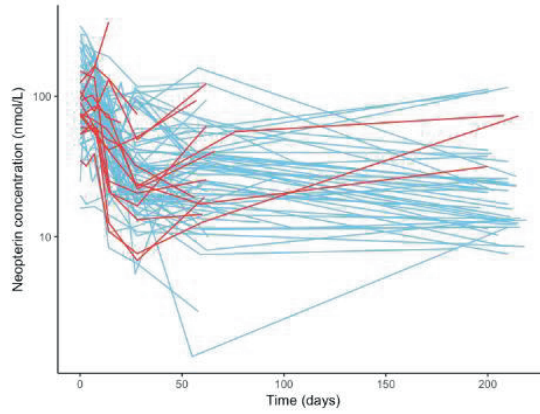
Figure 1: Observed neopterin dynamics stratified for the treatment outcome, where cured patient profiles are shown in blue, and relapsed in red.

3.2 The PK-PD model

Since neopterin is an endogenous compound, it is normally present in plasma of healthy individuals. Therefore, two separate modes of the neopterin production were considered given by the set of *Eq. 1.1 and 1.2*: 1) endogenous (healthy) production of neopterin representing a normal baseline, expressed as a steady-state concentration ($N_{endogenous}$), and 2) VL disease-activated production of neopterin representing a disease baseline, expressed as a concentration at the start of treatment indicated by $N_{disease,base}$. In the final model, the effect of miltefosine was defined as a second-order elimination rate constant (k_{dis}) on $N_{disease,base}$. After treatment, neopterin concentrations increased in a subset of patients, probably due to a regrowth of parasites. Thus, an exponential growth rate λ including between-subject variability (BSV) was implemented in the model after the end of the treatment to characterize this increase.

For t ≤ 28 days: $\frac{dN_{disease}}{dt} = - k_{dis} \cdot C_m \cdot N_{disease}$

For t > 28 days: $\frac{dN_{disease}}{dt} = - k_{dis} \cdot C_m \cdot N_{disease} + \lambda \cdot N_{disease}$ *Eq. 1.1*

$Y = N_{disease} + N_{endogenous} \cdot (1 + \varepsilon)$ *Eq. 1.2*

where $N_{disease}$ is disease-activated neopterin concentration that varies over time due to the drug effect, and is initialized in the model using an estimated steady-state baseline

(N$_{disease,base}$). Furthermore, N$_{endogenous}$ is the model-estimated endogenous steady-state neopterin, k$_{dis}$ is the disease inactivation rate, C$_m$ is the individual model-predicted plasma concentration of miltefosine in plasma, λ is the neopterin first-order regrowth rate after the end of treatment, while Y is the observed neopterin concentration including the residual error, with ε representing the proportional error assuming N (0, σ^2). In the final model, between-subject variability (BSV) was included on N$_{disease,base}$ (change (Δ) in the objective function value (OFV) – 313) , k$_{dis}$ (ΔOFV – 119) and λ (ΔOFV – 6) , while RUV was described by a proportional error model *(Eq. 3).* Available covariates were tested on all parameters, but no significant parameter – covariate relationship were identified.
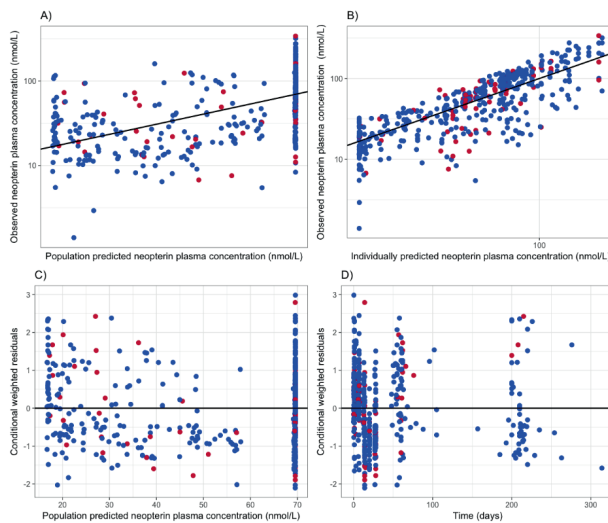
Figure 2: Goodness of fit plots for the final PK-PD model A) Observed versus individually predicted neopterin concentrations, B) observed versus population predicted neopterin concentrations, C) conditional weighted residuals (CWRES) versus population predicted concentrations, and D) CWRES versus time. Blue dots represent cured patients, while red dots represent relapsed patients.

Model-based estimates of the PD parameters and corresponding precision of parameter estimates are provided in the *Table 2*. The typical N$_{disease,base}$ was estimated at 70 nmol/L, (95% CI: 61.7 -78.6) but was variable among patients (BSV 30.4%, 95% CI: 21.3 – 45.6 %), while

$N_{endogenous}$ was estimated at 16.6 nmol/L (95% CI: 16.5 – 16.6). Moreover, during follow-up neopterin plasma levels increased again in a subset of patients (11 out of 78). The population value for λ was estimated at 0.0055 day^{-1}, with very high variability among patients (BSV 364%, 95% CI: 167 - 390 %) allowing empirical Bayesian estimates to approach zero for λ in patients who presented no increase in neopterin levels after end of treatment. However, inclusion of the multimodal distribution (implemented with $MIXTURE subroutine) on λ did not result in successful model convergence and was, therefore, not included in the model. Precision of the parameter estimates is summarized in the *Table 2*. Goodness of fit (GOF) plots colored for the clinical outcome indicate that the final model showed acceptable fit of the data during and after miltefosine treatment *(Figure 2)* for both cured and patients who relapsed.

Table 2: Pharmacodynamic model parameter estimates for neopterin pharmacodynamics in response to treatment of VL with miltefosine

Parameter (unit)		Model estimate (95 % CI*)
Disease inactivation rate constant	k_{dis} *(nmol^{-1}day^{-1})*	0.0073 (0.066 - 0.0079)
Neopterin disease baseline	$N_{disease,base}$*(nmol/l)*	70 (61.7 -78.6)
Neopterin healthy baseline	$N_{endogenous}$ *(nmol/l)*	16.6 (16.5 – 16.7)
Rate of the post-treatment neopterin increase	λ *(day^{-1})*	0.00055 (0.00055-0.00056)
BSV $N_{disease,base}$	*(%)*	165 (137 - 281 %)
BSV $N_{endogenous}$	*(%)*	30.4 (21.3 – 45.6 %)
BSV Rate of the post-treatment neopterin regrowth λ	*(%)*	364 (167 – 390 %)
Proportional error	*(%)*	38.7 (38.6 – 38.9 %)

*Values obtained using SIR

3.3 Model-based estimates for predicting the clinical outcome

In order to evaluate treatment response, model-based predictions of individual patient estimates for the various neopterin parameters at the end of the treatment and during follow up were evaluated by means of identifying those patients who may be at risk of relapse. From the last day of treatment (day 28) to the first follow up point (day 60), median neopterin increase in relapsed patients was 12 nmol/L, and it varied from a decrease of 5 nmol/L to an increase of 74.4 nmol/L. In cured patients, a mean neopterin decrease of 30.8 nmol/L was observed. Neopterin slightly elevated after treatment end in a few patients who were clinically evaluated as cure, with one patient surprisingly increasing by 117 nmol/L. In the box and whisker plots displayed in *Figure 3*, we show that the individual model-based predictions of neopterin concentrations at day 40 could be used to identify patients at risk of relapse. As represented in *Figure 4,* the ratio of individual model-based predicted neopterin concentrations at day 40/day 28 resulted in 92.86 % sensitivity and 56.25% specificity (AUC ROC 68.6% (CI: 61.1 – 76.2) in predicting clinical relapse at a cut off value 0.8. As such, despite suboptimal specificity of the current marker, its high sensitivity suggests this could be used to identify patients who are at higher risk of clinical relapse already at day 40, who could for instance be more intensively monitored.
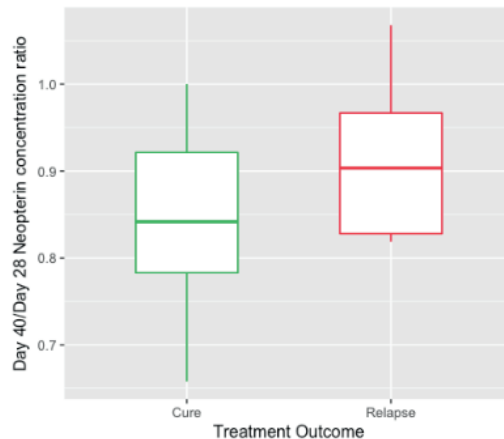
Figure 3: Box plots distributional characteristics for the post hoc parameter estimates of the neopterin concentration ratios at day 40 to day 28 stratified for the treatment outcome. The middle line within boxes represents the median, while the lower and upper line of the boxes are 25th and 75th percentiles of the interquartile range (IQR).
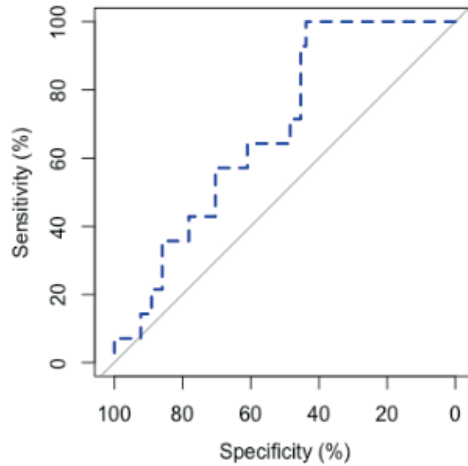
Figure 4: Area under the receiver operating characteristics (AUC ROC) curve of individual model-based predictions of neopterin concentrations as predictors of clinical relapse (cured patients=0, relapsed patients=1). Blue line represents concentration ratio from the day 40 over day 28. Integrated area under the curve (AUC) is 68.6 %.

4. Discussion

This is the first study to present an integrated PK-PD model neopterin concentrations in response to miltefosine treatment of VL in both pediatric and adult patients. Our previously developed PK models were used as the basis in the current sequential PK-PD analysis (2, 19). Given the slow accumulation of miltefosine in plasma, stable neopterin levels are observed in the first treatment week. Consequently, neopterin decline due to drug effect is expected with delay, as observed in graphical inspection of the data. Therefore, we included two modes of the neopterin production quantified by $N_{endogenous}$ and $N_{disease,base}$ in combination with a drug-driven neopterin elimination of $N_{disease,base}$. In this respect, neopterin dynamics were modelled with a direct effect model following a second-order drug-driven elimination. After the end of treatment, neopterin increased in a subset of patients, possibly indicating a (transient) recrudescence of *Leishmania* parasites or macrophage activation in these individuals. Interestingly not all patients with increased neopterin concentrations post-treatment were assessed as clinical relapses upon the final evaluation at 6 months, illustrating diverse immune responses among subjects. An exponential regrowth rate λ was included in the

model to describe this effect, with estimated variability across individuals. This resulted in a skewed distribution of BSV on λ, which must be cautiously taken into account when considering simulations based on this model.

A decrease in neopterin is widely used in evaluating cure in various infectious diseases (7, 20, 21). But up to date, only a few studies evaluated neopterin in the context of VL treatment (13, 18). In light of the other antileishmanial agents, it has been reported that successful treatment of Brazilian VL with antimonial therapy substantially decreased neopterin levels in comparison to relapsed patients when evaluated 30 days post-treatment (13). Recently, a single study reported neopterin concentrations in a patient cohort treated for VL with the miltefosine conventional dosing regimen, also included in the current model-based analysis. Here, it was proposed that an increase by 220% (2.2 ratio) of measured neopterin concentration of day 60 over day 28 may serve as an indicator of the patients who are at relapse risk (14). In comparison, with a model-based approach this study indicates that a decrease less than 20% (ratio of 0.8) of day 40 over day 28 could help identifying patients at higher risk of relapse. The identified ratio at day 40 over day 28 was below 1 because miltefosine, with a long elimination half-live, continues to eliminate neopterin production long after treatment.

The model-based predicted day 40/day 28 neopterin concentration ratio had a high sensitivity towards identifation of patients who eventually relapse, which provides a basis for intensified clinical follow-up for these patients. However, the low associated specificity of this marker suggests that its value as 'test of cure' on day 40 may be rather limited. This limitation is underlined by the observed increase in neopterin levels after treatment in patients who were clinically cured, therefore contributed to a lower specificity of neopterin parameters as surrogate markers of the clinical outcome in the present study. It could be speculated that increase in neopterin in these patients could be attributed to a possibly wide range of other inflammations, and/or stressors which are common in these patient populations. Moreover, these observations could also indicate asymptomatic carriers: patients who harbour *Leishmania* parasites, but have already developed effective immune responses in combating the disease.

Furthermore, in line with previous reports, individual patient estimates of $N_{disease,base}$ from the present study also illustrate that elevation of neopterin in VL largely surpass any other infectious disease (up to 32-fold), with no significant differences in neopterin dynamics

between children and adults, or sexes (13, 18). However, healthy endemic control levels for neopterin have not been reported in Eastern African population previously. We estimated an endogenous production of neopterin in an Eastern African VL patient population after the end of treatment indicated an endogenous healthy concentration of 16.6 nmol/L versus 8-13 nmol/L reported in other patient populations (9).

This population PK-PD analysis provides a more mechanistic understanding of the drug concentration-time-effect relationships between miltefosine and neopterin and disentangles the fraction of neopterin which is either disease-activated or associated with endogenous production, allowing the prediction of neopterin concentrations beyond those observed at sampling times. Hence, model-predicted neopterin concentrations for various time points after the end of treatment could be evaluated for their power to identify patients at risk of relapse. Given that model-based Bayesian estimates are derived from the same distribution, performing formal statistical tests was not appropriate. However, descriptive statistics analyses as illustrated by ROC analysis and box plots suggest that the neopterin concentration ratio day 40/day 28 provides helpful information for identifying patients at increased risk of relapse.

In conclusion, we developed a PK-PD model quantifying the relationship of miltefosine PK on neopterin dynamics in the context of VL, including an endogenous non-disease-driven production of neopterin. This model was used to derive a parameter which appeared highly sensitive in differentiating patients at higher risk of relapse, which could potentially be used to intensify clinical monitoring, for example by considering more frequent follow ups.

Funding

References

1. Dorlo TPC, Balasegaram M, Beijnen JH, de Vries PJ. 2012. Miltefosine: a review of its pharmacology and therapeutic efficacy in the treatment of leishmaniasis. J Antimicrob Chemother 67:2576–2597.

2. Palić S, Kip AE, Beijnen JH, Mbui J, Musa A, Solomos A, Wasunna M, Olobo J, Alves F, Dorlo TPC. Characterizing the non-linear pharmacokinetics of miltefosine in paediatric visceral leishmaniasis patients from Eastern Africa.

3. Palić S, Bhairosing P, Beijnen JH, Dorlo TPC. 2019. Systematic Review of Host-Mediated Activity of Miltefosine in Leishmaniasis through Immunomodulation. Antimicrob Agents Chemother 63.

4. Verhaar AP, Wildenberg ME, Peppelenbosch MP, Hommes DW, Van Den Brink GR. 2014. Repurposing miltefosine for the treatment of immune-mediated disease? J Pharmacol Exp Ther 350:189–195.

5. Mukhopadhyay D, Das NK, Roy S, Kundu S, Barbhuiya JN, Chatterjee M. 2011. Miltefosine effectively modulates the cytokine milieu in Indian post kala-azar dermal leishmaniasis. J Infect Dis 2011/09/22. 204.

6. Badaro R, Johnson WD. 1993. The role of interferon-gamma in the treatment of visceral and diffuse cutaneous leishmaniasis. J Infect Dis 167 Suppl:S13-7.

7. Hosp M, Elliott AM, Raynes JG, Mwinga AG, Luo N, Zangerle R, Pobee JO, Wachter H, Dierich MP, McAdam KP, Fuchs D. 1997. Neopterin, beta 2-microglobulin, and acute phase proteins in HIV-1-seropositive and -seronegative Zambian patients with tuberculosis. Lung 175:265–75.

8. Sacktor N, Liu X, Popescu M, Marder K, Stern Y, Mayeux R. 1995. Serum Neopterin Level Predicts Hiv-Related Mortality But not Progression to Aids or Development of Neurological Disease in Gay Men and Parenteral Drug Users. Arch Neurol 52:676–679.

9. Werner ER, Bichler A, Daxenbichler G, Fuchs D, Fuith LC, Hausen A, Hetzel H, Reibnegger G, Wachter H. 1987. Determination of neopterin in serum and urine. Clin Chem 33.

10. Cesur S, Aslan T, Hoca NT, Çimen F, Tarhan G, Çifçi A, Ceyhan I, Şipit T. 2014. Clinical importance of serum neopterin level in patients with pulmonary tuberculosis. Int J

Mycobacteriology 3:5–8.

11. Fuchs D, Hausen A, Kofler M, Kosanowski H, Reibnegger G, Wachter H. 1984. Neopterin as an index of immune response in patients with tuberculosis. Lung 162:337–46.

12. Mildvan D, Spritzler J, Grossberg SE, Fahey JL, Johnston DM, Schock BR, Kagan J. 2005. Serum Neopterin, an Immune Activation Marker, Independently Predicts Disease Progression in Advanced HIV-1 Infection. Clin Infect Dis 40:853–858.

13. Schriefer A, Barral A, Carvalho EM, Barral-Netto M. 1995. Serum soluble markers in the evaluation of treatment in human visceral leishmaniasis. Clin Exp Immunol 102:535–40.

14. Kip AE, Wasunna M, Alves F, Schellens JHM, Beijnen JH, Musa AM, Khalil EAG, Dorlo TPC. 2018. Macrophage activation marker neopterin: A candidate biomarker for treatment response and relapse in visceral leishmaniasis. Front Cell Infect Microbiol 8.

15. Carrillo E, Moreno J. 2019. Editorial: Biomarkers in Leishmaniasis. Front Cell Infect Microbiol 9:388.

16. Esteves S, Costa I, Amorim C, Santarem N, Cordeiro-da-Silva A. 2018. Biomarkers in Leishmaniasis: From Basic Research to Clinical ApplicationBiomarker - Indicator of Abnormal Physiological Process. InTech.

17. Lesko LJ, Atkinson AJ. 2001. Use of biomarkers and surrogate endpoints in drug development and regulatory decision making: criteria, validation, strategies. Annu Rev Pharmacol Toxicol 41:347–66.

18. Hamerlinck FF, van Gool T, Faber WR, Kager PA. 2000. Serum neopterin concentrations during treatment of leishmaniasis: useful as test of cure? FEMS Immunol Med Microbiol 27:31–4.

19. Dorlo TPC, Kip AE, Younis BM, Ellis SJ, Alves F, Beijnen JH, Njenga S, Kirigi G, Hailu A, Olobo J, Musa AM, Balasegaram M, Wasunna M, Karlsson MO, Khalil EAG. 2017. Visceral leishmaniasis relapse hazard is linked to reduced miltefosine exposure in patients from Eastern Africa: a population pharmacokinetic/pharmacodynamic study. J Antimicrob Chemother 72:3131–3140.

20. Demian S, Hamdy El-Sayed M, El-Sedfy A, Ahmed A, Ahmedai F. 2014. The role of

neopterin in patients with primary and metastatic breast cancer: correlation with clinicopathological data. J Immunother Cancer 2:P147.

21. Melichar B, Solichová D, Melicharová K, Malírová E, Cermanová M, Zadák Z. Urinary neopterin in patients with advanced colorectal carcinoma. Int J Biol Markers 21:190–8.

22. Wasunna M, Njenga S, Balasegaram M, Alexander N, Omollo R, Edwards T, Dorlo TPC, Musa B, Ali MHS, Elamin MY, Kirigi G, Juma R, Kip AE, Schoone GJ, Hailu A, Olobo J, Ellis S, Kimutai R, Wells S, Khalil EAG, Strub Wourgaft N, Alves F, Musa A. 2016. Efficacy and Safety of AmBisome in Combination with Sodium Stibogluconate or Miltefosine and Miltefosine Monotherapy for African Visceral Leishmaniasis: Phase II Randomized Trial. PLoS Negl Trop Dis.

23. Mbui J, Olobo J, Omollo R, Solomos A, Kip AE, Kirigi G, Sagaki P, Kimutai R, Were L, Omollo T, Egondi TW, Wasunna M, Alvar J, Dorlo TPC, Alves F. 2018. Pharmacokinetics, safety and efficacy of an allometric miltefosine regimen for the treatment of visceral leishmaniasis in Eastern African children: an open-label, phase-II clinical trial. Clin Infect Dis.

24. Dorlo TPC, Hillebrand MJX, Rosing H, Eggelte TA, de Vries PJ, Beijnen JH. 2008. Development and validation of a quantitative assay for the measurement of miltefosine in human plasma by liquid chromatography–tandem mass spectrometry. J Chromatogr B 865:55–62.

25.   R Core Team (2015). R: A language and environment for statistical computing. R Foundation for Statistical Computing, Vienna, Austria.

26. Zhang L, Beal SL, Sheiner LB. 2003. Simultaneous vs. Sequential Analysis for Population PK/PD Data II: Robustness of Methods. J Pharmacokinet Pharmacodyn 30:405–416.

27. Jusko WJ. 1971. Pharmacodynamics of chemotherapeutic effects: Dose-time-response relationships for phase-nonspecific agents. J Pharm Sci 60:892–895.

28. Mager DE, Jusko WJ. 2008. Development of translational pharmacokinetic-pharmacodynamic models. Clin Pharmacol Ther 83:909–12.

29. Carlsson KC, Savi RM, Hooker AC, Karlsson MO. 2009. Modeling subpopulations with the $MIXTURE subroutine in NONMEM: Finding the individual probability of belonging

to a subpopulation for the use in model analysis and improved decision making. AAPS J 11:148–154.

30.   Dosne AG, Bergstrand M, Karlsson MO. 2017. An automated sampling importance resampling procedure for estimating parameter uncertainty. J Pharmacokinet Pharmacodyn 44:509–520.

Skin pharmacokinetics and pharmacodynamics of miltefosine

Skin pharmacokinetics of miltefosine in the treatment of post kala-azar dermal leishmaniasis

Semra Palić[1], Ignace C. Roseboom[1], Shyam Sundar[2], Dinesh Mondal[3], Pradeep Das[4], Krishna Pandey[4], Sheeraz Raja[5], Suman Rijal[5], Abdullah Hamadeh[6], Paul R.V. Malik[6], Jos H. Beijnen[1], Alwin D.R. Huitema[1,7,8], Erik Sjögren[9,10], Fabiana Alves[11], Thomas P.C. Dorlo[1]

1. Department of Pharmacy & Pharmacology, The Netherlands Cancer Institute - Antoni van Leeuwenhoek Hospital, Amsterdam, The Netherlands
2. Banaras Hindu University, Varanasi, India
3. Centre for Nutrition and Food Security (CNFS), International Centre for Diarrhoeal Disease Research, Bangladesh (ICDDR,B), Dhaka, Bangladesh
4. Rajendra Memorial Research Institute of Medical Sciences (RMRIMS), Patna, India
5. Drugs for Neglected Diseases initiative (DNDi) South Asia, New Delhi, India
6. School of Pharmacy, University of Waterloo, Ontario, Canada
7. Department of Pharmacology, Princess M xima Center for Pediatric Oncology, Utrecht, the Netherlands
8. Department of Clinical Pharmacy, University Medical Center Utrecht, Utrecht University, Utrecht, The Netherlands.
9. Department of Pharmaceutical Biosciences, Uppsala University, Uppsala, Sweden
10. Pharmetheus AB, Uppsala, Sweden
11. Drugs for Neglected Diseases initiative (DNDi), Geneva, Switzerland

Chapter 4.1

Abstract

Background

Post-kala-azar dermal leishmaniasis (PKDL) is a dermal complication of visceral leishmaniasis (VL). Effective treatments for PKDL are lacking and skin distribution of antileishmanial compounds is unknown in human. The present study evaluated the skin distribution of miltefosine in PKDL patients, to better understand of target-site pharmacokinetics in PKDL.

Methods

Fifty-three PKDL patients were treated with Ambisome (20mg/kg) plus miltefosine by allometric dosing for 21 days. Miltefosine concentrations were measured in plasma on days 7, 14, 21, 29, while a punch skin biopsy was taken on day 22. A physiologically based PK (PBPK) model of miltefosine skin penetration was developed.

Results

Following the allometric weight-based dosing regimen, skin concentrations on day 22 were on median 48.1 µg/g (IQR: 24.1 − 66.7 µg/g) and in plasma 34.3 µg/ml (IQR: 26.8 − 62.4 µg/ml). The median concentration ratio of skin to plasma was 1.73 (IQR: 0.86 − 2.65). Approximately 90% of PKDL patients had exposure in the skin above a suggested PK target associated with *in vitro* activity (EC$_{90}$ of 10.6 mg/L). Simulations showed that residence time of miltefosine in the skin is nearly twice longer compared to blood plasma, estimated by mean residence time at 720 hours versus 397 hours respectively.

Conclusion

The present study provides the first accurate measurements of miltefosine penetration in the skin, estimating to which extent the parasite-loaded macrophages in the skin are exposed to miltefosine. As such, combined with parasitological and clinical data, this is a promising start for future optimization of miltefosine in treatment of PKDL.

1. Introduction

Leishmaniasis is an infectious disease caused by the protozoan parasite *Leishmania*, transmitted by sand flies. By primarily affecting the poorest populations, leishmaniasis remains one of the most neglected tropical diseases (1). The most common clinical presentation of the disease, which affects up to 2 million people per year, is cutaneous leishmaniasis (CL), leading to skin ulcers and lesions at the site of infection (2). The most severe form of leishmaniasis is visceral leishmaniasis (VL) or kala azar (3). VL affects internal organs, and is lethal within months without adequate treatment. In addition, some patients who were previously treated for VL develop post kala-azar dermal leishmaniasis (PKDL) months or years after treatment. Clinical manifestation of PKDL include skin rash in form of macular, nodular or mixed lesions (4, 5). In South Asia, PKDL develops in 5 – 10 % of VL treated patients within an average of 2 years after VL treatment and with predominance of the macular form (4). As *Leishmania* parasites reside in the skin, sand flies feeding on PKDL patients may become infected and further transmit the parasite. Therefore, patients with chronic PKDL serve as reservoirs for VL transmission, and all patients should be treated.

Miltefosine is the first and still only oral agent available in treatment of leishmaniasis. It is an alkylphosphocholine compound, consisting of long-chain alcohols in phosphocholine esters (6). Due to its chemical structure, with its long hydrophobic tail, miltefosine has a high affinity for lipid rafts, and is able to incorporate in the lipid bilayers of cell membranes, without disrupting the membrane itself (7, 8). With respect to pharmacokinetics (PK), miltefosine is slowly absorbed from the gastrointestinal tract, with reported saturable absorption in both preclinical and clinical studies (9, 10). In addition, plasma clearance is low, with elimination half-lives estimated at 7 and ~30 days (6). Due to these PK properties, miltefosine accumulates in plasma until the end of treatment (11, 12).

Treatment regimens with miltefosine have been established for CL and VL. In South Asia, current recommended treatment for PKDL is miltefosine for long period of 12 weeks, while recent studies have also shown the efficacy of Ambisome for the treatment of PKDL. Long treatment duration of 12 weeks together with poor tolerability may hinder treatment compliance. In addition, women of childbearing age require 8 months of contraception (during treatment and 5 months after treatment) due to miltefosine teratogenicity. Shorter

treatment durations are therefore needed, urging for adequate evidence-based treatment for PKDL. Due to a lack of studies investigating exposure-response relationships for miltefosine in the treatment of PKDL, it remains challenging to further optimize and rationalize treatment. The main burden of parasite biomass in PKDL is located in the dermis of the skin, however, no investigations have been performed on target-site exposure in the skin of any of the currently used antileishmanial drugs in the treatment of any type of dermal leishmaniasis (13). Such PK studies are pivotal to further optimize and rationalize treatment regimens for the various different clinical presentations of leishmaniasis. In the present study, we aimed to provide the first data on miltefosine exposure in skin tissue from PKDL patients treated with miltefosine, as a proxy of target-site exposure at the site of the parasite infection. Furthermore, we used a physiologically based PK (PBPK) modelling approach to further elucidate miltefosine PK in both skin and plasma after oral administration as a framework for target-site tissue predictions.

2. Patients and Methods

2.1 Clinical studies and patient cohorts

2.1.1 PKDL study

The clinical data originated from a non-comparative, open label, randomized phase II trial, which was conducted to assess the safety and efficacy of Ambisome monotherapy (total dose of 20 mg/kg) and Ambisome (20 mg/kg) in combination with miltefosine (allometric dosing) in treatment of PKDL patients from Bangladesh (study site of the International Centre for Diarrhoeal Disease Research) and India (study sites of Rajendra Memorial Research Institute of Medical Sciences, Patna and Kala Azar Medical Research Centre, Muzzafarpur, both in Bihar state), which will be reported in another manuscript. In the combination arm, oral miltefosine daily dose was divided in two administrations (with food) according to a previously determined allometric dose for a duration of 21 days. Allometric dosing algorithm increases mg/kg dose for patients with body weight < 30 kg (10, 14), while there is no difference no difference between the allometric scale and conventional dose of 2.5 mg/kg/day for patients > 30 kg. Enrolment criteria included patients with confirmed PKDL by clinical presentation and demonstration of parasites by microscopy skin smear or qPCR, with a documented stable or progressive disease lasting longer than 4 months. The age inclusion

criteria ranged from 6 to 60 years of age, and written informed consent from patients, or patient's parent or guardian for children younger than 18 years was obtained before the treatment initiation. Patients who had a prior treatment for PKDL in the last two years were not included in this study. The study further excluded pregnant and lactating women, women of childbearing potential did not accept to take effective contraception for the duration of treatment and 5 months thereafter, patients with contaminant infection such as tuberculosis or HIV, and severe underlying disease such as cardiac, renal or hepatic diseases, as well as individuals who presented severe malnutrition. Miltefosine plasma samples were collected on day 7, day 14, day 21, and day 29 after treatment onset correspondent to scheduled study visits on days 8, 15, 22 and 30, as well as at three months during the follow up period. In addition, on day 22 (approximately 24 hours after the last dose on day 21) a punch biopsy of the skin was taken from all patients randomized to the Ambisome/miltefosine treatment group.

2.1.2 CL study

Prior PK data from a study in CL patients were used to enable the development of the miltefosine PBPK model, as the PK data from the PKDL trial lacked plasma samples to accurately estimate drug absorption. Thirty-one Dutch military personnel who were infected with CL (*Leishmania major*) and were otherwise systemically healthy were included in the present analysis. A population PK analysis of this trial has been previously reported (15). Plasma samples were obtained at 2, 4, and 6 hours post first dose on the first day of treatment, then weekly during the treatment on an outpatient basis, as well as during 5 months of follow up (15).

2.2 Quantification of miltefosine concentrations

2.2.1 In plasma

Miltefosine was quantified in plasma by liquid chromatography coupled to tandem mass spectrometry (LC-MS/MS) in both studies, previously validated with the lowest limit of quantification (LLOQ) of 4 ng/ml and 10 ng/ml for the CL and PKDL studies, respectively (16). Samples from the PKDL study were measured at the bioanalytical laboratory of Lambda Therapeutic Research, in Ahmedabad, India Samples from the CL study were measured at the

bioanalytical laboratory of the Antoni van Leeuwenhoek hospital / Netherlands Cancer Institute in Amsterdam.

2.2.2 In skin

Collected biopsies were stored at -70 °C and transported on dry ice to the bioanalytical laboratory. Detailed bioanalytical assay development and validation will be reported in a separate publication (manuscript in draft). In short, the assay employed chemical skin tissue digestion, followed by solid phase extraction (SPE) and quantification using LC-MS/MS, similar to the miltefosine plasma PK methodology. Prior to digestion, the skin tissue was washed using 250 µL cold phosphate buffer saline (PBS). This was followed by skin tissue transfer from the washing buffer. The washing buffer was diluted 1:1 (vol/vol) with 4% bovine serum albumin (BSA). Following the washing step, skin tissue was transferred to a clean reaction tube containing 500 µL digestion buffer [2% BSA in 5 mM $CaCl_2$ 25 mM Tris (pH 7.5) and 5 mg/mL collagenase A]. A volume of 50 µL miltefosine-d4 stable isotope internal standard (IS) was added. Subsequently, the skin tissue was incubated overnight at 37°C, using a thermos shaker. After incubation, 275 µL homogenized human skin tissue, including IS, was extracted using phenyl-bonded SPE cartridges. Seven hundred microliter 2.5 M ammonium acetate (pH 4.5) was added to homogenized skin tissue, and centrifuged at 5°C for 5 minutes at 23,100 g, before adding the supernatant to the SPE cartridge. For the SPE cartridge, 1 mL ACN conditioning solvent and subsequently 1 mL 2.5 M ammonium acetate (pH 4.5) activation solvent was added before transferring the supernatant of human skin tissue mixture. The SPE cartridge was then washed with 1 mL water/MeOH (1:1, vol/vol) and eluted using 1.5 mL 0.1% TEA in MeOH. The elution solvent was transferred to glass autosampler vials. The LC-MS/MS instruments were modernized relative to the Dorlo et al. method, employing a UPLC LC-30AD pump with an inline degasser connected to a UPLC LC-30AMCP autosampler, set at 4 °C and CTO-20AC column oven (Nexera X2 series, Shimadzu Corporation, Kyoto, Japan). The validated concentration range for a standardized skin biopsy sample weight of 15 mg, was 4 – 1000 ng/ml, converted into µg/g miltefosine in skin biopsy using the mass of each individual human skin tissue sample. Mass/charge transitions at m/z 408.5 to 125.1 and at 412.6 to 129.2, were monitored for miltefosine and miltefosine-d4, respectively. The relative error was ±2.3% for the concentrations above LLOQ and ±6.6% at LLOQ level. The coefficient of variation

in terms of method precision was <1.9% for the concentrations above LLOQ, and <2.5% at LLOQ level.

2.3 PBPK Model development

This work applied middle-out strategies to facilitate PBPK model development. As such, firstly the PBPK model was developed based on the databases containing drug-specific, system-specific parameters, in vitro and preclinical data regarding miltefosine PK. Next, clinical data was used to optimize the model parameters.

2.3.1 Software

PBPK modeling was performed using the Open System Pharmacology Suite including the modeling software PK-Sim® and MoBi® (Open Systems Pharmacology Suite 9.0, https://www.open-systems-pharmacology.org). Graphical evaluation and statistical analyses were performed in R and R Studio (version 3.6.3 and 3.4.3) (17).

2.3.2 Miltefosine PBPK model building

At start, the miltefosine drug model was built using drug physicochemical properties. The model was informed by available data regarding the processes of absorption, distribution, metabolism and elimination (ADME). The literature was reviewed through the PubMed database to collect drug-specific parameter values. In case of multiple values identified for a parameter, either a range of values was tested on the model, or when that was not possible, each value was tested for its ability to result in a simulation that adequately fitted the observed data. Parameters were identified by minimization of the residuals between observed data and corresponding simulation output adopting the optimization functionality and the Levenberg-Marquardt algorithm included in PK-Sim®.

Secondly, a full body PBPK model was built for miltefosine adopting the generic model for small molecules within the software PK-Sim. This is a full body PBPK model accommodating 15 different organs with rich information regarding the volumes, blood flow rates, metabolism etc (18). Each of these organs further consists of compartments representing the plasma, interstitial and intracellular space. At start, the miltefosine drug model was informed by available data regarding drug physicochemical properties and the processes of absorption, distribution, metabolism and elimination (ADME). The literature was reviewed through the

PubMed database to collect drug-specific parameter values. In case of multiple values identified for a parameter, either a range of values was used as input in the model and tested for its ability to result in a simulation that adequately fitted the observed data. To further improve model performance drug-related parameters were further optimized towards PK data from two clinical studies of miltefosine PK in CL and PKDL patients. Parameters were identified by minimization of the residuals between observed data and corresponding simulation output adopting the optimization functionality and the Levenberg-Marquardt algorithm included in PK-Sim®. On basis of the pooled data of miltefosine concentrations in plasma, distribution and elimination were parametrized by optimizing parameters such as lipophilicity, specific intestinal permeability (transcellular) and specific drug clearance (normalized to the enzyme concentration of 1 μmol/l). In addition, since miltefosine has a long hydrophobic chain, it was expected to be incorporated into the cell membrane, and subsequently enter the cell. This unspecific binding was accommodated in the model by including an unspecific binding partner located at the cell membranes. MoBi was then employed to facilitate simulation output representative for clinical reference skin concentration measurements by creating an observer to trace the concentration of the drug sequestered in the cell membrane, while conserving drug mass balance within the original PBPK model. Membrane binding of miltefosine was explicitly represented by the cell membrane accumulation factor, determined by the equilibrium constant K_d, and the dissociation constant k_{off}. In physiological terms, this factor represents all lipid membranes to which miltefosine binds. In this respect, K_d, and the relative expression of the cell membrane binding partner was optimized in the skin based on the measured miltefosine concentrations in patient biopsies, and then subsequently fixed for the other organs. As this membrane binding is applicable for all organs, the same structure is assumed, thus the estimated corresponding relative expression are scaled by the volumes of organs, plasma compartments and blood flow rates. The mass transfer of the drug from plasma into each organ is then determined by the K_d, volumes of the compartments and the concentration of drug

A number of simulations were performed based on the virtual patient populations representative of the patient cohorts of the included clinical data. For each of simulations, the dosing regimen of miltefosine corresponding to the clinical study was used. For this purpose, virtual populations of individuals were created utilizing the in-built population algorithm in PK-Sim and based on the population characteristics stated in the respective publication. System-dependent parameters, such as age, weight, height, organ weights, blood flow rates, tissue composition, etc., were varied by the implemented algorithm in PK-Sim (19). Simulations of miltefosine in plasma and the skin were used for the final parameter identification step. At last, the optimized PBPK model was used to simulate PK profiles of miltefosine in the spleen and liver.

3. Results

3.1 Patients and data

In total, PK data of 52 patients was available from the PKDL study. The details of patient demographics, as well as the dosing of miltefosine are provided in *table 1*. A total of 273 miltefosine plasma concentrations, and 52 skin biopsies were available for this analysis.

3.2 Observed skin penetration of miltefosine and comparison with exposure in plasma

The miltefosine concentrations that were measured in the collected skin biopsies, represent a combination of intracellular and interstitial concentrations, since extracellular miltefosine and dermal blood were washed off during the sample preparation. Observed miltefosine concentrations in the skin and plasma are presented in the *figure 1*. Miltefosine concentrations in the skin on day 22 were on median 48.1 µg/g (IQR: 24.1 – 66.7 µg/g) while median concentrations in plasma at the same time point were 34.3 µg/ml (IQR: 26.8 – 62.4 µg/ml). High interindividual variability (IIV) in concentrations of miltefosine was observed for both skin and plasma (coefficient of variation (CV)% of 65.9 and 38.8%, respectively). The median concentration ratio of skin to plasma was 1.73 (IQR: 0.86 – 2.65). In total 15 patients had a ratio of skin to plasma < 1, while 37 had this ratio >1. Individual plasma and skin miltefosine concentrations showed a moderate degree of correlation with a correlation coefficient of 0.53.

Table 1: Patient demographics and the dosing of miltefosine for the clinical studies included in the PBPK model development

Parameter	Median value (interquartile range)
PKDL study	
Bangladesh	
Total number of patients	14
Age (years)	27 (15 – 38)
Weight (kg)	44 (39 -53)
Height (cm)	160 (153 – 164)
Dose (mg/kg/day)	2.27 (1.89 – 2.60)
India	
Total number of patients	38
Age (years)	22 (15 – 33)
Weight (kg)	47 (41 -53)
Height (cm)	153 (147 -161)
Dose (mg/kg/day)	2.16 (1.87 – 2.39)

Table 2: Summary of miltefosine drug model parameters used in simulations

Parameter	Value	Unit
Physiochemical parameter		
Molecular weight	407.58	g/mol
Fu (plasma)	0.03	
pKa (acid)	2	
pKa (base)	7.2	
Aqueous diffusion coefficient	$2.9 * 10^{-4}$	cm^2/min
Solubility (at reference pH)	2.5 (7.2)	mg/ml

Fu (plasma): fraction unbound in plasma, pKa: acid dissociation constant
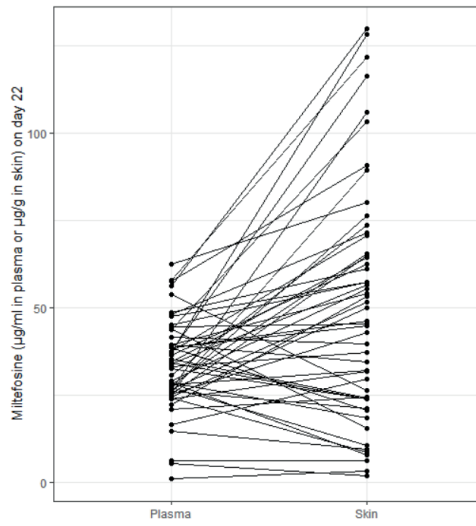
Figure 1: Observed miltefosine concentrations in plasma and skin after 21-day treatment with an allometric weight-based dosing regimen. Individual patient measurements for both plasma and skin are paired by individual lines.

Table 3: Simulated pharmacokinetic parameters of miltefosine following the dosing regimen utilized in the clinical studies

Global PK analyses		
Parameter	Value	Unit
Vss (plasma)	648	ml/kg
Vd (plasma)	664	ml/kg
Vss (phys-chem)	633	ml/kg
Total plasma clearance	0.03	ml/min/kg
Plasma PK		
C_max	101	μmol/l
t_max	576	h
AUC_tEnd	4.46×10^6	μmol*min/l
Elimination Half-Life	282	h
MRT	397	h
Vss (plasma)/F	648	ml/kg
Skin PK		
C_max	124	μmol/l
t_max	528	h
AUC_tEnd	6.29×10^6	μmol*min/l
Elimination Half-Life	286	h
MRT	720	h
Spleen PK		
C_max	128	μmol/l
t_max	576	h
AUC_tEnd	5.65×10^6	μmol*min/l
Elimination Half-Life	283	h
MRT	397	h
Vss (plasma)/F	512	ml/kg
Liver PK		
C_max	182	μmol/l
t_max	576.	h
AUC_tEnd	8.08×10^6	μmol*min/l
Elimination Half-Life	282.	h
MRT	397	h
Vss (plasma)/F	**358**	ml/kg

Vss: volume at steady state, C_max: maximum (compartment) concentration, t_max: the time take to reach C_max, AUC_tEnd: area under the concentration time curve until the end of treatment, MRT: mean residence time

Table 4: Optimized model parameters of the full PBPK model based on the clinical observations of miltefosine in skin and plasma

Optimized Parameter	Value	Unit
Physiochemistry		
Lipophilicity	3	log
Specific intestinal permeability	1.5	cm/min
CLspec*	1.99 *10-3	1/min
Cell membrane binding partner		
K_d	1	µmol/l
k_{off}	101.8	1/min
Reference concentration	100.5	µmol/l

*Specific clearance normalized to the enzyme concentration of 1 µmol/l

K_d: equilibrium constant, k_{off}: dissociation constant

3.3 Miltefosine PBPK model and simulations

Summary of the model parameters utilized in the drug model are given in *table 2.* Simulated PK parameters are given in *table 3.* Identified parameters are in line with previous reports (20) and are summarized in *table 4.* Skin concentrations were used to estimate parameters of the cell membrane binding partner *(table 4).* The developed model adequately predicted typical miltefosine concentrations in the two compartments for which observations were available, i.e. plasma and skin. Accumulation of the drug in the skin exceeded concentrations in plasma, as illustrated in *figure 2,* which is in line with higher median observations of miltefosine in the skin than in patients' plasma. The model-based simulations indicated that the residence time of miltefosine in the skin is nearly twice as long compared to residence time in blood plasma, as estimated by mean residence time (MRT) for the skin at 720 hours compared to 397 hours in plasma. The established PBPK model can be used to derive predicted exposure of other tissues of interests, which should be validated further *(figures 2).* Simulated PK parameters for the spleen and liver are further summarized in the *table 3.* Lastly, the PK target for miltefosine in VL has been previously been suggested as the time the miltefosine concentration is above the in vitro susceptibility EC_{90} value of 10.6 mg/L (12). Present data show that 90% of PKDL patients had exposure in the skin above this target value. Typical time > EC_{90} in the skin as simulated by the PBPK model was 52 days (from day 2 till day 54).

Evaluation of this target was not performed in any PKDL study till now, while could be appropriate since it is same parasite causing different disease manifestations.
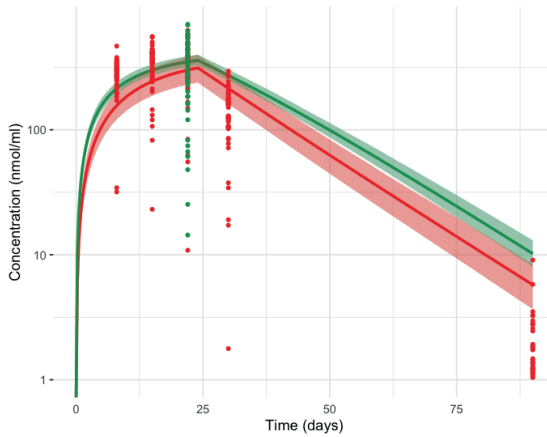

Figure 2: Observed and simulated miltefosine concentrations in plasma and skin tissues. Red dots represent observed concentrations in plasma while red line represents model simulation of miltefosine in plasma. Green dots represent observed miltefosine concentrations in the skin while the green line illustrates the simulated skin concentration based on the PBPK model. Shaded areas indicate 95% CI of the mean.
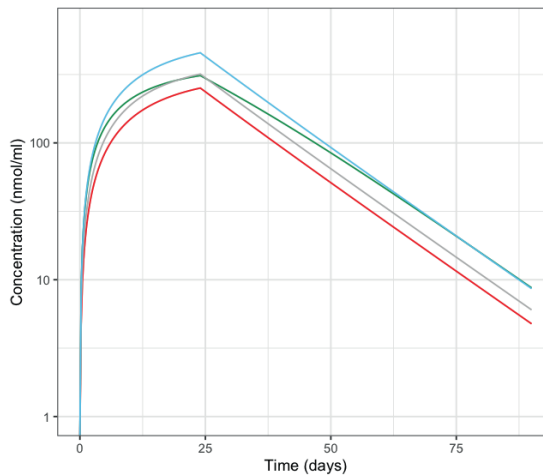
Figure 3: Model based simulations of miltefosine pharmacokinetics in various organs following allometric weight-based dosing regimen in duration of 21 days. Red line (plasma), gray line (spleen), green line (skin), blue line (liver).

4. Discussion

The present study quantified miltefosine exposure in the skin following an allometric weight-based dosing regimen of 21 days in PKDL patients treated with a combination of Ambisome and miltefosine therapy. Several dosing regimens have previously been evaluated for miltefosine in the treatment of VL, such as the conventional linear weight-based dosing (2.5 mg/kg/daily for 28 days) or an allometric weight-based dosing (up to 3.9 mg/kg/day for 28 days), while for PKDL considerably longer 12 week of miltefosine treatment was previously suggested. This study provides the first evidence of miltefosine skin exposure and target-site PK in PKDL, which together with parasitological and clinical response to treatment will be of crucial value for future optimization and rationalization of miltefosine treatment in PKDL.

Miltefosine concentrations in the skin were highly variable between patients, which has also been observed for miltefosine in plasma in various previous studies (10–12). In having available only a single time point measurement of skin concentrations, empirical PK modeling could not be applied to further characterize skin PK of miltefosine. Therefore, we applied more advanced methods of PBPK modeling utilizing drug-specific and system-specific information to further predict skin PK. Furthermore, this approach allowed us to characterize target-site PK (e.g. MRT), parameters that could otherwise not be derived from a single observation.

Results of PK target achievement in the skin are in line with previous evaluations of the allometric weight-based dosing regimen in plasma (10, 12), suggesting that this dosing regimen achieves sufficient target exposure of the parasites in skin tissue, also after 21 days. Since the target was defined based on the concentration of miltefosine required to induce intracellular susceptibility of *Leishmania donovani*, it could be assumed that such exposure is sufficient for killing of the same parasite localized within the dermis. In the present study, 90% of the patients reached this target. However, due to the invasive nature of the biopsy sampling, which limited the number of samples which could be collected (only one per patient), this study was limited for a longitudinal individual patient evaluation in target exposure attainment over time. It remains to be assessed in future studies, whether reaching this target exposure in skin is associated with parasitological and clinical response to treatment.

We also developed a PBPK model of miltefosine, further used to simulate concentrations in the organs known to be affected by *Leishmania* parasites. With the here collected skin concentrations along with pooled data of plasma concentrations, we were able to inform the PBPK model and introduce a cell membrane binding partner which represents the membrane binding capacity. It can be anticipated that this cell membrane binding property is not tissue-specific. Mechanisms of miltefosine binding to the membrane is similar for all cell types, thus the extent of membrane binding is related to the number of cells in any compartment. Nonetheless, in having limited data to validate this model, further simulated exposures in spleen and liver should be interpreted with caution. The PBPK model-based predicted concentration-time curve in the skin suggested that typical target attainment ($T > EC_{90}$) after this 21-day regimen is twice higher (52 days) than previously reported $T > EC_{90}$ values in plasma of VL patients treated for 28 days (~24-27 days) (10, 12).

In conclusion, in this study we showed that miltefosine penetrates to a large extent into the skin after oral administration and that skin concentrations are potentially high enough to exert activity on the dermal parasites in PKDL. Bridging the gap in knowledge of miltefosine disposition in human skin, the present study provides a promising start for future optimization of miltefosine in the treatment of PKDL. The PBPK model enabled the prediction of miltefosine concentrations in various other organ tissues, such as spleen and liver affected in VL, which would be unfeasible to sample in clinical trials. In future studies, such predictions and extrapolations from the developed model might be valuable to characterize miltefosine exposure and parasite killing response in respective organs or tissues.

References

1. Alvar J, Vélez ID, Bern C, Herrero M, Desjeux P, Cano J, Jannin J, de Boer M. 2012. Leishmaniasis worldwide and global estimates of its incidence. PLoS One.

2. Eiras DP, Kirkman LA, Murray HW. 2015. Cutaneous Leishmaniasis: Current Treatment Practices in the USA for Returning Travelers. Curr Treat options Infect Dis 7:52–62.

3. Arenas R, Torres-Guerrero E, Quintanilla-Cedillo MR, Ruiz-Esmenjaud J. 2017. Leishmaniasis: A review. F1000Research 6.

4. Zijlstra EE, Musa AM, Khalil EA, el-Hassan IM, el-Hassan AM. 2003. Post-kala-azar dermal leishmaniasis. Lancet Infect Dis 2003/02/01. 3:87–98.

5. Ismail A, Khalil EAG, Musa AM, EL Hassan IM, Ibrahim ME, Theander TG, EL Hassan AM. 2006. The pathogenesis of post kala-azar dermal leishmaniasis from the field to the molecule: Does ultraviolet light (UVB) radiation play a role? Med Hypotheses 66:993–999.

6. Dorlo TPC, Balasegaram M, Beijnen JH, de Vries PJ. 2012. Miltefosine: a review of its pharmacology and therapeutic efficacy in the treatment of leishmaniasis. J Antimicrob Chemother 67:2576–2597.

7. Baumer W, Wlaz P, Jennings G, Rundfeldt C. 2010. The putative lipid raft modulator miltefosine displays immunomodulatory action in T-cell dependent dermal inflammation models. Eur J Pharmacol 2009/11/18. 628:226–232.

8. Mukherjee AK, Gupta G, Adhikari A, Majumder S, Kar Mahapatra S, Bhattacharyya Majumdar S, Majumdar S. 2012. Miltefosine triggers a strong proinflammatory cytokine response during visceral leishmaniasis: role of TLR4 and TLR9. Int Immunopharmacol 2012/03/01. 12:565–572.

9. Ménez C, Buyse M, Farinotti R, Barratt G. 2007. Inward Translocation of the Phospholipid Analogue Miltefosine across Caco-2 Cell Membranes Exhibits Characteristics of a Carrier-mediated Process. Lipids 42:229–240.

10. Palić S, Kip AE, Beijnen JH, Mbui J, Musa A, Solomos A, Wasunna M, Olobo J, Alves F, Dorlo TPC. 2020. Characterizing the non-linear pharmacokinetics of miltefosine in

paediatric visceral leishmaniasis patients from Eastern Africa. J Antimicrob Chemother https://doi.org/10.1093/jac/dkaa314.

11. Dorlo TPC, Huitema ADR, Beijnen JH, de Vries PJ. 2012. Optimal dosing of miltefosine in children and adults with visceral leishmaniasis. Antimicrob Agents Chemother 56:3864–72.

12. Dorlo TPC, Kip AE, Younis BM, Ellis SJ, Alves F, Beijnen JH, Njenga S, Kirigi G, Hailu A, Olobo J, Musa AM, Balasegaram M, Wasunna M, Karlsson MO, Khalil EAG. 2017. Visceral leishmaniasis relapse hazard is linked to reduced miltefosine exposure in patients from Eastern Africa: a population pharmacokinetic/pharmacodynamic study. J Antimicrob Chemother 72:3131–3140.

13. Roseboom IC, Rosing H, Beijnen JH, Dorlo TPC. 2020. Skin tissue sample collection, sample homogenization, and analyte extraction strategies for liquid chromatographic mass spectrometry quantification of pharmaceutical compounds. J Pharm Biomed Anal. Elsevier B.V.

14. Mbui J, Olobo J, Omollo R, Solomos A, Kip AE, Kirigi G, Sagaki P, Kimutai R, Were L, Omollo T, Egondi TW, Wasunna M, Alvar J, Dorlo TPC, Alves F. 2018. Pharmacokinetics, safety and efficacy of an allometric miltefosine regimen for the treatment of visceral leishmaniasis in Eastern African children: an open-label, phase-II clinical trial. Clin Infect Dis.

15. Dorlo TPC, Van Thiel PPAM, Huitema ADR, Keizer RJ, De Vries HJC, Beijnen JH, De Vries PJ. 2008. Pharmacokinetics of miltefosine in old world cutaneous leishmaniasis patients. Antimicrob Agents Chemother 52:2855–2860.

16. Dorlo TPC, Hillebrand MJX, Rosing H, Eggelte TA, de Vries PJ, Beijnen JH. 2008. Development and validation of a quantitative assay for the measurement of miltefosine in human plasma by liquid chromatography–tandem mass spectrometry. J Chromatogr B 865:55–62.

17. R Core Team (2015). R: A language and environment for statistical computing. R Foundation for Statistical Computing, Vienna, Austria.

18. Willmann S, Lippert J, Sevestre M, Solodenko J, Fois F, Schmitt W. 2003. PK-Sim®: A

physiologically based pharmacokinetic "whole-body" model. Drug Discov Today BIOSILICO. Elsevier Ltd.

19.   Willmann S, Höhn K, Edginton A, Sevestre M, Solodenko J, Weiss W, Lippert J, Schmitt W. 2007. Development of a physiology-based whole-body population model for assessing the influence of individual variability on the pharmacokinetics of drugs. J Pharmacokinet Pharmacodyn 34:401–431.

20.   Miltefosine | C21H46NO4P - PubChem.

Pharmacokinetics of an allometric miltefosine regimen and its relation to skin lesion healing in Bangladeshi pediatric patients treated for post kala-azar dermal leishmaniasis

Chapter 4.2

Semra Palić[1], M.G. Hasnain[2], Anke E. Kip[1], M. A. Mural[2],
Jos H. Beijnen[1], J. Baker[2], Dinesh Mondal[2], Thomas P.C. Dorlo[1]

1. Department of Pharmacy & Pharmacology, The Netherlands Cancer Institute
   / Antoni van Leeuwenhoek Hospital, Amsterdam, The Netherlands
2. Centre for Nutrition and Food Security (CNFS), International Centre for
   Diarrhoeal Disease Research, Bangladesh (ICDDR,B), Dhaka, Bangladesh

Abstract

Background

Post-kala-azar dermal leishmaniasis (PKDL) is a complication of visceral leishmaniasis (VL) developing months or years upon VL treatment completion. An allometric dosing regimen of miltefosine was recently proposed for pediatric patients. This study aims to evaluate miltefosine pharmacokinetics (PK) following an allometric dosing regimen of 12 weeks and relate it to skin healing dynamics in pediatric and adolescent PKDL patients.

Methods

Seventy-nine patients (age 4-17 years) from Bangladesh were treated with oral miltefosine for 12 weeks. Miltefosine was quantified in dried blood spots by LC-MS/MS. Treatment response was evaluated by skin lesion scores, quantified by a picture-based scoring system. A population pharmacokinetic-pharmacodynamic (PK-DP) model was developed to characterize the exposure-treatment response relationship.

Results

Miltefosine PK was described by a two-compartment model following first order absorption and linear elimination. In contrast to previous results from Eastern Africa, non-linearities in PK were not observed in this study. Next, the dynamics of skin lesion healing were modeled using a transit compartment model. The typical estimated baseline skin lesion score was 54.5 units with a high between-subject variability (BSV) of 158%. Mean transit time of the delay in drug effect was estimated at 170 days (BSV 22.5%), while the estimated time to reach resolution of 90% lesion score was 193 days (IQR: 180 – 293), achieved by 86% of the patients at 12 months follow up.

Conclusion

The developed PK-PD model quantified the dynamics of skin lesion score resolution in PKDL patients in response to miltefosine and captured high variability among patients in treatment response delay.

1. Introduction

Post-kala-azar dermal leishmaniasis (PKDL) is a complication of kala-azar or visceral leishmaniasis (VL) which can develop months or years upon treatment completion. While VL is a systemic and lethal form of leishmaniasis, PKDL is not life threatening, and is characterized by nodular, macular or maculopapular skin rash.(1) In addition, although prevalent in all endemic regions including Eastern Africa and South Asia, there remain important geographical differences in pathogenesis and clinical manifestations in PKDL. For example, PKDL develops in patients suffering from VL caused by infection with *Leishmania donovani*, and rarely with *L. infantum* (2, 3). In Eastern Africa, PKDL can develop in 50 – 60% of VL cases, while in Southeast Asia, PKDL develops in 5 – 10 %, and typically requires treatment.(4) Moreover, 90% of the PKDL cases in East Africa are manifested with papular rash usually within the first 12 months post VL treatment, while in Southeast Asia, 90% of the cases exhibit a macular rash developing 2- or 3-years post VL treatment. In Bangladesh, PKDL is common across all ages, but it mostly affects children and adolescents (5, 6).

Patients with PKDL are found to contribute to transmission of *Leishmania* parasites during inter-epidemic periods of VL, jeopardizing elimination efforts in the context of VL (7, 8). Previously, various other agents have been used in treatment of PKDL, including sodium stibogluconate (SSG), amphotericin B, and paromomycin. Up to date, there is no standard treatment regimen for PKDL, while miltefosine is the only oral drug available for the treatment of leishmaniasis. Pharmacokinetics (PK) of miltefosine is characterized with slow absorption and long elimination half-life (approximately 7 days), with steady-state concentrations only reached from the fourth week of treatment. Pharmacokinetic–pharmacodynamic (PK-PD) relationships for miltefosine have been previously established in treatment of VL (9, 10) and CL (11), while the characterization of an exposure-effect relationship for miltefosine in the context of PKDL is currently lacking. In absence of established exposure-effect relationships, it remains challenging to deliver more rational miltefosine dosing regimens for the treatment of PKDL. To this end, there is a need for an objective marker or scoring system representing a pharmacodynamic response following antileishmanial treatment in PKDL. For this purpose, a new picture scoring system has been developed to quantify the clinical treatment effect on the PKDL skin lesions. The aim of the present model-based analysis was to evaluate the relationship between miltefosine exposure

and dynamics of skin lesion resolution, in pediatric and adolescent PKDL patients. Secondly, we wanted to investigate whether previously found non-linearities in the pharmacokinetics of miltefosine in VL pediatric patients, were also present in this PKDL pediatric population.

2. Materials and Methods

2.1 Study set-up and patients

The current analysis is based on a non-randomized single group study which was registered with ClinicalTrials.gov under NCT02193022, after approval by the Research Review Committee and Ethical Review Committee (ERC) of the International Centre for Diarrhoeal Disease Research, Bangladesh (ICDDR,B) (12). Written informed consent from all participants or their legal guardians was obtained prior the trial start. Miltefosine (Impavido, Paladin Labs, Montréal, Canada) was administered orally based on the allometric dosing regimen in duration of 12 weeks. The allometric dosing regimen is based on height, weight and sex of the patient (10). Follow up was conducted every three months after the end of treatment up to twelve months. Treatment response was evaluated by the assessment of a skin lesion score, quantified by total number of squares affected by skin lesions for the total body area of the patient, as previously described in the published study protocol (12).

2.2 Pharmacokinetic sample collection and bioanalysis

Dried blood spot (DBS) samples for the quantification of miltefosine were collected prior to the treatment, and then nominally on days 14, 28 and 84 of the treatment. Post-treatment DBS samples were taken on days 114, 175, 267 and day. All samples were collected roughly three 3 hours after the dose (range 1.5-4.5 hours). Upon collection, samples were air-dried at room temperature for a minimum of 3 hours, then stored in a zip-lock bag for storage and transportation to the bioanalytical laboratory of the Netherlands Cancer Institute, department of Pharmacy & Pharmacology. Here, miltefosine concentrations were determined by previously validated method of liquid chromatography coupled to tandem mass spectrometry (LC-MS/MS), with a lower limit of quantitation (LLOQ) of 10 ng/ml. Previously, it has been reported that miltefosine distributes equitably between plasma and erythrocytes, with a paired miltefosine DBS/plasma concentration ratio reported at 0.99 (13). Given this, determined miltefosine concentrations in DBS samples were considered representative of the miltefosine concentration in plasma. Clinical validation of the analytical

DBS method showed that hematocrit correction was not required in calculation of the plasma concentrations analyzed in this manner (13).

2.3 Lesion score

The skin area affected by lesions was quantified using a scoring system in which skin lesions were plotted in squares of pre-determined area and then counted. The total number of squares affected by lesions quantified the skin lesion score, which was evaluated at the treatment initiation as well as at the end of the treatment and at each three months of the follow up.

2.4 PK-PD model development

2.4.1 Software

Nonlinear mixed-effects modeling was applied for estimation of both population pharmacokinetic and pharmacodynamic parameters, using the first-order conditional estimation method with interaction (FOCE+I) in NONMEM (version 7.4, ICON Development Solutions, USA). Model deployment was automated by Perl-speaks-NONMEM (PsN version 4.7.0), with Pirana (version 2.9.7) used as graphical interface. Management of the data, as well as graphical evaluation was performed in R and R Studio (versions 3.6.3 and 3.4.3). Computational analyses were carried out on a high-performance computing cluster of the Netherlands Cancer Institute.

2.4.2 Pharmacokinetic analysis

Guided by prior knowledge, miltefosine PK was described using a two-compartment model following first-order absorption and linear elimination from the central compartment. Next, the stochastic model was built where between subject variability (BSV) was tested on all PK parameters using an exponential error model *(Eq. 1)* while between occasion variability (BOV) was further tested on bioavailability to account for and evaluate reported treatment adherence issues.

$$P_i = P_{pop} \cdot \exp(\eta_i, \text{BSV} + \eta_i, \text{BOV}) \hspace{3cm} Eq.(1)$$

*wh*ere P_i represents the individual parameter estimate for individual i, P_{pop} represents the typical population parameter estimate, η_i either BSV or BOV effect for subject individual i where η_i assumes normal distribution following N $(0, \sigma^2)$. Occasions were defined for each individual treatment week. Residual unexplained variability (RUV) was explored using proportional error model as given in the equation below.

$$C_{obs,ij} = C_{pred,ij} \cdot (1 + \varepsilon 1_{p,ij}) \qquad\qquad Eq.\ (2)$$

where $C_{obs,ij}$ represents the observed concentration for an individual i and observation j, and respectively $C_{pred,ij}$ represents the individual predicted concentration, while $\varepsilon 1_{p,ij}$ represents the proportional error, assuming normal distribution following N $(0, \sigma^2)$.

2.4.3 Pharmacodynamic analysis

Sequential PK-PD modeling was performed using an Individual PK Parameter (IPP) approach, using posterior individual empirical Bayes estimates from the final PK model to further inform the PD model development (14). The lesion score was used to model the treatment efficacy and quantify the concentration-effect relationships. In this respect a variety of continuous PD models were tested, including an effect compartment model, a direct effect model, a lag time model, and a transit compartment model.

2.4.4 Covariate analysis

Stepwise generalized additive models were employed in identifying potential covariates. Available covariates used in screening included age, sex and body weight. Significance of the covariate effect was assessed as explained in the following paragraph for hierarchical models.

2.4.5 Model selection and evaluation

The same model selection criteria were applied to both PK and PD analyses, where discrimination between models was initially guided by physiological plausibility, and finally by the objective function value (OFV), goodness of fit (GOF) plots, prediction corrected visual predictive checks (pcVPC), as well as precision of parameter estimates. Hierarchical models were assessed by a decrease in OFV where a significant improvement was determined by drop of ≥ 6.63 points, corresponding to a $P < 0.01$ (χ^2-distribution with 1 degree of freedom).

Both GOF and pcVPC were evaluated in assessing the adequacy of the model fit to data. Parameter precision was evaluated by standard errors, inspection of the correlation matrix as well as ε- and η-shrinkage. The final parameter precision was obtained using Sampling Importance Resampling (SIR) (15). Concentrations below the LLOQ were excluded from this analysis (15).

2.4.6 Model based assessment of treatment efficacy

The developed model was used to evaluate the exposure-response relationship. Efficacy in this study is assessed by resolution of the skin lesions, quantified by the lesion score. The model was used to calculate the time needed for lesion resolution by 50% (half-response) and 90% of the maximal response, which defines the clinical cure in respect to skin healing. Furthermore, the response to treatment evaluated between individuals in range of exposures to miltefosine. These results are then used in evaluating the duration of follow up time needed for a complete resolution of lesion.

3. Results

3.1 Patients

Seventy-nine pediatric patients (aged 4-17 years) from Bangladesh (district of Mymensingh) treated at the Mymensingh Medical College Hospital were included in this PK-PD study. All patients received miltefosine based on the allometric weight-based dosing regimen, once daily for a duration of 12 weeks. Details of patient demographics are summarized in *table 1*.

3.2. Data

In total, 547 miltefosine plasma concentrations were available for the PK analysis during both treatment and follow up, while 474 skin lesion score counts were available for the PD analysis. There were only 4 PK measurements below the LLOQ at the last follow up period, which were excluded from the analysis. Observed lesion score profiles for each patient individually are displayed in *figure 1*.

Table 1: Patient demographics, dosing information and lesion score utilized in efficacy assessment

Parameter	Total	Male	Female
Number of patients	79	37	43
Age	10 (4 - 17)	10 (4 - 17)	10 (5 - 16)
Body weight	27.6 (14.0 - 62.2)	25.3 (14.0 - 55.2)	29.2 (14.8 - 62.2)
Height	134 (95 - 168)	133 (95 - 168)	140 (95 - 158)
Fat free mass	23.1 (10.8 - 46.8)	24.0 (12.9 - 46.8)	22.4 (10.8 - 38.8)
Miltefosine dose (mg/kg/day)	2.8 (1.8 - 3.9)	3.2 (2.4 - 3.9)	2.6 (1.8 - 3.90)
Lesion score at treatment initiation (day 0)	81 (2 - 545)	90 (3 - 483)	74 (2 - 545)
Lesion score at the end of the treatment (day 84)	54 (0 - 530)	65 (2 - 355)	51 (0 - 530)
Lesion score at follow up (day 120)	20 (0 – 493)	17 (1 – 195)	21 (0 – 493)
Lesion score at follow up (day 180)	6 (0 – 400)	5 (0 -132)	8 (0 – 400)
Lesion score at follow up (day 270)	2 (0 – 347)	1 (0 – 94)	3 (0 – 347)
Lesion score at follow up for cure assessment (day 365)	0 (0 – 305)	0 (0 -44)	0 (0 – 305)

All values are displayed as median (range).
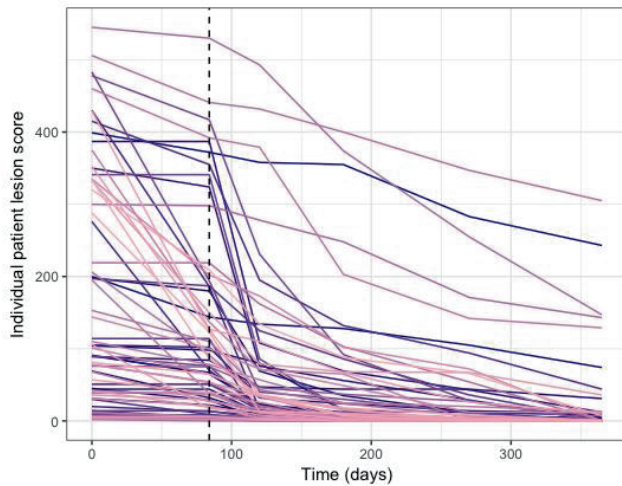
Figure 1: Observed dynamics of individual patient lesion score. The dashed line represents the end of treatment.

3.3 Population PK model

Miltefosine PK was described by a two-compartment model following first order absorption and linear elimination. Model estimates of the PK parameters, as well as precision of parameter estimates are given in *table 2*. All PK parameter estimates are in line with previous analyses (9, 16). However, previously estimated lower F in the first treatment week, as well as reduction in F as a result in increase of cumulative dose following miltefosine allometric weight-based dosing regimen in VL patients were not found in the present study, using the previously developed PK model including these non-linearities led to an consistent underprediction of the current data. BOV was included on F to account for possible non-adherence according to *Eq.(1)*. Although missed doses were incorporated in the dosing input of the model, 8.2 % BOV was found to result in a significant decrease in OFV (Δ -19, p-value 0.05). Ten patients showed an approximately 30% decline in miltefosine accumulation after day 28, which could potentially be due to non-adherence. In addition, BSV could be estimated on clearance (Cl), volume of distribution in the central (V_c), and peripheral compartment (V_p). RUV was modeled using a proportional error model. The model adequately fitted the observed plasma PK of miltefosine, as illustrated by the GOF plots in *figure 2*, additionally it performed satisfactory in terms of predictive ability as shown in *figure 3*. None of the tested

covariates were found significant in explaining BSV on any of the tested estimated PK parameters. Total treatment miltefosine exposure as given by the area under the plasma drug concentration-time curve (AUC) was also calculated based on the final PK model, and is given in *table 3*.

3.4 Population pharmacodynamic model

Due to the delay in drug action and the slow skin lesion recovery and re-epithelialization, a delay in treatment response was observed. At start, an effect compartment approach was evaluated, but was insufficient in describing the variability in delay of response. Next, lag and transit time models were evaluated. In theory, both a lag time and a transit compartment model are potential structural models to model delays, and adequately fitted these data. However, in physiological terms, a transit compartment was considered more suitable for describing underlying physiological processes while a lag time model is a more empirical approach and could be implemented in absence of sufficient data to estimate the transit compartment model. Evaluation of the model fit to these data showed adequate model-based predictions, as illustrated by the GOF plots in *figure 2.*
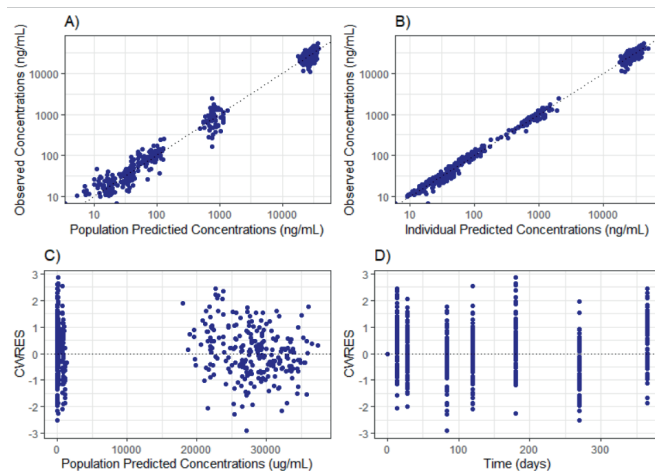
Figure 2: Goodness-of-fit plots for the final miltefosine PK model, (A) Observed versus population predicted miltefosine concentrations, (B) observed versus individually predicted miltefosine concentrations, (C) conditional weighted residuals (CWRES) versus population predicted concentrations and (D) CWRES versus time after start of treatment.
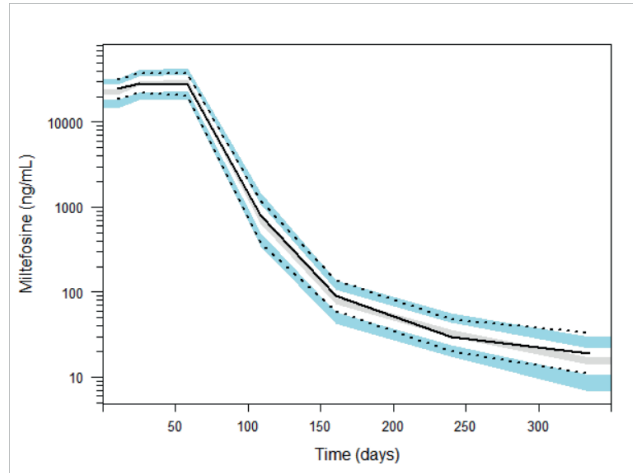
Figure 3: Prediction corrected VPCs based on 1000 simulations of the final miltefosine PK model for the 12-week allometric dosing regimen in Bangladeshi pediatric PKDL patients. The solid line represents the observed median concentrations, and gray shading shows the simulated values. The dotted lines are representative of the 5th and 95th percentiles of the observed data, while blue shaded areas represent the 95% CI for the simulated data.

In this respect, the dynamics of skin healing as quantified by the skin lesion score fitted in a transit compartment model, mimics the delay in response, and represents both the delay in miltefosine effect on the skin parasite loads, and subsequently the recovery of the lesion itself. A single slope parameter was structurally more appropriate than sigmoid E_{max} concentration effect. A schematic representation of the developed PK-PD model is illustrated in the *figure 4*. Three transit compartments were found most optimal in the final model. The miltefosine drug effect on the skin lesion score was modeled as a second order inactivation rate (K_d), where the drug concentration (C_M) estimated in the central compartment of the PK model induces parasite killing and consequently skin healing. All transit compartments were initialized with the baseline estimate for lesion score (S_0), assuming a steady-state at baseline. Consequently, transit compartments assume the loss or reduction of the lesion into the next compartment.(17) Population value for the lesion score at baseline (S_0) was estimated at 54.7, but was highly variable among patients (BSV 158%, 95% CI: 187.1 -345).

In addition, mean transit time (Mtt) was estimated at 170 days for this patient population (BSV 22.5%, 95% CI: 15.9 – 32.3). All parameter estimates, as well as parameter precision are given in *table 2*. BSV was estimated for K_d, Mtt and S_0. RUV was described by a combined error model given in *Eq 2.* The differential equations used in the final PD model are given below.

$$\frac{dS_1}{d_t} = -K_d \cdot C_M \cdot S_1 - K_{tr} \cdot S_1 \qquad Eq.(3)$$

$$\frac{dS_j}{d_t} = K_{tr} \cdot (S_{j-1} - S_j) \qquad Eq.(4)$$

$$Mtt = \frac{(n+1)}{K_{tr}} \qquad Eq.(5)$$

Herein, S is the lesion score, C_M is the estimated miltefosine concentration from the PK model. S_j is the amount of lesion score in the compartment, while K_{tr} is the transit rate between the linked compartments. Mtt stands for the mean transition time and represents response delay, and j is the number of transit compartments.
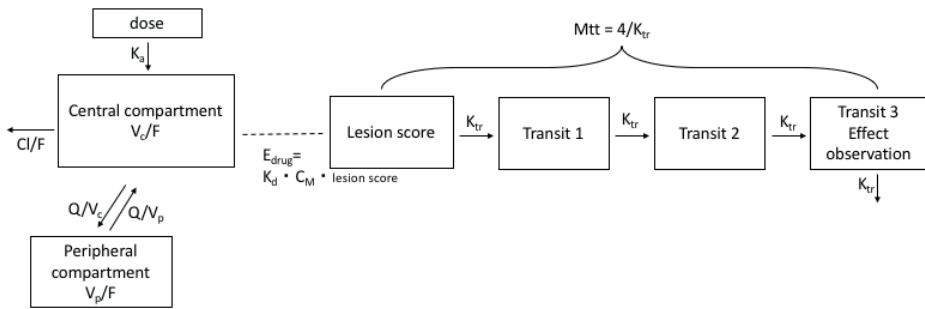
Figure 4: Schematic representation of the developed PK-PD model

F: Apparent Bioavailability, CL/F: apparent clearance, V_c/F: apparent volume in the central compartment, K_a: absorption rate constant, Q/F: apparent intercompartmental clearance, V_p/F: apparent volume in the peripheral compartment, K_d: disease inactivation rate constant, Mtt: mean transit time, C_M is the estimated miltefosine concentration from the PK model, K_{tr} is the transit rate between the linked compartments, and E_{drug} is the drug effect

Table 2: Model-based estimates and precisions of the PK and PD parameters

Parameter (unit)	Estimate	95 % CI*
Pharmacokinetics		
Fixed Effects		
Apparent clearance **CL/F** (L/day)	2.1	1.77 - 2.52
Apparent volume in the central compartment **V_c/F** (L)	18.4	16.9 – 19.95
Absorption rate constant **k_a** (/day)	1.61 fixed [A]	-
Apparent intercompartmental clearance **Q/F** (L/day)	0.026	0.019 -0.04
Apparent volume in the peripheral compartment **V_p/F** (L)	2.33	1.79 – 3.06
Apparent Bioavailability **F**	1 fixed	-
Between-subject variability		
CL/F (%)	9.9	0.7 – 10
V_c/F (%)	16.6	1.2 – 24.2
V_p/F (%)	13.6	0.2 – 17.9
Between – Occasion variability		
F (%)	8.2	1.7 – 22.4
Residual Unexplained Variability		
Proportional error (%)	21.3%	15.4 – 32.7
Pharmacodynamics		
Fixed Effects		
Lesion score at baseline **S_0**	54.7	52.4 – 57.4
Disease inactivation rate constant **K_d** ($ng/mL^{-1}day^{-1}$)	78.7	76.1 – 81.6
Mean transit time **Mtt** (days)	170	167.6 – 172.9
Between-subject variability		
S_0	158	187.1 -345
K_d (%)	170	52.8 - 611
Mtt (%)	22.5	15.9 – 32.3

Residual Unexplained Variability		
Proportional error (%)	42.3	38.3–46.9
Additive error [B]	70% fixed for the score <1	-

*Values obtained using SIR

[A] Fixed based on the previous estimate from the PK model for miltefosine after the allometric dosing regimen

[B] Applied to avoid computational difficulties
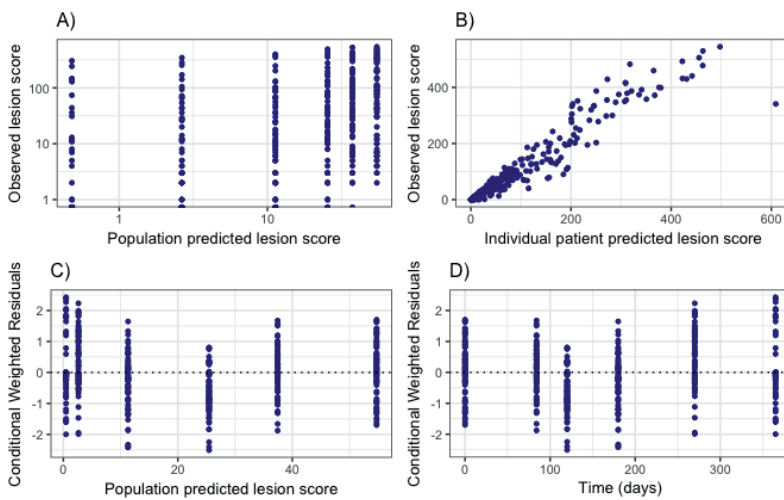
Figure 5: Goodness-of-fit plots for the final PD model, (A) Observed versus population predicted lesion score, (B) observed versus individually predicted lesion score, (C) conditional weighted residuals (CWRES) versus population predicted lesion score and (D) CWRES versus time after start of treatment.

3.5 Therapeutic response assessment

The developed PK-PD model was employed to further assess and quantify the individual treatment response. Treatment response was evaluated in terms of two targets to be obtained, i.e. resolutions of 50%, and 90% of the total lesion score in reference to the baseline lesion score at treatment initiation. Reduction in 90% of the lesion score, along with a negative qPCR essay for skin and peripheral blood defines clinical cure, evaluated at the last follow up on day 365. The results show that with the allometric weight-based dosing regimen, all patients achieved resolution of the lesion by 50% as summarized in the *table 3*. 30% patients have already reached this effect during the treatment, while 70% patients reach this effect during the follow up. No statistically significant difference was found in baseline score between groups that had a fast or a slow response to treatment. Furthermore, 86% patients reached the 90% resolution of the lesion score, on median at day 193 of follow up (interquartile rage (IQR) 180 - 293 days).

Table 3: Model-based evaluation of the target attainment

	Target	
	Resolution of 50% lesion score	Resolution of 90% lesion score
Percentage of patients reaching the effect	100%	86%
Time to reach the effect (days)	106 (84 − 189)*	193 (180 − 293)*

*Values represent median (the interquartile range (IQR))

4. Discussion

The current study evaluated miltefosine PK following a 12-week allometric dosing regimen for the treatment of pediatric PKDL patients and quantified the relationship between miltefosine exposure and treatment response in terms of skin lesion healing. Regarding PK, as in line with previous studies, miltefosine PK was adequately described by a two-compartment model following first-order absorption and elimination (16, 18). The allometric weight-based dosing regimen of 4 weeks of miltefosine has recently been evaluated for the treatment of pediatric VL patients in Eastern Africa, where a decrease in F in the first treatment week and dose-related nonlinearities in miltefosine PK were observed (19, 20). In our previous study (16), we have explained and characterized these nonlinearities in PK, while. Despite a similar daily dosage, but a longer treatment duration of the Bangladeshi pediatric patients, we could not confirm such nonlinear PK characteristics, upon evaluating post-hoc individual predictions of miltefosine PK of the present cohort based on the previously developed PK model from the allometric dosing regimen (16). Discrepancies in miltefosine PK among these studies could be explained by difference in disease severity between VL and PKDL, since patients suffering from PKDL are systemically healthy, and VL patients have a systemic infection altering internal organs. In this respect, a decrease in F found in VL patients in the first week of treatment is likely due to patient malnourishment and infection-driven effects on the gastrointestinal system, impairing absorption of the drug. Similarly, the previously characterized cumulative dose-effect on bioavailability mainly limiting accumulation of the drug from the 4th week of treatment, could not be confirmed in this study population either, possibly due to differences in saturation of absorption.

With respect to PD, this study investigated a longitudinal treatment response, and quantified the dynamics of skin healing in terms of lesion score. Before the PD model development, we evaluated the data of the individual baseline lesion score and the treatment response in terms of reaching the target of 90% reduction from baseline, however no clear relationship between these two variables were found. Therefore, the model was developed to further quantify the effect of the treatment and depict the lesion score resolution in response to miltefosine. For the PKDL lesions characterized by maculopapular rash, suggested mechanisms for PKDL pathogenesis include cytokine cascades dominated by interleukin (IL)-10 during chronic inflammation, further followed by IL-2 simulation and granuloma formation (21). The

treatment induced host immune activation, or eventual spontaneous priming of IL-12, and production of interferon gamma (INF-γ) leads to a parasite killing within macrophages and lesion healing (22). Complex interplay between the disease-driven anti-inflammatory and treatment-induced pro-inflammatory effects may take a substantial amount of time depending on the level of inflammation, resulting in expectably large variability in the onset of treatment response. Moreover, variability in delay of the treatment response is also underlined by dynamics of the cascade of skin healing, involving a number of processes such as scar formation and tissue regeneration, expectedly variable among individuals. This is also demonstrated in the results of this study, where only 30% patients achieved 90% reduction in lesion score during the treatment period, and most reached this target within a year after completion of treatment. In the current study, 14% of patients did not reach 90% reduction in lesion score, suggesting that a longer follow up for these patients may be needed. In conclusion, the present PK-PD study established and quantified the relationship between miltefosine PK following an allometric dosing regimen and skin lesion PD, in terms of an objective skin lesion score, where we characterized a large variability in delay of treatment response. Essentially, the established relationship could be used to inform future dosing regimens of miltefosine in PKDL treatment.

References

1. Singh S, Sharma U, Mishra J. 2011. Post-kala-azar dermal leishmaniasis: Recent developments. Int J Dermatol 50:1099–1108.

2. Kemp M, Kurtzhals JAL, Kharazmi A, Theander TG. 1994. Dichotomy in the human CD4 $^+$ T-cell response to *Leishmania* parasites. APMIS 102:81–88.

3. Sudeck H. 2006. Kala azar: Rare import and significant differential diagnosis. Internist 47:825–834.

4. Zijlstra EE, Musa AM, Khalil EA, el-Hassan IM, el-Hassan AM. 2003. Post-kala-azar dermal leishmaniasis. Lancet Infect Dis2003/02/01. 3:87–98.

5. Lukeš J, Mauricio IL, Schönian G, Dujardin JC, Soteriadou K, Dedet JP, Kuhls K, Tintaya KWQ, Jirků M, Chocholová E, Haralambous C, Pratlong F, Oborník M, Horák A, Ayala FJ, Miles MA. 2007. Evolutionary and geographical history of the Leishmania donovani complex with a revision of current taxonomy. Proc Natl Acad Sci U S A 104:9375–9380.

6. Kuhls K, Mauricio IL, Pratlong F, Presber W, Schönian G. 2005. Analysis of ribosomal DNA internal transcribed spacer sequences of the Leishmania donovani complex. Microbes Infect 7:1224–1234.

7. Bern C, Courtenay O, Alvar J. 2010. Of Cattle, Sand Flies and Men: A Systematic Review of Risk Factor Analyses for South Asian Visceral Leishmaniasis and Implications for Elimination. PLoS Negl Trop Dis 4.

8. Mondal D, Bern C, Ghosh D, Rashid M, Molina R, Chowdhury R, Nath R, Ghosh P, Chapman LAC, Alim A, Bilbe G, Alvar J. 2019. Quantifying the infectiousness of post-kala-azar dermal leishmaniasis toward sand flies. Clin Infect Dis 69:251–258.

9. Dorlo TPC, Rijal S, Ostyn B, de Vries PJ, Singh R, Bhattarai N, Uranw S, Dujardin J-C, Boelaert M, Beijnen JH, Huitema ADR. 2014. Failure of Miltefosine in Visceral Leishmaniasis Is Associated With Low Drug Exposure. J Infect Dis 210:146–153.

10. Dorlo TPC, Huitema ADR, Beijnen JH, de Vries PJ. 2012. Optimal dosing of miltefosine in children and adults with visceral leishmaniasis. Antimicrob Agents Chemother 56:3864–72.

11. Kip AE, Castro M del M, Gomez MA, Cossio A, Schellens JHM, Beijnen JH, Saravia NG, Dorlo TPC. 2018. Simultaneous population pharmacokinetic modelling of plasma and intracellular PBMC miltefosine concentrations in New World cutaneous leishmaniasis and exploration of exposure–response relationships. J Antimicrob Chemother

73:2104–2111.

12. Mondal D, Hasnain MG, Hossain MS, Ghosh D, Ghosh P, Hossain H, Baker J, Nath R, Haque R, Matlashewski G, Hamano S. 2016. Study on the safety and efficacy of miltefosine for the treatment of children and adolescents with post-kala-azar dermal leishmaniasis in Bangladesh, and an association of serum vitamin E and exposure to arsenic with post-kala-azar dermal leishmaniasis: A. BMJ Open 6.

13. Kip AE, Rosing H, Hillebrand MJX, Blesson S, Mengesha B, Diro E, Hailu A, Schellens JHM, Beijnen JH, Dorlo TPC. 2016. Validation and clinical evaluation of a novel method to measure miltefosine in leishmaniasis patients using dried blood spot sample collection. Antimicrob Agents Chemother 60:2081–2089.

14. Zhang L, Beal SL, Sheiner LB. 2003. Simultaneous vs. Sequential Analysis for Population PK/PD Data II: Robustness of Methods. J Pharmacokinet Pharmacodyn 30:405–416.

15. Dosne AG, Bergstrand M, Karlsson MO. 2017. An automated sampling importance resampling procedure for estimating parameter uncertainty. J Pharmacokinet Pharmacodyn 44:509–520.

16. Palić S, Kip AE, Beijnen JH, Mbui J, Musa A, Solomos A, Wasunna M, Olobo J, Alves F, Dorlo TPC. 2020. Characterizing the non-linear pharmacokinetics of miltefosine in paediatric visceral leishmaniasis patients from Eastern Africa. J Antimicrob Chemother https://doi.org/10.1093/jac/dkaa314.

17. Friberg LE, Henningsson A, Maas H, Nguyen L, Karlsson MO. 2002. Model of chemotherapy-induced myelosuppression with parameter consistency across drugs. J Clin Oncol 20:4713–4721.

18. Ostyn B, Hasker E, Dorlo TPC, Rijal S, Sundar S, Dujardin J-C, Boelaert M. 2014. Failure of miltefosine treatment for visceral leishmaniasis in children and men in South-East Asia. PLoS One 9:e100220.

19. Dorlo TPC, Kip AE, Younis BM, Ellis SJ, Alves F, Beijnen JH, Njenga S, Kirigi G, Hailu A, Olobo J, Musa AM, Balasegaram M, Wasunna M, Karlsson MO, Khalil EAG. 2017. Visceral leishmaniasis relapse hazard is linked to reduced miltefosine exposure in patients from Eastern Africa: a population pharmacokinetic/pharmacodynamic study. J Antimicrob Chemother 72:3131–3140.

20. Mbui J, Olobo J, Omollo R, Solomos A, Kip AE, Kirigi G, Sagaki P, Kimutai R, Were L, Omollo T, Egondi TW, Wasunna M, Alvar J, Dorlo TPC, Alves F. 2018. Pharmacokinetics,

safety and efficacy of an allometric miltefosine regimen for the treatment of visceral leishmaniasis in Eastern African children: an open-label, phase-II clinical trial. Clin Infect Dis.

21. Wadhone P, Maiti M, Agarwal R, Kamat V, Martin S, Saha B. 2009. Miltefosine promotes IFN-gamma-dominated anti-leishmanial immune response. J Immunol2009/05/21. 182:7146–7154.

22. Palić S, Bhairosing P, Beijnen JH, Dorlo TPC. 2019. Systematic Review of Host-Mediated Activity of Miltefosine in Leishmaniasis through Immunomodulation. Antimicrob Agents Chemother 63.

Conclusion and perspectives

Chapter V

It has been nearly two decades since miltefosine was approved for treatment of leishmaniasis and since then the drug has been considered a major therapeutic breakthrough against leishmaniasis. Today, miltefosine still remains the only oral drug available in treatment of this neglected disease, witnessing the lack of sufficient research and development. Although there are several new chemical entities with proposed antileishmanial activity in early phases of drug development, undergoing long processes of clinical trials, potential approvals and registration will take a number of years, and are unpredictable. Therefore, it is highly important to optimize treatment of leishmaniasis with the existing antileishmanial drugs. This thesis focuses in particular on the clinical pharmacokinetics (PK) and pharmacodynamics (PD) of miltefosine for treatment optimization in leishmaniasis.

Advanced mathematical methodologies in clinical pharmacology to rationalize treatment of leishmaniasis

Clinical trials in neglected tropical diseases, especially those including children yield sparse data, and often include limited number of patients. Since these are vulnerable patients, limited sampling strategies are typically used in these trials to prevent these patients from experiencing additional pain or harm. Research performed in this thesis applied advanced methods of population pharmacokinetic-pharmacodynamic (PK-PD) modeling and simulation, based on the methodological concept of non-linear mixed effects modeling and simulation, and physiologically-based PK modeling and simulation. These methods employ mathematical models to explain how drugs interact with physiological, anatomical and biochemical systems, as well as how those influence PK of drugs. In contrast to methods employed in here, there are traditional PK methodologies which require frequent and homogeneous sampling in PK studies in a group of individuals, preferably with similar characteristics. Data is then analyzed first to calculate PK parameters, and in the next step, means and variability are calculated. In a population PK-PD approach, the models are developed utilizing data from all individuals, and analyzed simultaneously, to be able to differentiate between the population and individuals, allowing for simultaneous estimation of the typical estimate and between-subject variability of the parameters. The modeling and simulation methodologies have a number of advantages over the traditional PK methods, such as 1) allowing for analysis of heterogenous data, 2) analysis of sparse data, and thus do not necessarily require frequent sampling, 3) all information contained in the available data

points is utilized in the estimation of PK parameters, through which individual estimates can be derived even for individuals with sparse sampling , 4) provide more accurate estimates of variability and parameter precisions, 5) provide possibility to differentiate between patient-specific, system-specific and drug-specific characteristics, as well to quantify relationships between those characteristics, 6) parameter-covariate relationships can be quantified to essentially explain why PK-PD varies among individuals, 7) sub-groups of patients can be distinguished given quantification of PK-PD relationships and their variability in such way that it is possible to predict which patients are at higher risk of receiving ineffective dose, etc, 8) models can allow extrapolation between populations, and finally 9) models can be used to simulate various clinical scenarios and help decide what an optimal treatment actually is.

Adequate exposure to miltefosine is critical for favorable treatment response

PK characteristics are essential determinants of treatment efficacy. Therefore, in order to be able to understand, and possibly predict treatment responses, understanding the PK of a drug is fundamental.

PK dictates drug exposure, and various relationships between exposure and clinical outcome have been established for leishmaniasis. Conventional 2.5 mg/kg/day dosing of miltefosine was previously shown to be less effective in pediatric VL patients compared to adults in Eastern Africa, which led to an investigation of an increased mg/kg miltefosine dosing based on an allometric formula in pediatric VL patients in Uganda and Kenya. Results of this trial showed substantially improved efficacy, but lower than expected increase in treatment exposure. Non-linearities in miltefosine PK are explored in **chapter 2.1** of this thesis. In here, we explain that non-linearities in miltefosine PK in Eastern African pediatric VL patients are dose-dependent, signifying that increase in exposure is not proportional with the dose administered. Our model-analysis estimated that stagnation in miltefosine accumulation in plasma occurred after a cumulative daily dose of 70 mg/kg/day was reached in these patients, perhaps due to a slow accumulation of miltefosine in the gastrointestinal membrane cells and subsequent dose-dependent saturation of transcellular transport. In spite of the fact that the allometric dose regimen did not result in completely equivalent exposure of miltefosine in children compared to adult patients, it led to a doubled exposure in the first treatment week where the parasite burden is the highest, and led to a faster PK target achievement. The allometric dose regimen led to an adequate increased efficacy of miltefosine monotherapy in

Eastern African VL patients of 90% (7). Therefore, the adoption of allometric weight-based dosing in pediatric VL patients is further recommended.

In addition, these non-linearities in miltefosine PK were not observed when children suffering from PKDL were treated with this dosing regimen. Patients suffering from VL have systemic infection of the internal organs, while PKDL patients are only affected by dermal lesions. In **chapter 2.2** and **chapter 3.2** of this thesis, we discuss that these discrepancies in miltefosine PK are likely disease- or population-specific between and within VL and PKDL patients, which highlights the need for PK studies in all of these different (geographical) populations and the difficulty of extrapolating findings between clinical leishmaniasis presentations and populations. In summary this clearly shows that a "one size fits all" approach does not apply to the treatment of different clinical leishmaniasis presentations with miltefosine. From these studies we gained a better understanding of the sources of the PK variability which provide a better understanding of how miltefosine should be included in future treatment combinations with miltefosine. Various new oral drug candidates are currently in phase I or phase II clinical trials. Our PK results provide a deeper insight on how miltefosine can be included in future oral combination regimens for leishmaniasis.

Elucidating PK-PD relationships of miltefosine treatment regimens

Modeling of treatment response provides valuable information for monitoring treatment, and has a potential to enable individualization of therapy. Understanding exposure – response relationships is therefore essential for predicting treatment outcome. Miltefosine PD responses were investigated in this thesis, in the context of both VL and PKDL treatment. In **chapter 3.1** we systematically reviewed host-mediated immunomodulatory effects of miltefosine in both preclinical and clinical studies. Here we showed that miltefosine exerts effects on activation of T-helper cell type-1 (Th1) cytokines, essential to combat intracellular pathogens such as *Leishmania* parasites. Next, in light of immunomodulatory effects, in **chapter 3.2**, we quantified the relationship between miltefosine PK and PD responses of inflammatory biomarker neopterin, elucidating which levels of neopterin increase after the treatment end may indicate patients at a higher risk of treatment failure. Neopterin is an endogenous compound, it is normally present in plasma of healthy individuals. We developed a PKPD model with two separate modes of neopterin production including endogenous (healthy) production and VL disease-activated production of neopterin. This model illustrates

how an endogenous immunological marker is influenced by treatment and may serve an example for other biomarkers which are affected by drugs acting on the host immunity. Furthermore, in **chapter 4.2**, we developed a mechanistic PK-PD model of skin lesion score resolution after miltefosine treatment of PKDL. This model quantified the exposure and time needed for 90% reduction in lesion score, and also captured high variability in treatment response delay among patients.

Whether lesion score or neopterin could be used as a surrogate endpoint in clinical trials requires future clinical and research efforts, as our findings are only based on relatively small numbers of patients. Nonetheless both these markers could potentially be used to identify patients who require more intensive follow-up as they are at a higher risk of relapse or eventual treatment failure . Overall, these studies illustrate the potential of establishing PK-PD relationship specifying groups of patients, exposure thresholds, or biomarker levels which are associated with the clinical outcome and should be further optimized to inform dosing regimens of miltefosine in the treatment of VL or PKDL.

Miltefosine accumulates in human skin

Up til now miltefosine exposure in the skin could be only approximated from the systemic exposure in plasma. In this thesis, we present the first evidence of miltefosine penetration into the skin of PKDL patients after oral administration. **Chapter 4.2** provides the first study on miltefosine target-site PK which allows evaluation of miltefosine exposure on the site of the parasite infection in the dermal clinical phenotypes of leishmaniasis. Demonstrating that these concentrations are above previously defined PK target of the time that the miltefosine concentration is > EC_{90} (10.6 mg/L) for *Leishmania donovani*, these data suggest that exposure to miltefosine following the allometric dose regimen, in these patients was high enough to exert activity on the dermal parasites in PKDL. These data were further incorporated into a full body PBPK approach to develop a model of miltefosine disposition in the skin, and miltefosine binding within the cellular membrane. The developed PBPK model provided a promising start for target-site tissue predictions of miltefosine exposure in any organ or tissue of interest. Membrane binding of miltefosine was modelled by the cell membrane binding partner, determined by an equilibrium and dissociation constants, as well as reference concentration. Mechanisms of miltefosine membrane binding could be assumed to be similar for all cell types, meaning that the extent of binding is rather related to the

number of cells in a tissue or organ. In physiological terms, this factor represents all lipid bilayers in which miltefosine is incorporated as a phospholipid derivative, potentially allowing prediction of miltefosine exposure in other organ tissues, such as spleen and liver affected in VL, that are unfeasible to sample in clinical trials.

Concluding remarks

Taken together, this thesis presents the most recent insights into the clinical pharmacology of miltefosine in the treatment of the neglected tropical disease leishmaniasis. By application of advanced methodologies of PK-PD modeling and simulation, we aimed to provide answers to various clinically relevant questions regarding e.g., optimal dosing regimens in pediatric patients, exposure target attainment following various dosing regimens, treatment-response predictions in both VL and PKDL, etc. Important knowledge can be gained about PK and PD of drugs by applying these methodologies in the future drug development for leishmaniasis. Developed models not only characterize PK-PD relationships that are difficult to understand by conventional noncompartmental analyses, but they can also be further used to simulate new dosing regimens, and inform future clinical trial designs. In addition, various questions in pharmacology. Besides, these methods are increasingly becoming an integrated part of drug development, and should also be applied in drug development for leishmaniasis, and any other neglected disease in that regard.

Appendix

Summary

Leishmaniasis is a devastating and still insufficiently recognized health burden. Caused by the heterogeneous *Leishmania* parasite species, the disease manifests in various clinical forms from a cutaneous infection to an infection of the internal organs that is fatal if left untreated. Miltefosine is the first and still only oral drug available for treatment of leishmaniasis. This thesis investigated the clinical pharmacokinetics (PK) and pharmacodynamics (PD) of miltefosine in the treatment of leishmaniasis.

In **chapter I**, we provided a comprehensive and updated review of the clinical pharmacology of miltefosine. Here we discussed the current dosing recommendation in various clinical presentations of leishmaniasis including cutaneous leishmaniasis (CL), visceral leishmaniasis (VL) and future prospects in treatment of post kala-azar dermal leishmaniasis (PKLD). **Chapter II** focused on clinical PK, and **chapter III** explored clinical PD of miltefosine. Studies included in these chapters employed methods of population PK-PD modeling and simulation, as well as physiologically-based PK (PBPK) modeling. Using a population PK-PD modeling approach, we aimed to characterize and interpret miltefosine PK and PD responses in different patient populations including adult and pediatric patients, in different clinical presentations of leishmaniasis, i.e. VL and PKDL. In **chapter 2.1** we characterized non-linear PK of miltefosine in pediatric VL patients from Eastern Africa treated with an allometric dosing regimen. Here we characterize that underlying reasons leading to nonproportional increase in exposure given the increase in dose were related to decrease in bioavailability of the drug. This decrease was dose-dependent, and likely due to saturable absorption of miltefosine. In **chapter 2.2** we present the first population PK analysis of a short course allometric dosing regimen of miltefosine in the treatment of PKDL in South Asian patients. Next, to optimize treatment efficacy, exposure-response relationships are of crucial essence. Thus, in **chapter 3.1** we provided a systematic overview of host-mediated effects of miltefosine through immunomodulation. This study summarized both pre-clinical and clinical data of various effects miltefosine exerts on the immune system of the host, and how those further affect the parasite response. In **chapter 3.2** we presented a PKPD model of the endogenous macrophage-activation marker neopterin in VL patients and its dynamics following treatment with miltefosine.

The above-mentioned studies focused on systemic exposure of miltefosine, and its relationship with PK and PD, while target-site exposure of miltefosine in dermal leishmaniases was previously unknown. For this reason, we further applied a PBPK modeling and simulation approach. This enabled us to create a mechanistic model based on physiological, anatomical and biochemical information entirely separate from drug model, in order to evaluate mechanisms by which physiological processes dictate disposition of miltefosine in human. In **chapter 4.1** we present first evidence of miltefosine penetration into the human skin after oral administration in the context of the treatment of PKDL patients. To further characterize and quantify the target-site PK of miltefosine, we developed a PBPK model of miltefosine penetration into the skin. By modeling how miltefosine binds to or is incorporated into cell membranes, this study further proposes exposure to miltefosine in various other tissues and organs. As such, results obtained with the developed PBPK model enabled conclusions and perspectives which extend beyond the scope of clinical observations.

In conclusion, this thesis described the results of several clinical PK and PD studies of miltefosine in the treatment of leishmaniasis. We demonstrated various examples of applying advanced methods of (mathematical) modeling and simulation to improve the treatment options with miltefosine for leishmaniasis. Using these methods, we were able to answer clinically relevant questions that would be rather difficult or even impossible to answer using traditional methods. Model-based investigations into PK-PD relationships of miltefosine are also needed because these relationships have been shown to suffer from non-linearities and delays. Taken together, this thesis contributed towards a better understanding of clinical pharmacology of miltefosine, which further enabled a more optimized treatment with miltefosine, currently alone, and in future combination antileishmanial therapies.

Samenvatting

Leishmaniasis is een levensgevaarlijke en verwaarloosde parasitaire aandoening. Deze wordt veroorzaakt door de *Leishmania* parasiet en manifesteert zich in verschillende klinische vormen, van een huidinfectie tot een infectie van de inwendige organen, welke fataal kan zijn indien deze onbehandeld blijft. Miltefosine is het eerste en enige orale geneesmiddel dat beschikbaar is voor de behandeling van leishmaniasis. Dit proefschrift onderzoekt de klinische farmacokinetiek (PK) en farmacodynamiek (PD) van miltefosine in de behandeling van leishmaniasis. In **hoofdstuk I** wordt een uitgebreid overzicht gepresenteerd van de recente literatuur over de klinische farmacologie van miltefosine. Hierin bespreken we de huidige doseringsaanbevelingen en toekomstperspectieven voor de behandeling van verschillende klinische presentaties van leishmaniasis, waaronder cutane leishmaniasis (CL), viscerale leishmaniasis (VL) en post-kala-azar dermale leishmaniasis (PKDL). In **hoofdstuk II** wordt gefocust op klinische PK, en in **hoofdstuk III** wordt de klinische PD van miltefosine onderzocht. Voor de studies die in deze hoofdstukken zijn opgenomen wordt gebruik gemaakt van populatie PK-PD modellering en simulatie en fysiologisch gebaseerde PK (PBPK) modellering. Het doel was om de PK en PD respons van miltefosine te karakteriseren en interpreteren voor verschillende patiëntenpopulaties, waaronder volwassen en pediatrische patiënten, tijdens de behandeling van VL en PKDL, door middel van populatie PK-PD modellering. In **paragraaf 2.1** hebben we de niet-lineaire PK van miltefosine gekarakteriseerd in pediatrische VL patiënten uit Oost Afrika, die behandeld werden met een allometrisch doseringsschema. Hier identificeerden we dat de onderliggende redenen die leiden tot een niet-proportionele toename in blootstelling gegeven de verhoging van de dosis, gerelateerd zijn aan de afname van de biologische beschikbaarheid van het geneesmiddel. Deze afname was afhankelijk van de dosis en komt mogelijk door verzadigbare absorptie van miltefosine. In **paragraaf 2.2** presenteren we de eerste populatie PK analyse van een kort allometrisch doseringsschema van miltefosine in de behandeling van PKDL in Zuid Aziatische patiënten. Om de effectiviteit van de behandeling te optimaliseren zijn blootstelling-respons relaties van cruciaal belang. Daarom hebben we in **paragraaf 3.1** een systematisch overzicht gepresenteerd van gastheer-afhankelijke effecten van miltefosine door middel van immunomodulatie. Deze studie vat zowel preklinische als klinische data samen van de verschillende effecten die miltefosine heeft op het immuunsysteem van de gastheer en hoe deze de parasitaire respons verder beïnvloeden. In **paragraaf 3.2** hebben we een PK-PD model gepresenteerd van neopterine,

een endogene marker voor activatie van macrofagen, in VL patiënten en de dynamiek ervan tijdens en na behandeling met miltefosine. Bovengenoemde onderzoeken waren gericht op systemische blootstelling aan miltefosine en de relatie tussen systemische PK en PD, terwijl lokale blootstelling aan miltefosine in de huid waar de parasieten gelokaliseerd zijn bij dermale *Leishmania*-infecties voorheen onbekend was. Om deze reden hebben we een PBPK-modellering en simulatiebenadering toegepast. Dit stelde ons in staat om een mechanistisch model te creëren op basis van fysiologische, anatomische en biochemische informatie om mechanismen te evalueren waarmee fysiologische processen de dispositie van miltefosine in de mens bepalen. In **paragraaf 4.1** presenteren we het eerste bewijs van penetratie van miltefosine in de menselijke huid na orale toediening in de context van de behandeling van PKDL patiënten. Om de lokale PK van miltefosine in de huid verder te karakteriseren en kwantificeren, hebben we een PBPK model van miltefosine penetratie in de huid ontwikkeld. Door te modelleren hoe miltefosine bindt aan of wordt geïncorporeerd in celmembranen, wordt in deze studie ook een indicatie gegeven van de blootstelling aan miltefosine in andere weefsels en organen. De resultaten verkregen uit het ontwikkelde PBPK-model hebben geleid tot conclusies en perspectieven die verder gaan dan het bereik van de klinische observaties.

Ter conclusie, in dit proefschrift zijn resultaten gepresenteerd van verschillende klinische PK en PD studies van miltefosine voor de behandeling van leishmaniasis. We hebben verschillende voorbeelden gepresenteerd van het toepassen van geavanceerde methoden op basis van (wiskundige) modellen en simulaties, om de behandelingsmogelijkheden met miltefosine te verbeteren voor leishmaniasis. Met behulp van deze methoden hebben we klinisch relevante vragen kunnen beantwoorden die moeilijk of zelfs onmogelijk te beantwoorden zouden zijn met behulp van traditionele methoden. Modelgebaseerd onderzoek naar PK-PD verbanden van miltefosine is ook nodig omdat is aangetoond dat deze verbanden niet-lineair gedrag en vertragingen vertonen. Samenvattend heeft dit proefschrift bijgedragen aan een beter begrip van de klinische farmacologie van miltefosine, welke een meer geoptimaliseerde behandeling met miltefosine mogelijk maakt, zowel in monotherapie, als in toekomstige combinaties met andere antileishmaniale geneesmiddelen.

Author affiliations

Fabiana Alves

Drugs for Neglected Diseases initiative,
Geneva, Switzerland

Jos H. Beijnen

Department of Pharmacy & Pharmacology, The Netherlands Cancer Institute - Antoni van Leeuwenhoek Hospital, Amsterdam, The Netherlands

Patrick Bhairosing

Scientific Information Service, The Netherlands Cancer Institute, Amsterdam, The Netherlands

Pradeep Das

Rajendra Memorial Research Institute for Medical Sciences, Patna, India

Thomas P. C. Dorlo

Department of Pharmacy & Pharmacology, The Netherlands Cancer Institute - Antoni van Leeuwenhoek Hospital, Amsterdam, The Netherlands

M.G. Hasnain

Centre for Nutrition and Food Security (CNFS), International Centre for Diarrhoeal Disease Research, Bangladesh (ICDDR,B), Dhaka, Bangladesh

Abdullah Hamadeh

School of Pharmacy, University of Waterloo, Ontario, Canada

Alwin D.R. Huitema

Department of Pharmacy & Pharmacology, The Netherlands Cancer Institute - Antoni van Leeuwenhoek Hospital, Amsterdam, The Netherlands

Princess Máxima Center for Pediatric Oncology, Utrecht, the Netherlands

Eltahir A.G. Khalil

Institute of Endemic Diseases, University of Khartoum, Khartoum, Sudan

Anke E. Kip

Department of Pharmacy & Pharmacology, The Netherlands Cancer Institute - Antoni van Leeuwenhoek Hospital, Amsterdam, The Netherlands

Paul R.V. Malik

School of Pharmacy, University of Waterloo, Ontario, Canada

Jane Mbui

Centre for Clinical Research, Kenya Medical Research Institute, Nairobi, Kenya

Dinesh Mondal

International Centre for Diarrhoeal Disease Research, Bangladesh (ICDDR,B)

Dhaka, Bangladesh

M. A. Mural

Centre for Nutrition and Food Security (CNFS), International Centre for Diarrhoeal Disease Research, Bangladesh (ICDDR,B), Dhaka, Bangladesh

Ahmed Musa   Institute of Endemic Diseases, University of Khartoum,
                              Khartoum, Sudan

Joseph Olobo   Department of Immunology and Molecular Biology, College of
                              Health Sciences, Makerere University,
                              Kampala, Uganda

Krishna Pandey   Rajendra Memorial Research Institute for Medical Sciences,
                              Patna, India

Sheeraz Raja   Drugs for Neglected Diseases Initiative South Asia,
                              New Delhi, India

Suman Rijal   Drugs for Neglected Diseases Initiative South Asia,
                              New Delhi, India

Ignace C. Roseboom   Department of Pharmacy & Pharmacology, The Netherlands
                              Cancer Institute - Antoni van Leeuwenhoek Hospital,
                              Amsterdam, The Netherlands

Erik Sjögren   Department of Pharmaceutical Biosciences, Uppsala University,
                              Uppsala, Sweden
                              Pharmetheus AB, Uppsala, Sweden

Alexandra Solomos   Drugs for Neglected Diseases initiative,
                              Geneva, Switzerland

Shyam Sundar

Department of Medicine, Institute of Medical Sciences, Banaras Hindu University,

Varanasi, India

Monique Wasunna

Drugs for Neglected Diseases initiative,

Nairobi, Kenya

List of publications

Peer-reviewed articles

- van den Brink WJ, **Palić S**, Köhler I, de Lange ECM. 2018. Access to the CNS: Biomarker Strategies for Dopaminergic Treatments. Pharm Res 35:64.

- Brussee JM, Yu H, Krekels EHJ, **Palić S**, Brill MJE, Barrett JS, Rostami-Hodjegan A, de Wildt SN, Knibbe CAJ. 2018. Characterization of Intestinal and Hepatic CYP3A-Mediated Metabolism of Midazolam in Children Using a Physiological Population Pharmacokinetic Modelling Approach. Pharm Res 35:182.

- Brussee JM, Krekels EHJ, Calvier EAM, **Palić S**, Rostami-Hodjegan A, Danhof M, Barrett JS, de Wildt SN, Knibbe CAJ. 2019. A Pediatric Covariate Function for CYP3A-Mediated Midazolam Clearance Can Scale Clearance of Selected CYP3A Substrates in Children. AAPS J 21:81.

- **Palić S**, Bhairosing P, Beijnen JH, Dorlo TPC. 2019. Systematic Review of Host-Mediated Activity of Miltefosine in Leishmaniasis through Immunomodulation. Antimicrob Agents Chemother 63(7):e02507.

- **Palić S**, Kip AE, Beijnen JH, Mbui J, Musa A, Solomos A, Wasunna M, Olobo J, Alves F, Dorlo TPC. 2020. Characterizing the non-linear pharmacokinetics of miltefosine in paediatric visceral leishmaniasis patients from Eastern Africa. J Antimicrob Chemother 75(11):3260-3268.

Conference proceedings

- **Palić S,** Kip AE, Beijnen JH, Wasunna M, Alves F, Dorlo TPC. 2018. Exploring dose-dependent pharmacokinetics of miltefosine in pediatric visceral leishmaniasis patients from East Africa, PAGE 27th meeting.

- **Palić S**, Alves F, Huitema ADR, Beijnen JH, Dorlo TPC. 2019. Neopterin dynamics in pediatric patients after miltefosine treatment of visceral leishmaniasis, PAGE 28th meeting.

- Palić S, Kip AE, Beijnen JH, Mbui J, Wasunna M, Alves F, Dorlo TPC. 2020. Clinical pharmacokinetics of allometric dosing regimen in treatment of peadiatric visceral leishmaniasis in East Africa: Results from an open label, Phase II clinical trial. ESPID Virtual Meeting

- Palić S, Huitema ADR, Alves F, Beijnen JH, Dorlo TPC. 2021. Pharmacodynamics of the Macrophage Activation Marker Neopterin Following Miltefosine Treatment of Visceral Leishmaniasis in Eastern African Patients. World Conference on Pharmacometrics, Abstracts CPT: Pharmacometrics & Systems Pharmacology - Wiley Online Library

Curriculum Vitae

Semra Palić was born on March 3rd, 1994 in Žepa, and grew up in Sarajevo, Bosnia and Herzegovina. She graduated from International Baccalaureate Diploma Programme at Druga gimnazija in Sarajevo in 2012, and moved to the Netherlands to study at Amsterdam University College. She majored in sciences, following subjects within the biomedical and chemistry tracks. In 2015, she graduated with honors, and obtained a joint Bachelor's degree from the University of Amsterdam (UvA) and Vrije Universiteit Amsterdam (VU). After obtaining her Bachelor's degrees, she entered a research-oriented master's program in Biopharmaceutical sciences at Leiden University, specializing in Systems Biomedicine and Pharmacology. During her masters, she conducted clinical research projects at Leiden Academic Centre for Drug Research, and University Medical Center Utrecht. She was awarded Leiden University Excellence Scholarship and graduated *cum laude* in 2017. In the same year, Semra started her PhD which is presented in this thesis, at the department of Pharmacy & Pharmacology at Netherlands Cancer Institute - Antoni van Leeuwenhoek hospital in the research group lead by prof.dr. Jos Beijnen. Her research focused on the oral drug miltefosine, and its optimization in treatment of neglected tropical disease leishmaniasis. During her doctorate, Semra was a member of the Steering Committee International Society of Pharmacometrics (ISoP) Student Community, representing PhD students in pharmacometrics from the Netherlands. In 2019, she was also a guest researcher at department of Pharmacy at Uppsala University in Sweden.